Stony Brook University

Three Novel rRNA Methyltransferases in Mammalian Mitochondria

A Dissertation Presented

by

Ken-Wing Lee

to

The Graduate School

in Partial Fulfillment of the

Requirements

for the Degree of

Doctor of Philosophy

in

Molecular and Cellular Pharmacology

Stony Brook University

August 2014

Stony Brook University

The Graduate School

Ken-Wing Lee

We, the dissertation committee for the above candidate for the

Doctor of Philosophy degree, hereby recommend

acceptance of this dissertation.

Professor Daniel Bogenhagen, MD – Dissertation Advisor
Department of Molecular and Cellular Pharmacology

Professor Bruce Demple, PhD – Chair of Thesis Committee
Department of Molecular and Cellular Pharmacology

Associate Professor Miguel Garcia-Diaz, PhD – Committee Member
Department of Molecular and Cellular Pharmacology

Associate Professor Wali Karzai, PhD – Committee Member
Department of Biochemistry and Cell Biology

Assistant Professor Kevin Czaplinski, PhD – Outside Member
Department of Biochemistry and Cell Biology

This dissertation is accepted by the Graduate School

Charles Taber
Dean of the Graduate School

Three Novel rRNA Methyltransferases in Mammalian Mitochondria

by

Ken-Wing Lee

Doctor of Philosophy

in

Molecular and Cellular Pharmacology

Stony Brook University

August 2014

Mammalian mitochondria maintain their double-stranded circular genome in DNA-protein complexes known as nucleoids, similar to bacteria. While bacterial and yeast mitochondrial nucleoids have been studied more extensively, much is unknown about the protein composition and events that occur at mammalian mitochondrial nucleoids. Recent work has identified many novel mitochondrial nucleoid proteins by mass spectrometry, however the functions of many of these proteins are not well understood. One of the interesting proteins identified by mass spectrometry is RNMTL1, a putative RNA methyltransferase. A search for related mitochondrial proteins in proteomic databases revealed MRM1 and MRM2 as potential RNA methyltransferases as well. The work reported in this thesis includes an initial characterization of the three novel rRNA methyltransferase proteins. We provide data on the subcellular localization of these proteins and the macromolecular complexes in which they exist. We have slightly focused more on RNMTL1, since neither RNMTL1 nor any known homologues have previously been characterized, and provide data on its protein interacting partners. We also provide evidence that RNMTL1 has an important role in mammalian

mitochondrial translation. In addition, we have assigned the three methyltransferases to their specific substrate sites on the mitochondrial large ribosomal subunit rRNA. MRM1, MRM2 and RNMTL1 methylate the 2'-O-ribose of G^{1145}, U^{1369} and G^{1370}, respectively. These methyltransferases are also likely involved in mitochondrial ribosome assembly and/or stability.

Dedication Page

The thesis presented here is dedicated to my family and my best friends, who have been my greatest support throughout many challenging years. My parents worked full-time every day of the week for more than thirty years and sacrificed everything to give their children the best. My parents sacrificed going on vacation, buying luxury items and enjoying their hobbies to put their full attention to their children. My brothers not only supported me when I was right but they also supported me when I was wrong, and taught me to be a better person. My friends were there to lift me up when the road was rough. I hope that upon graduation I have made them all proud and that their sacrifices did not go to waste.

Frontispiece

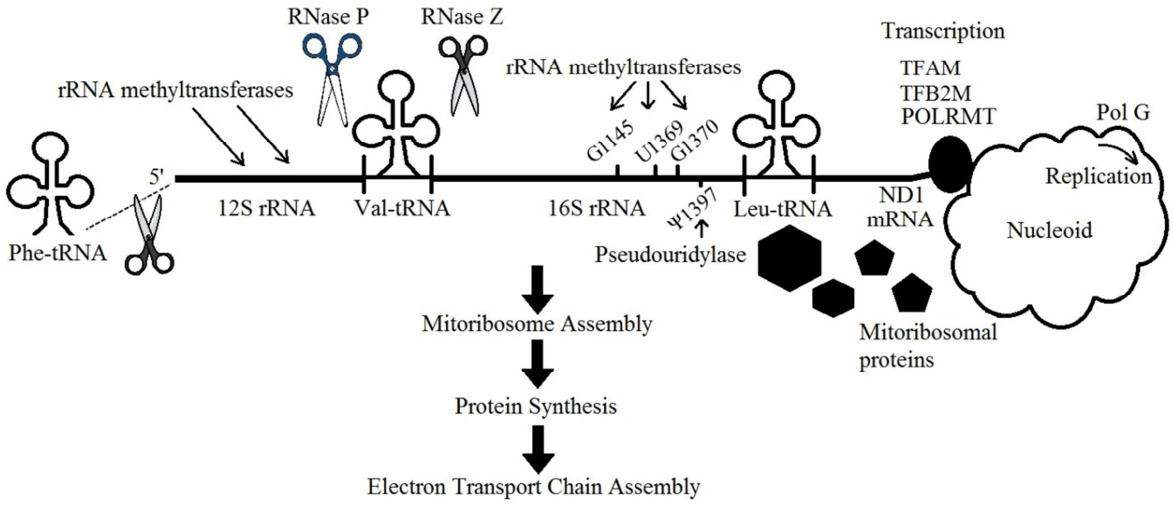

Mitochondrial nucleoids are the sites of biogenesis.

Table of Contents

List of Figures viii
List of Tables x
List of Abbreviations xi
Preface xvi
Acknowledgments xviii
Chapter 1 – Introduction 1
A. The Significance and Diverse Functions of Mammalian Mitochondria 1
B. Mammalian Mitochondrial Genetics 3
C. Post-transcriptional Regulation of Mitochondrial RNA 19
D. Mitochondrial Ribosomes and Translation 21
Chapter 2 – Materials and Methods 42
Chapter 3 – Initial Characterization of Three Novel Mitochondrial rRNA Methyltransferases .. 56
A. RNMTL1, MRM1 and MRM2 are mitochondrial proteins 56
B. RNMTL1, MRM1 and MRM2 are associated with mitochondrial nucleoids and ribosomal complexes 57
C. Murine RNMTL1 interacts with mitochondrial LSU components and other proteins 61
D. RNMTL1 is involved in mitochondrial protein synthesis 63
E. Analysis of activity in recombinant RNA methyltransferase family members 64
Chapter 4 – Assignment of Three Mitochondrial rRNA Methyltransferases to their Substrate Sites 83
A. Mapping the site of modification attributable to RNMTL1 using primer extension 84
B. Mapping the 2'-O-methylation sites on 16S rRNA with DNAzymes 85
Chapter 5 – Conclusion and Perspectives 98
References 104

List of Figures

Figure 1 – Map of the human mitochondrial genome.

Figure 2 – tRNA punctuation model.

Figure 3 – The secondary structure of human mitochondrial 12S and 16S rRNAs and their modifications.

Figure 4 – RNMTL1, MRM1 and MRM2 are members of the methyltransferase family.

Figure 5 – MRM1, MRM2 and RNMTL1 tagged with Eos localize to foci in the vicinity of nucleoids.

Figure 6 – Endogenous RNMTL1 is localized in foci in the vicinity of mitochondrial nucleoids.

Figure 7 – RNMTL1 and MRM1 sediment with nucleoid and ribosomal complexes on a non-denaturing glycerol gradient, while MRM2 only sediments with ribosomal complexes.

Figure 8 – RNMTL1 and MRM1 sedimenting in the nucleoid fraction remains associated with nucleoids after centrifugation through an iodixanol (OptiPrep) gradient.

Figure 9 – RNMTL1 and MRM2 sedimenting with ribosomes in glycerol gradient fractions remain associated with ribosomes after centrifugation through an iodixanol gradient.

Figure 10 – RNMTL1 is associated with the LSU in a sucrose gradient supplemented with $MgCl_2$.

Figure 11 – Affinity chromatography purification of RNMTL1-3FH and associated proteins.

Figure 12 – Recombinant hsRNMTL1 does not interact with MTERF3.

Figure 13 – siRNA-mediated depletion of RNMTL1 in HeLa cells decreased mitochondrial translation without drastically affecting mitochondrial transcript levels.

Figure 14 – Recombinant RNMTL1 and MRM1 do not cross-link to [^{3}H]AdoMet under conditions that permit cross-linking for NSUN4 and MRM2.

Figure 15 – Recombinant hsRNMTL1, mmMRM1 and mmMRM2 behave as monomeric proteins.

Figure 16 – The methylation sites on mitochondrial 16S rRNA that are conserved in bacteria contribute to secondary structures participating in the peptidyl transferase center.

Figure 17 – Depletion of RNMTL1 increases reverse transcriptase extension past G^{1370} in domain 6 of 16S rRNA.

Figure 18 – DNAzymes cleave unmodified RNA and are an effective tool for studying 2'-O-ribose methylation of rRNA.

Figure 19 – siRNA effectively depletes MRM1 and MRM2 protein levels in HeLa cells.

Figure 20 – Schematic of the application of siRNA and DNAzymes to assign 2'-O-methyltransferases to their substrate sites.

Figure 21 – DNAzymes allow the assignment of 2'-O-methyltransferases to their substrate sites.

List of Tables

Table 1 – Mammalian mitochondrial rRNA modifications and their corresponding sites in bacteria (*E. coli*) and yeast (*S. cerevisiae*) mitochondria.

Table 2 – rRNA modifications across various species, sorted by the type of modification.

Table 3 – GTPases involved in ribosome assembly, sorted by homologues in different species.

Table 4 – DNA oligonucleotide sequences used in this thesis.

Table 5 – Predicted attributes of MRM1, MRM2 and RNMTL1 proteins.

Table 6 – Well-represented non-ribosomal mitochondrial proteins that were co-immunoprecipitated by RNMTL1-3FH.

Table 7 – Recombinant hsRNMTL1, mmMRM1 and mmMRM2 do not catalyze *in vitro* methylation of 16S rRNA.

Table 8 – Quantification of the effects of siRNA on DNAzyme-mediated 16S rRNA cleavage.

List of Abbreviations

$^{32}P_i$	Inorganic phosphate, radioactively labeled with atomic weight of 32
A	Adenosine
AdoMet / SAM	S-adenosyl methionine
ADP	Adenosine diphosphate
ATP	Adenosine triphosphate
BSA	Bovine serum albumin
C	Cytosine
CBB	Coomassie brilliant blue
CM	Crude mitochondria
CMC	1-cyclohexyl-3-(2-morpholinoethyl)carbodiimide metho-p-toluene sulfonate
Cryo-EM	Cryo-electron microscopy
CSB II	Conserved sequence box II
CTP	Cytosine triphosphate
DEPC	Diethylpyrocarbonate
D-foci	Degradation foci
DMEM	Dulbecco's modified Eagle's medium
DMSO	Dimethyl sulfoxide
dNTPs	Deoxyribonucleic acid triphosphates
DTT	Dithiothreitol
E. coli	*Escherichia coli*
EDTA	Ethylenediaminetetraacetic acid
ETC	Electron transport chain (see OXPHOS)

f^5C	5-Formylcytidine
FADH	Flavin adenine dinucleotide
FBS	Fetal bovine serum
$FLAG_3His_6$	Three FLAG peptides in tandem with six histidine residues
γ-[^{32}P]ATP	ATP radioactively-labeled at the gamma phosphate
G / Gm	Guanosine / 2'-O-methyl guanosine
GTP	Guanosine triphosphate
GTPase	Guanosine triphosphatase
h	Hour(s)
HEPES	4-(2-Hydroxyethyl)piperazine-1-ethanesulfonic acid
Hom	Homogenate (of cells)
HRP	Horseradish peroxidase
hsRNMTL1	*Homo sapiens* RNMTL1
IMM	Inner mitochondrial membrane
IMS	Intermembrane space
IPTG	Isopropyl β-D-1-thiogalactopyranoside
K_2HPO_4	Potassium phosphate
KCl	Potassium chloride
kDa	Kilodalton
LC-MS/MS	Liquid chromatography with tandem mass spectrometry
LHON	Leber's hereditary optic neuropathy
LSU	Large ribosomal subunit
M	Molarity

MELAS	Mitochondrial encephalomyopathy lactic acidosis stroke-like episodes
MERRF	Myoclonic epilepsy with ragged red fibers
$MgCl_2$	Magnesium chloride
MIB	Mitochondrial isolation buffer
μg	Microgram
min	Minute(s)
Mitoribosome	Mitochondrial ribosome
μl	Microliter
ml	Milliliter
MLS / MTS	Mitochondrial localization/targeting signal/sequence
μm	Micrometer (micron)
mM	Millimolar
mmMRM1	*Mus musculus* MRM1
mmMRM2	*Mus musculus* MRM2
$MnCl_2$	Manganese chloride
MOPS	3-(N-morpholino)propanesulfonic acid
mRNA	Messenger RNA
MRP	Mitochondrial ribosomal protein
MSH	Mannitol, sucrose, HEPES buffer
mtDNA	Mitochondrial DNA
NaCl	Sodium chloride
NADH	Nicotinamide adenine dinucleotide
ng	Nanogram

nm	Nanometer
nM	Nanomolar
nt	Nucleotide(s)
OD_{600}	Opitcal density measured at 600 nanometer wavelength
O_H	Origin of heavy strand replication
O_L	Origin of light strand replication
OXPHOS	Oxidative phosphorylation
PALM	Photoactivated localization microscopy
PBS	Phosphate buffered saline
PCR	Polymerase chain reaction
pI	Isoelectric point
pmol	Picomole
PM	Purified mitochondria
PMS	Post-mitochondrial supernatant
PMSF	Phenylmethylsulfonyl fluoride
PNS	Post-nuclear supernatant
PTC	Peptidyl transferase center
PVDF	Polyvinylidene fluoride
Q	Queuosine
RA-GTPase	Ribosome-assembly GTPase
RNMTL1-3FH	RNMTL1 tagged at the 3’ terminus with $FLAG_3His_6$
ROS	Reactive oxygen species
RT-PCR	Reverse-transcriptase / real-time polymerase chain reaction

rRNA	Ribosomal RNA
S. cerevisiae	*Saccharomyces cerevisiae*
SDHA	Succinate dehydrogenase complex, subunit A
SDS	Sodium dodecyl sulfate
SDS-PAGE	Sodium dodecyl sulfate polyacrylamide gel electrophoresis
SILAC	Stable isotope labeling by amino acids in cell culture
siRNA	Silencing RNA
SMEM	Minimum essential medium Eagle Spinner Modification
snoRNP	Small nucleolar ribonucleoproteins
SSC	Saline sodium citrate
SSU	Small ribosomal subunit
TAS	Termination-associated sequence
TE	Tris EDTA buffer
τm^5U	5-Taurinomethyluridine
τm^5s^2U	5-Taurinomethyl 2-thiouridine
Tris	Tris(hydroxymethyl)aminomethane
tRNA	Transfer RNA
$tRNA^{Met}$	Methionine-tRNA
Ψ	Pseudouridine
U / Um	Uridine / 2'-O-methyluridine
UTR	Untranslated region
UV	Ultraviolet
V	Volts

Preface

While biochemical analysis of cell fractions began to reveal some of the functions of mitochondria around the 1950s (Ernster and Schatz, 1981), proteomic studies to identify specific mammalian mitochondrial proteins were initiated in 1981, using two-dimensional gel electrophoresis (Anderson, 1981). Technological advances by 1998 to 2001 allowed the large scale identification of mitochondrial proteins by utilizing the powerful tool of mass spectrometry (Calvo and Mootha, 2010). The vast amount of information on mitochondrial proteins has been organized into databases such as the MitoCarta (Pagliarini et al., 2008), MitoMiner (Smith et al., 2012; Smith and Robinson, 2009) and others (Calvo and Mootha, 2010). Patterns found within the N-termini of mitochondrial proteins have helped generate tools such as MitoProt, which analyzes the amino acid sequence of any given protein and calculates the probability of the protein to be naturally imported into mitochondria, as well as the expected cleavage site after import. This tool is particularly useful since most mitochondrial matrix proteins have an N-terminal sequence that is proteolytically cleaved subsequent to translocation into the organelle. The exact functions of hundreds of putative mitochondrial proteins remain unknown.

The Bogenhagen lab was among the first to pioneer methods for isolating highly purified mitochondrial nucleoids from higher eukaryotes and perform proteomic analysis of the proteins in these complexes (Bogenhagen et al., 2003). This led to a model in which the nucleoid core consists of mitochondrial DNA tightly packaged by TFAM and mtSSB, and is handled by a set of “core” proteins functioning in DNA repair, replication and transcription (Bogenhagen et al., 2008). The periphery of the nucleoid core consists of RNA processing enzymes, proteins involved in translation, protein folding and ribosome assembly factors. However, many of the

nucleoid proteins are still uncharacterized. We began to study some of these proteins and found an interesting group of putative RNA methyltransferases: RNMTL1, MRM1 and MRM2, which is the basis for this dissertation.

Acknowledgments

The work presented here would not be possible without the support and leadership from my advisor, Professor Daniel Bogenhagen and my thesis committee. I am truly thankful for the opportunity to work on an interesting project and to have received very helpful advice from the most intelligent people that I know. I am also thankful for learning how to be critical when analyzing data and understanding the limitations of each technique. I thank the Miguel Garcia-Diaz lab for reagents and consultation. I thank my fellow classmates for their moral support. I thank Joseph F. LaComb, who had done a great job maintaining the lab and helping with training rotation students, undergraduates and high school students. I thank Cynthia Okot-Kotber, whom I had the experience of teaching in her undergraduate career. I thank the Molecular and Cellular Pharmacology Department at Stony Brook University for investing in my education. I also thank the many great scientists whose work had set the foundation for our studies reported here, since none of it would have been possible without previously established concepts and methods. And lastly, I thank those who help fund scientific research.

Chapter 1 – Introduction

A. The Significance and Diverse Functions of Mammalian Mitochondria

Mitochondria are double-membrane organelles that are unique to eukaryotes and are believed to have evolved from the endosymbiotic incorporation of an α-proteobacterium most similar to the present-day Rickettsiales into a host cell over 1.5 billion years ago (Dyall et al., 2004; Gray et al., 1999). It is not surprising that about two-thirds of the approximately 1,100 known mitochondrial proteins in humans have bacterial origins (Vafai and Mootha, 2012). Interestingly, other mitochondrial proteins such as DNA Polymerase γ, RNA polymerase (POLRMT) and TWINKLE helicase are similar to T-odd bacteriophage proteins (Filee et al., 2002; Ringel et al., 2011; Shutt and Gray, 2006). Mitochondria are most well known for their role in oxidative phosphorylation by the respiratory chain (OXPHOS complexes, also known as the electron transport chain (ETC)) at the inner mitochondrial membrane, which provides the host cell with energy in the form of ATP. An historical account of the major discoveries in mitochondria, including the development of Mitchell's hypothesis of respiratory chain function, is reviewed by Ernster and Schatz (Ernster and Schatz, 1981). It is proposed that by maintaining its own genome dedicated to producing energy, separate from the nuclear genome, mitochondria have allowed the evolution of complexity in higher eukaryotes (Lane and Martin, 2010). In higher eukaryotes, mitochondria also have important functions in apoptosis, metabolism, heat generation, calcium storage, immunity, cell signaling via reactive oxygen species (ROS) (Finkel, 2011), and the synthesis of iron-sulfur complexes (Beilschmidt and Puccio, 2014) and steroids (Miller, 2013). Therefore it is no surprise that mitochondrial dysfunction is found in a vast array of human diseases that affects various organs and causes diverse, often debilitating symptoms.

Over 150 distinct mitochondrial syndromes are defined, and most are caused by abnormal respiratory chain function, occurring in at least 1 in 5,000 live births (Vafai and Mootha, 2012). Mitochondria are heterogeneous in an organ-specific basis to allow specialization of diverse functions, likely explaining the organ-specific clinical presentations of some mitochondrial diseases. Over 300 mutations in mitochondrial DNA (mtDNA) and over 110 mutations in nuclear-encoded proteins have been found to lead to mitochondrial disease. The first disease-causing human mtDNA mutations were identified by the labs of Wallace (Wallace et al., 1988) and Harding (Holt et al., 1988). Mitochondrial diseases include mitochondrial encephalopathy lactic acidosis and stroke-like syndrome (MELAS), myoclonic epilepsy with ragged red fibers (MERRF), Leigh syndrome, Leber's hereditary optic neuropathy (LHON), cardiomyopathy, deafness, muscular dysfunction, anemia, diabetes, Parkinson's disease and Alzheimer's disease (DiMauro and Schon, 2003; Stumpf and Copeland, 2011; Taylor and Turnbull, 2005; Vafai and Mootha, 2012; Wallace, 1999, 2012). Mitochondrial dysfunction is also heavily implicated in aging (Bogenhagen, 2010; Bratic and Larsson, 2013; Trifunovic et al., 2004). Organs with a high energy demand such as the brain, the heart, the liver and skeletal muscles are often the most severely affected by dysfunctional mitochondria. The synthesis of mitochondrial ribosomes (mitoribosomes) and respiratory complexes is regulated by the coordinated expression of two genomes, the nuclear and the mitochondrial genomes. Thus, mutations in either source may lead to defects in mitochondrial biogenesis and mitochondrial disorders. Mitochondria undergo fusion and fission to share components to maintain a functional population and to re-distribute mitochondria, which is especially important in polarized cell types (Detmer and Chan, 2007). Dysfunctional mitochondria are believed to be removed from the cell through mitophagy, a

process mediated by PINK1 and Parkin, proteins that are mutated in a subset of Parkinson's disease patients (Kane et al., 2014).

The current treatments for mitochondrial disorders attempt to mitigate the symptoms, but do not deal with the underlying cause. Therapies are only palliative and include vitamins, cofactors, ROS scavengers and exercise (DiMauro and Schon, 2003; Gardner et al., 2007; Koene and Smeitink, 2009; Smeitink et al., 2006). Methods of specifically eliminating mutant mtDNA without depleting normal mtDNA are under development *in vitro*, including expression of a mitochondrial-localized restriction enzyme (Srivastava and Moraes, 2001) or zinc-finger nuclease (Minczuk et al., 2010). However the clinical translation of these ideas is still far away. Since mtDNA is completely maternally inherited, strategies are being explored to prevent transmission of defective mtDNA prior to birth. Progress in pro-nuclear transfer and spindle transfer technology with human cells offers promise of a "three-parent" model to prevent inheritance of defective mtDNA and are on the verge of entering clinical trials in the United Kingdom and possibly in the United States (Amato et al., 2014; Craven et al., 2010; Tachibana et al., 2013a; Tachibana et al., 2013b; Tachibana et al., 2009; Vogel, 2014). Recently, polar body genome transfer in mice has also shown promise as an alternative method for bypassing the transmission of mitochondrial diseases (Wang et al., 2014b).

B. Mammalian Mitochondrial Genetics

1. Mitochondrial Genome and Mitochondrial Nucleoids

The human mtDNA is an approximately 5 μm circular molecule of 16,569 base pairs, coding for 13 mRNAs, 2 rRNAs and 22 tRNAs (**Fig 1**). The double-stranded genome consists of a heavy strand and a light strand, named so because the heavy strand is G-rich while the light

strand is C-rich and can thus be separated by mass on alkaline cesium chloride gradients (Falkenberg et al., 2007). tRNAs are dispersed throughout the genome and in all but two cases separate the rRNAs and mRNAs. The rRNAs and tRNAs are components of the mitochondrial ribosome (mitoribosome) and translation machinery, while the mRNAs are translated on mitoribosomes to generate protein subunits of the oxidative phosphorylation (OXPHOS) complexes. mtDNA encodes components of Complexes I, III, IV and V, while Complex II is composed of four nuclear-encoded subunits. Thus, mtDNA is solely dedicated to producing the electron transport chain (ETC). The coordination of the mitochondrial and nuclear genomes are required for assembly of the ETC. Complex I utilizes the NADH generated by the citric acid cycle in the mitochondrial matrix, whereas Complex II utilizes succinate and $FADH_2$. Complexes I and II transfer their electrons to Coenzyme Q, which then subsequently passes the electrons through Complex III, cytochrome c and Complex IV, initiating proton pumping from the mitochondrial matrix into the intermembrane space (IMS) at each step. This generates a proton electrochemical gradient across the inner mitochondrial membrane (IMM), consisting of a membrane potential ($\Delta\Psi$) and a proton concentration gradient (ΔpH). The protons re-enter the mitochondrial matrix through Complex V (ATP synthase), driving the phosphorylation of ADP to ATP. Uncoupling of the proton entry through ATP synthase and the ATP synthesis reaction by uncoupling protein 1 (UCP1) is a mechanism of heat generation.

mtDNA is packaged similarly to bacterial DNA into nucleoids by various proteins and not compartmentalized within a membrane (Bogenhagen, 2012). A comparison of the physical properties of mitochondrial nucleoids across several species is provided by (Chen and Butow, 2005). In vivo imaging of mammalian mitochondrial nucleoids over time shows that they are dynamic structures (Bereiter-Hahn and Voth, 1996; Garrido et al., 2003; Iborra et al., 2004;

Legros et al., 2004). Super-resolution microscopy surpasses the diffraction limit of light, which is approximately 200 nm and has improved the visualization of nucleoids. Recently, TFAM, one of the core protein components of nucleoids, was expressed with a photoactivatable fluorescent mEos2 tag in mouse fibroblasts and imaged with super-resolution photoactivated localization microscopy (PALM) (Brown et al., 2011). TFAM serves not only to tightly package DNA but also regulates its accessibility to other proteins. It is estimated that there are between 1.4 to 7.3 mtDNA copies per nucleoid and an estimated range of 50 to 1,700 molecules of TFAM are available per mtDNA (Bogenhagen, 2012). PALM imaging of TFAM-mEos2 revealed that nucleoids have an average diameter of approximately 70 nm and have an ellipsoidal shape (Brown et al., 2011), consistent with the previously reported range of nucleoid diameters of 31 to 132 nm measured by electron microscopy (Iborra et al., 2004). Nucleoids often exclude freely diffusible matrix proteins but these proteins can access the nucleoids through remodeling events (Brown et al., 2011). By combining electron microscopy and PALM, nucleoids were shown to be tightly associated with the IMM (Kopek et al., 2012), consistent with the co-fractionation of mtDNA with membranes (Albring et al., 1977) and the identification of IMM proteins in proteomic analyses of nucleoids (Wang and Bogenhagen, 2006). Yeast mitochondrial nucleoids are also believed to be associated with the membranes (Chen and Butow, 2005).

Studies on yeast mitochondrial nucleoids have been informative for understanding nucleoids in mammals and other higher eukaryotes (Garrido et al., 2003; Spelbrink, 2010). However, the protein components and events that occur at nucleoids are not well defined. Chemical crosslinking of proteins to DNA within nucleoids allowed the purification and identification of some of the nucleoid components in the yeast system (Kaufman et al., 2000). The Bogenhagen lab was the first to isolate highly purified mitochondrial nucleoids from higher

eukaryotes (*Xenopus* oocytes) and identified the proteins via mass spectrometry (Bogenhagen et al., 2003). *Xenopus* oocytes were chosen as the starting material since they each contain about 100,000 copies of mtDNA and are therefore abundant in nucleoids. The Bogenhagen lab and others have also isolated nucleoids from several mammalian cell lines and rat liver (Bogenhagen et al., 2008; He et al., 2012b; Wang and Bogenhagen, 2006), as reviewed by (Hensen et al., 2014). Nucleoids are often purified as native complexes by sedimentation through gradients or by immunoprecipitation, except in one case in which nucleoids were first crosslinked with formaldehyde prior to isolation in stringent conditions (Bogenhagen et al., 2008), a method previously performed on yeast nucleoids (Kaufman et al., 2000). These approaches provide information on the average composition of nucleoids. It is interesting that some nucleoid proteins are bifunctional, possibly acting as a sensor of the metabolic state of the cell to regulate mitochondrial nucleoid dynamics. Only recently, an aspect of nucleoid dynamics has been factored into proteomic studies by using a non-radioactive heavy-isotope amino acid labeling approach known as stable isotope labeling with amino acids in cell culture (SILAC) (Bogenhagen et al., 2014). Cells are briefly grown in the presence of heavy-amino acids to label newly synthesized proteins (pulse), and then the labeling medium is removed (chase). Macromolecular complexes were isolated from mitochondria from these cells and labeled proteins were distinguished from non-labeled proteins by mass spectrometry. The SILAC technique helped to reveal that many newly-synthesized nuclear-encoded mitochondrial ribosomal proteins (MRPs) localize to the nucleoid for the initiation of ribosome assembly and then dissociate into ribosomal complexes (see below).

Human mtDNA has an approximately 10-fold higher mutation rate than nuclear DNA (Brown et al., 1979; Wallace and Fan, 2009). Some of the contributing factors to the high rate of

mtDNA mutation include a lack of repair pathways that are present in the nucleus. Mitochondria are capable of short-patch and long-patch base excision repair, and possibly mismatch repair and single-strand break repair, but lack nucleotide excision repair (Bogenhagen, 1999; Kazak et al., 2012; Liu et al., 2008; Mason and Lightowlers, 2003; Mason et al., 2003; Pinz and Bogenhagen, 1998). While yeast and plant mtDNA undergo homologous recombination, the ability to repair double-strand breaks in mammalian mitochondria is still debated.

Mammalian mitochondria only possess one DNA polymerase, DNA Polymerase γ. The fidelity of DNA Polymerase γ is dependent on its proofreading exonuclease domain, which is essential for health, as demonstrated by the "mutator mouse", which has a D257A mutation in the Polymerase γ 3'→5' exonuclease domain. mtDNA in the mutator mouse accumulates a 3- to 5-fold increase in point mutations. These mice present with signs of premature aging, including weight loss, reduced subcutaneous fat, alopecia, extreme spinal curvature, osteoporosis, anemia, reduced fertility, enlarged heart and reduced longevity (Kujoth et al., 2005; Trifunovic et al., 2004). Nonetheless, due to the many copies of mtDNA within cells, cells can be perfectly healthy in a state of heteroplasmy, a condition in which wild-type and mutant mtDNA co-exist. There are about 1,000 to 10,000 mtDNA molecules per somatic cell, and over 100,000 copies in an oocyte (Falkenberg et al., 2007). Mitochondrial nucleoids have been shown to be able to share protein components while faithfully maintaining mtDNA in their respective nucleoids, a concept known as functional complementation (Gilkerson et al., 2008; Jacobs et al., 2000). Thus a subset of mtDNA encoding functional genes can compensate for a percentage of dysfunctional genomes, and thus diseases do not present until a threshold level of heteroplasmy is reached, typically 60-90% (Gardner et al., 2007). Interestingly, cell cultures can survive and grow in the absence of mtDNA (as rho-zero (ρ0) cells) when the culture medium is supplemented with

uridine (Desjardins et al., 1985; King and Attardi, 1989), however, higher eukaryotes cannot survive as an intact organism without functional mtDNA.

The mammalian mitochondrial genome is extremely compact, as demonstrated by the lack of introns or untranslated mRNA regions. Most of the mtDNA-encoded mRNAs require polyadenylation to provide the stop codon. Interestingly, the mitochondrial genome slightly diverges from the "universal" genetic code (Barrell et al., 1980; Barrell et al., 1979); AUA and AUU code for methionine instead of isoleucine, AGA and AGG encodes stop codons instead of arginine, and UGA codes for tryptophan instead of a stop codon. It is unclear why mitochondria utilize a unique genetic code, but the mitochondrial-specific tRNA modifications (see below) contribute to the usage of only 22 tRNAs rather than the full set of 32 required for recognition of the "universal" genetic code.

Mitochondria follow a strict maternal inheritance, although in only one known case, a patient was found to have inherited some paternal mtDNA (Schwartz and Vissing, 2002). Transmission of mtDNA is not yet fully understood, but there appears to be "bottleneck" that operates to permit only a small number of mtDNA molecules to be inherited from the mother. One possible mechanism of the bottleneck is that there is a significant reduction in mtDNA content during early oogenesis, prior to a rapid expansion in mtDNA during oocyte maturation, leading to a random shift in mtDNA mutational load between oocytes (Chinnery and Hudson, 2013). Thus, a mother with a sub-threshold level of mtDNA heteroplasmy may be healthy, but give birth to diseased children (Chinnery and Hudson, 2013). This bottleneck theory helps explain how mutant mtDNA that acquire a replicative advantage are not continuously propagated in the host's lineage in a process called "Muller's ratchet" (Wallace, 2007).

It is proposed that by maintaining a separate genome entirely dedicated to producing energy, mitochondria have allowed the evolution of complexity (Lane and Martin, 2010). It is believed that over an evolutionary timescale, most α-proteobacterial genes have been exported to the nucleus, while the host nuclei also evolved new proteins that bind and package mtDNA (Kucej and Butow, 2007). Eukaryotic cells developed a system to synthesize nuclear-encoded mitochondrial proteins by translating the proteins on cytosolic ribosomes, importing them into mitochondria and sorting to the proper sub-mitochondrial location, as reviewed by (Schmidt et al., 2010). Most matrix proteins are synthesized as pre-proteins with a positively-charged N-terminal mitochondrial localization signal (MLS; mitochondrial targeting sequence (MTS)), which is cleaved upon entry into the matrix. Other mitochondrial proteins have an internal targeting signal that is not cleaved. The process of mitochondrial protein import is dependent on the electrochemical membrane potential, thus defective mitochondria may be culled by starving for an influx of proteins needed for maintenance and biogenesis. It is unknown why mtDNA have retained a specific set of genes and whether or not mtDNA is still undergoing evolution to transfer its genes into the nucleus.

2. Mitochondrial DNA Replication and Transcription

mtDNA replicates independently of the cell cycle and nuclear DNA replication. There are several models of mammalian mtDNA replication (Falkenberg et al., 2007): 1) the strand displacement model (Clayton, 1982, 1991; Robberson et al., 1972), 2) the RNA incorporated throughout the lagging strand (RITOLS) model (Holt and Reyes, 2012), and 3) the strand-coupled model (Holt and Reyes, 2012). The strand displacement model accounts for the high conservation of the non-coding origins of replication, and is discussed below. Transcription is

initiated by a complex of POLRMT, TFAM and TFB2M at one of three promoters: Light-strand promoter (LSP), Heavy-strand promoter 1 (HSP1), or Heavy-strand promoter 2 (HSP2) (Clayton, 2003; Yakubovskaya et al., 2014). Transcripts that initiate at LSP occur upstream of the Origin of heavy strand replication (O_H). LSP transcripts can be synthesized as near full-genome length polycistronic RNA encoding mRNAs and tRNAs, but in some cases terminate at Conserved Sequence Box II (CSBII) (Pham et al., 2006) to generate DNA primers for mtDNA replication. The transcription complex undergoes a polymerase switching event at CSBII, allowing DNA Polymerase γ to elongate the RNA primer. A subset of these DNA-extended RNA primers is terminated at the termination-associated sequence (TAS) to generate 7S DNA, while a small percentage continues past the TAS to replicate the heavy strand. The region of mtDNA encompassing the 7S DNA is called the D-loop, in which the 7S DNA is paired with the light strand and a region of the heavy strand is looped out (Nicholls and Minczuk, 2014). Heavy strand replication proceeds about two-thirds the length of the genome until it encounters the Origin of light strand replication (O_L). At O_L, replication of the light strand begins in the opposite direction while replication of the heavy strand continues to completion. mtDNA replication is assisted by mtSSB, a nucleoid protein that binds to single-strand DNA, Twinkle, the mtDNA helicase, and mtDNA topoisomerases I, IIB and IIIa (Sobek and Boege, 2014).

HSP1 transcripts initiate upstream of the phenylalanine tRNA gene and may be terminated by MTERF1 downstream of the 16S rRNA gene. MTERF1 is proposed to bind to HSP1 and tRNA-Leu (UUR), putting the transcription machinery on a loop known as a "ribomotor" (Guja and Garcia-Diaz, 2012). This is consistent with the much higher levels of mitochondrial rRNAs compared to mRNAs; rRNAs are estimated to be approximately 50-fold more abundant than mRNAs (Terzioglu et al., 2013). Transcripts that initiate from HSP2 begin

upstream of the 12S rRNA gene and generate a near full-genomic length polycistronic RNA. The polycistronic RNAs are then processed and modified, as described below. RNA is not significantly imported into or exported from mammalian mitochondria, although PNPase was reported to mediate RNA import (Wang et al., 2010; Wang et al., 2012).

3. RNA Processing and Modifications

a. RNase P and RNase Z cleave at tRNA junctions in polycistronic transcripts

At the same time the human mitochondrial genome was sequenced by the Sanger method (Anderson et al., 1981), the mRNAs were also characterized (Montoya et al., 1981). The 5' ends of most mRNAs either begin with a start codon or very proximal to a start codon, and are immediately flanked by tRNAs (Montoya et al., 1981) (Fig. 1). Mitochondrial transcripts synthesized from the heavy strand and the light strand are polycistronic precursors, and the rRNAs and all but two stretches of mRNAs are separated by tRNAs. It was therefore proposed that RNase P and RNase Z (ELAC2) are endonucleases that recognize the secondary structure of tRNAs within the nascent polycistronic messages and cleave at their 5' and 3' ends, respectively, to separate the individual tRNAs from rRNAs and mRNAs. This RNA processing mechanism is also known as the "tRNA punctuation" model (Battey and Clayton, 1980; Ojala et al., 1980; Ojala et al., 1981) (**Fig 2**). The RNases cleave sequentially; RNase P cleavage occurs prior to RNase Z cleavage (Manam and Van Tuyle, 1987; Rossmanith et al., 1995). Data supporting the model that processing occurs on nascent RNA synthesized from the nucleoid has recently been provided by the co-localization of RNase P and RNase Z to mitochondrial nucleoids (Bogenhagen et al., 2014).

RNase P was first discovered in bacteria as a protein-RNA complex in which the catalytic activity was attributed to its RNA component (Guerrier-Takada et al., 1983). In the human nucleus, RNase P is found to be a protein-RNA complex consisting of at least ten protein subunits serving to process precursor tRNAs (Jarrous, 2002). An RNA-free RNase P was identified in human mitochondria and an active complex consisting of three proteins, MRPP1, MRPP2 and MRPP3, was reconstituted *in vitro* (Holzmann et al., 2008). In addition to its role in RNA processing, MRPP1 was found to have methyltransferase activity at m^1G9 and m^1A9 positions on tRNA (Vilardo et al., 2012). MRPP2 is multi-functional protein with broad substrate specificity and is also known as hydroxysteroid (17-β) dehydrogenase 10 (HSD17B10), amyloid-beta binding alcohol dehydrogenase (ABAD) or Type II 3-hydroxyacyl-CoA dehydrogenase (HADH2), among other names. Due to its ability to bind amyloid-beta, MRPP2 was implicated in Alzheimer's disease, but recent data shows that this is not the case (Vilardo and Rossmanith, 2013). A missense mutation in MRPP3 was recently described as a nuclear genetic determinant of mitochondrial tRNA modification and accounts for about 22% of the variance in mitochondrial RNA sequences within and among individual blood cells (Hodgkinson et al., 2014). RNase Z (ELAC2) mutations have been found to be associated with hypertrophic cardiomyopathy due to defective RNA processing (Haack et al., 2013), as well as pathogenesis-related mutations in tRNA genes that affect 3' end processing (Levinger et al., 2004a; Levinger et al., 2004b; Levinger and Serjanov, 2012; Yan et al., 2006), highlighting the importance of separating the individual messages from precursor transcripts for proper mitochondrial translation. Recently, GRSF1 was described to interact with RNase P in distinct foci and mediate its tRNA 5' end processing activity and the subsequent dispersal of the RNA (Jourdain et al., 2013), however the functions of GRSF1 are contentious (Antonicka et al., 2013) (see below).

b. mRNA Polyadenylation

In comparison to mitochondrial tRNAs and rRNAs, which undergo various base-specific nucleotide modifications (see below), mitochondrial mRNA only have one type of modification, polyadenylation, which affects the mRNA stability. Unlike yeast mtDNA, the mammalian mitochondrial genome is extremely concise, as demonstrated by the lack of intronic sequences in mRNAs as well as the lack of 5' and 3' untranslated regions (UTRs), with minor exceptions (Montoya et al., 1981; Temperley et al., 2010b). It is noteworthy that mammalian mtDNA is so compact that 7 of the 11 mRNAs (two remain polycistronic after RNA cleavage) are not encoded with stop codons, but require polyadenylation to provide the final A residue(s) in the termination codon (Chang and Tong, 2012; Gagliardi et al., 2004; Rackham et al., 2012; Temperley et al., 2010b). Mitochondrial polyadenylation is mediated by hmtPAP, which surprisingly does not appear to have bacterial origins, but is rather similar to the cytosolic PAPs (Rorbach and Minczuk, 2012). 10 of the 11 mitochondrial transcripts are polyadenylated, and the length of polyadenylation can vary among cell types and even within a cell (Rackham et al., 2012; Rorbach and Minczuk, 2012), but in human cells, they are predominantly about 45 nucleotides long (Rackham et al., 2012; Rorbach and Minczuk, 2012; Temperley et al., 2010b). ND6 is the only mitochondrial mRNA that is not polyadenylated. The role of polyadenylation besides completion of stop codons is unclear, as changes in polyadenylation can increase or decrease the stability of certain messages (Gagliardi et al., 2004; Rorbach and Minczuk, 2012). Since polyadenylation is a determinant of transcript stability, it is difficult to determine whether polyadenylation has a direct role in mediating mitochondrial translation.

Mammalian mitochondrial mRNAs are also unique in that they lack the 5' 7-methylguanosine cap present on cytosolic mRNAs and do not completely follow the universal genetic code. Interestingly, AUG, AUA and AUU serve as initiation codons, while only one $tRNA^{Met}$ gene is encoded by mtDNA. Thus, the initiator Met-$tRNA^{Met}$ must be formylated by MTFMT (Tucker et al., 2011) and the unmodified $tRNA^{Met}$ is used during translation elongation. Another unique feature of mitochondrial mRNAs is that COXI and ND6 form secondary structures to initiate a -1 frameshifting event, thereby allowing recognition of their stop codons, AGA and AGG, respectively, by the translation termination factor mtRF-1a (Lightowlers and Chrzanowska-Lightowlers, 2010; Richter et al., 2010a; Temperley et al., 2010a).

c. tRNA Modifications

The tRNAs found in bacteria and eukaryotic cytosol (Type 0 tRNAs) have a canonical cloverleaf secondary structure, characterized from the 5' to 3' direction of the tRNA by an acceptor stem, D-stem, D-loop (not to be confused with the mtDNA D-loop), anticodon stem, anticodon loop, extra loop, T-stem, T-loop, and CCA terminus. In contrast, mitochondrial tRNAs have three forms of non-canonical tRNAs: Type I, which have a shortened D-loop and shortened extra loop, Type II, which have variable length and sequence in their D-loop and T-loop, and Type III, which lacks the D-loop (Suzuki and Nagao, 2011b). Mitochondrial tRNAs have a lower melting temperature than canonical tRNAs and therefore their post-transcriptional modifications are likely necessary to assist in their folding and stability. Fifteen species of modified nucleosides have been identified on 118 positions on mitochondrial tRNAs, three of which are specific to mitochondria: 5-formylcytidine (f^5C), 5-taurinomethyluridine (τm^5U) and 5-taurinomethyl-2-thiouridine (τm^5s^2U) (Suzuki, 2014; Suzuki and Nagao, 2011b). The other

tRNA modifications include base methylation and pseudouridylation. Mitochondrial tRNAs lack 2'-O-methylation, which is found on bacterial tRNAs and the mammalian mitochondrial large ribosomal subunit rRNA.

The wobble position nucleosides of mitochondrial tRNAs are: 1) f^5C, 2) queuosine (Q), 3) taurine-containing uridines and 4) unmodified guanosine or uridine. f^5C at the wobble position is required to recognize the AUA and AUG codons, while Q and unmodified guanosine allow detection of pyrimidine-ending codons, and unmodified uridine recognizes all four of the nucleosides in the opposing codon. The expansion of modified nucleosides at the wobble position in mitochondria allows broad specificity and decoding of 60 different sense codons by using only 22 tRNAs, in contrast to the minimal set of 32 tRNAs required for the standard genetic code (Suzuki and Nagao, 2011b). Similarly to the canonical tRNAs, the 3' termini of mitochondrial tRNAs undergo CCA addition by TRNT1, allowing for aminoacylation (Nagaike et al., 2001). Aminoacyl-tRNA synthetases may recognize the relatively truncated mitochondrial tRNAs by utilizing their N-terminal distal helix as a compensation mechanism (Watanabe, 2010). Approximately half of the 400 identified pathogenic mutations in mitochondrial disease are located on mitochondrial tRNA genes (Suzuki, 2014) and mutations that affect RNA processing are known to be pathogenic (Levinger et al., 2004a; Levinger et al., 2004b; Levinger and Serjanov, 2012). The lack of taurine modifications in tRNAs is also known to cause diseases such as MELAS and MERRF (Suzuki and Nagao, 2011a), again highlighting the importance of mitochondrial translation.

d. rRNA Modifications

The mitochondrial-encoded 12S (954 nt) and 16S (1,558 nt) rRNAs are components of the small and large ribosomal subunits, respectively. Baer and Dubin identified the mammalian mitochondrial rRNA methylation sites by double radioactive labeling of BHK-21 hamster cells with $^{32}P_i$ and [methyl-^{3}H] methionine, which label all nucleotides and only methylated nucleotides, respectively, followed by purification of mitochondrial rRNA and RNA fingerprinting (Baer and Dubin, 1981). The predicted secondary structure of the 12S and 16S rRNAs with identified modification sites are shown in **Fig 3**. All five of the mitochondrial rRNA base methylations are found on 12S rRNA, while 16S rRNA has only three 2'-O-ribose methylation sites and one pseudouridylation site (Baer and Dubin, 1981; Rorbach and Minczuk, 2012) (**Table 1**). In addition to supporting ribosomal function, rRNA modifications may be crucial for ribosome assembly and/or stability (Decatur and Fournier, 2002). The 2'-O-ribose methylations may serve to support RNA folding, RNA secondary structure and/or recognition by proteins (Decatur and Fournier, 2002; Motorin and Helm, 2011). Similar to mammalian mitochondria, the most common modifications in yeast and human cytosolic rRNAs are 2'-O-ribose methylations and pseudouridylations (Table 2). Surprisingly, the modifications of mammalian mitochondrial rRNA are in stark contrast to those of bacterial rRNA, which are predominantly base methylations and only few are 2'-O-ribose methylations.

Four of the five base methylations on mammalian mitochondrial 12S rRNA have been assigned to corresponding methyltransferases. TFB1M, the mammalian homologue of bacterial KsgA, is responsible for the dimethylation of two adjacent adenosines $m^6{}_2A^{936}$ and $m^6{}_2A^{937}$, as demonstrated by primer extension assays with reverse transcriptase (Seidel-Rogol et al., 2003), while NSUN4 is responsible for m^5C^{841}, as demonstrated by bisulfite sequencing (Metodiev et al., 2014). TFB1M and NSUN4 are necessary for embryonic development in mice, as genetic

deletion of these genes causes embryonic lethality at approximately 8.5 days (Metodiev et al., 2009; Metodiev et al., 2014). Mice with a heart-specific knockout of either TFB1M or NSUN4 mediated by cre recombinase driven by the Ckmm promoter are born, but develop mitochondrial cardiomyopathy. Heart-specific depletion of TFB1M caused decreased 12S rRNA stability and impaired assembly of the small mitoribosomal subunit, with an apparent increase in the LSU (Metodiev et al., 2009). Interestingly, heart-specific depletion of NSUN4 leads to increased levels of 12S rRNA and accumulation of both small and large mitoribosomal subunits at the expense of the complete monosome (Metodiev et al., 2014). Upregulation of 12S rRNA and ribosomal subunits may be a compensation response mechanism for the lack of functional monosomes. The activity of TFB1M may be regulated, since patients who are susceptible to aminoglycoside-induced deafness carry an A1555G mutation in the 12S rRNA gene, which causes TFB1M-mediated hypermethylation of its substrate adenosine residues. Hypermethylation of 12S rRNA leads to subsequent ROS-dependent AMPK signaling to E2F1 and apoptosis of hair cells in the ear (Raimundo et al., 2012).

Studies on catalytic-inactive mutations of methyltransferases are informative. A catalytic mutant of Dim1p, the yeast cytosolic homologue of TFB1M, was generated and revealed that Dim1p has an essential methyltransferase-independent role in pre-rRNA processing that is sufficient to support normal growth (Lafontaine et al., 1998). The catalytic activity of TFB1M is crucial for mitochondrial function, as demonstrated by overexpressing a methyltransferase-deficient TFB1M carrying the point mutation G65A in HeLa cells (Cotney et al., 2009). TFB2M is also believed to have methyltransferase activity that overlaps with that of TFB1M, but cells overexpressing a G105A point mutation in the catalytic site did not reveal any obvious deleterious phenotypes (Cotney et al., 2009), consistent with a much more significant role of

TFB2M in initiation of transcription (Falkenberg et al., 2007). Catalytically-inactive mutant methyltransferases are informative in the context of ribosome assembly as discussed below.

The 2'-O-ribose methylation sites on 16S rRNA are Gm^{1145}, Um^{1369} and Gm^{1370}. The Gm^{1145} and Um^{1369} methylations and corresponding methyltransferases are conserved in evolution, as the corresponding sites on bacterial and yeast mitochondrial rRNA are methylated by RlmB (bacteria) or Pet56p / MRM1 (yeast mitochondria), and RrmJ (bacteria) or FtsJ2 / MRM2 (yeast mitochondria), respectively (Caldas et al., 2000a; Lovgren and Wikstrom, 2001; Pintard et al., 2002; Sirum-Connolly et al., 1995). The Gm^{1370} methylation site and its corresponding methyltransferase, RNMTL1, are novel and apparently restricted to higher eukaryotes (Lee et al., 2013), although the corresponding residue in yeast cytosolic rRNA, Gm^{2918}, is also 2'-O-methylated (Decatur and Fournier, 2002; Rorbach et al., 2014). RNMTL1 has recently been referred to as MRM3 (Rorbach et al., 2014). The sole pseudouridylation site on 16S rRNA, Ψ^{1397}, was identified by CMC modification of RNA followed by incubation in basic conditions and a reverse-transcriptase-based primer extension assay (Ofengand and Bakin, 1997). The data presented in this thesis supports the assignment of MRM1, MRM2 and RNMTL1 to the methylation of G^{1145}, U^{1369} and G^{1370}, respectively (Lee and Bogenhagen, 2014; Lee et al., 2013), which is consistent with data presented by Rorbach, et al (Rorbach et al., 2014). While an indirect mechanism of rRNA methylation has not yet been excluded, mitochondrial rRNA methyltransferases likely resemble bacterial stand-alone proteins that recognize and methylate a specific target site, rather than nuclear snoRNP complexes that utilize a guide RNA strand to methylate nucleo-cytosolic rRNAs, as no guide RNAs have been identified in mammalian mitochondria (Decatur and Fournier, 2002; Motorin and Helm, 2011).

The 2'-O-ribose methylation sites on 16S rRNA are localized to regions participating in the peptidyl transferase center (PTC) of the mitoribosome, indicating a role for these modifications in the catalytic function of the rRNA. Based on the high-resolution crystal structures of bacterial and archaeal ribosomes, the conserved sites corresponding to mammalian mitochondrial Gm^{1145} and Um^{1369} are expected to fold into the P-loop and A-loop, respectively, and the modified nucleotides are in close contact or directly interact with the 3'- end of tRNAs in the P- and A-sites of the ribosome (Blanchard and Puglisi, 2001; Decatur and Fournier, 2002). Since Gm^{1370} is adjacent to Um^{1369}, it is also expected to fold into the A-loop. Thus, all three modified nucleotides are likely involved in catalyzing the transfer of the elongating peptide from the P-site tRNA onto the A-site aminoacyl tRNA. This is consistent with the observation that RNA is the catalytic component of bacterial ribosomes (Cech, 2000; Steitz and Moore, 2003). In addition to methylation and pseudouridylation, 12S and 16S rRNAs are oligoadenylated (Mercer et al., 2011).

C. Post-transcriptional Regulation of Mitochondrial RNA

Post-transcriptional regulation of mitochondrial transcripts is extremely important for mitochondrial function as mitochondria are dynamic organelles and must regulate the expression of their genes in response to signals and their environment. Mitochondrial RNA decay is perhaps equally important to RNA synthesis, processing and modifications. Since transcripts are nearly full-genomic length, non-coding RNAs may anneal to and inhibit the function of coding RNAs, consistent with the finding of long, non-coding RNAs and small RNAs derived from tRNA genes in mitochondria (Mercer et al., 2011; Rackham et al., 2011). Mitochondrial mRNA half-life ranges from 25 minutes to almost 4 hours (Gelfand and Attardi, 1981; Nagao et al., 2008),

while rRNA half-life ranges from 2.5 to 3.5 hours (Gelfand and Attardi, 1981). Despite the estimated abundance of rRNAs existing as 50 times greater than the other transcripts, one report found 16S rRNA to exist at twice the abundance of 12S rRNA, suggesting a yet finer mechanism of transcript regulation (Mercer et al., 2011). There is also an unexplained discrepancy in the amount of rRNAs produced per rRNA gene in mitochondria compared to the cytosol, known as the "copy number paradox". The ratio of rRNA produced per rRNA gene is approximately 100 times greater for cytosolic rRNAs than mitochondrial rRNAs (Attardi and Schatz, 1988; Bai et al., 2000). The suggestion that ND5 mRNA expression tightly regulates mitochondrial respiration highlights the importance of maintaining appropriate RNA levels (Bai et al., 2000).

As mentioned above, polyadenylation may affect transcript stability but the mechanism and pattern is unclear (Slomovic et al., 2005). Mitochondrial proteins that participate in post-transcriptional regulation include the LRPPRC/SLIRP complex, which has multiple roles on regulating RNA and is disrupted in a French-Canadian subtype of Leigh's syndrome (Chujo et al., 2012; Mootha et al., 2003; Ruzzenente et al., 2012; Sasarman et al., 2010; Xu et al., 2004), C1qR (p32), which binds to all mitochondrial mRNAs and affects their translation (Yagi et al., 2012), PDE12, which removes 3' terminal polyA tails (Rorbach et al., 2011), PTCD1, which is inversely related to levels of leucine tRNA (Lightowlers and Chrzanowska-Lightowlers, 2008, 2013; Rackham et al., 2009; Sanchez et al., 2011), PTCD2, which promotes processing of ND5-Cytb transcripts (Xu et al., 2008) and GRSF1, which may have a role in precursor RNA processing or localization of transcripts into ribosomal particles (Antonicka et al., 2013; Jourdain et al., 2013). GRSF1 was found to bind nascent transcripts and siRNA-mediated knockdown in mammalian cells led to changes in abundance of some mitochondrial messages (Antonicka et al., 2013), suggesting a role in the stabilization of RNA. GRSF1 is also suggested to have a role in

mitochondrial translation and/or ribosome assembly (Jourdain et al., 2013). Mitochondrial RNases that may be involved in RNA turnover include the PNPase-SUV3 complex, which forms "degradation-foci" (D-foci) (Borowski et al., 2013; Chen et al., 2006; Portnoy et al., 2008; Wang et al., 2014a; Wang et al., 2009), REXO2, a 3'→5' exoribonuclease and RNase L (Rorbach and Minczuk, 2012). A human genomic analysis of 107 putative mitochondrial RNA binding proteins was conducted and implicated FASTKD4 functioning in the stability of a subset of mRNAs (Wolf and Mootha, 2014). Nuclear-encoded RNAs were found in mitochondria at low abundance, but it is possible that these are contaminants bound on the outside of mitochondria, despite the use of RNase in the mitochondrial isolation procedure (Mercer et al., 2011).

D. Mitochondrial Ribosomes and Translation

1. General Properties of Mammalian Mitochondrial Ribosomes (Mitoribosomes)

The earliest study to show that mammalian mitochondria synthesized their own proteins was by McLean and others in the Simpson lab in 1958, whereby radioactively labeled amino acids were incorporated into rat muscle and liver mitochondria in an ATP-dependent manner (McLean et al., 1958). At the time, the field was highly skeptical of mitochondrial translation, due to the much greater abundance of cytosolic ribosomes or the possibility of bacterial contamination. This important discovery was further advanced when O'Brien and Kalf isolated mammalian mitoribosomes and began to characterize them, first from rat livers (O'Brien and Kalf, 1967a, b), and then from cows, pigs and rabbits (O'Brien, 1971). The isolation of mitoribosomes was made possible by improvements in differential centrifugation techniques of cell lysates and buffers that maintain ribosome stability. Within this time period, the Schatz

group provided evidence that yeast mitochondria also synthesized their own proteins, separately from cytosolic translation machinery (Schatz, 1997).

Isolation of mitoribosomes provided a means of studying their protein constituents and structure, especially as technology improved. Proteomic studies have identified most, if not all of the MRPs (Goldschmidt-Reisin et al., 1998; Graack et al., 1999; Koc et al., 2001a; Koc et al., 2001b; Koc et al., 2013; O'Brien et al., 1999; O'Brien et al., 2000; Suzuki et al., 2001a), while cryo-EM studies provided single-digit Angstrom-resolution models of the mitoribosome (Agrawal and Sharma, 2012; Greber et al., 2014; Kaushal et al., 2014; Mears et al., 2006; Sharma et al., 2003). Mammalian mitoribosomes are often compared to bacterial ribosomes because of the wealth of knowledge on the latter and the ancestral relationship between the two. Mitoribosomes are similar in size to their prokaryotic counterparts at about 2.6 mega-Daltons. The organization of the rRNA secondary structure into six domains is conserved, as well as approximately half of the ribosomal proteins. However, mitoribosomes are composed of approximately two-thirds protein by mass and one-third rRNA, while the inverse is true of bacterial ribosomes, making mitoribosomes less dense. Mitochondria have evolved shorter rRNAs by truncating a number of helices and have expanded their protein repertoire (Koc et al., 2010). In addition to mitoribosomes having ribosomal proteins that lack homologues in bacteria, MRPs that have ancestral counterparts often have N- and C-terminal extensions compared to the bacterial proteins. It was originally proposed that the increased number and size of MRPs would structurally compensate for the shortened rRNA regions (O'Brien, 2002; Suzuki et al., 2001b), but cryo-EM studies show that only approximately 20% of the “missing” rRNA is replaced by protein. Many of the mitochondrial-specific proteins occupy new positions on the mitoribosome, which may be necessary to accommodate the unique features of mitochondrial translation,

including the non-universal genetic code, unique tRNAs and leaderless, uncapped mRNAs. Deproteinized bacterial rRNA has been shown to possess catalytic activity. This is supported by the lack of protein density at the catalytic region of the peptidyltransferase center and the resistance to translation-targeting antibiotics afforded by certain rRNA mutations (Cech, 2000; Noller, 1991; Steitz and Moore, 2003). Although mitochondrial rRNAs are much less extensively modified than bacterial rRNAs, most of the remaining modifications occur at conserved sites presumably important for ribosome assembly and/or function (see below).

The complete mammalian mitoribosome (55S; monosome) consists of a small subunit (28S; SSU) and a large subunit (39S; LSU). The SSU is a complex of 12S rRNA and approximately 31 MRPs, containing the decoding center that recognizes the 5' ends of mRNAs during translation initiation. The LSU is a complex of 16S rRNA and approximately 51 MRPs, containing the peptidyltransferase center that catalyzes the transfer of the elongating peptide chain in the P-site to the incoming aminoacyl-tRNA in the A-site. Mitoribosome components are known to vary across different tissues (Pagliarini et al., 2008; Vafai and Mootha, 2012), and possibly even within cells, as MRPS18, a member of the SSU, is expressed in three different isoforms (Koc et al., 2001a). Mitoribosomes are completely dedicated to synthesizing thirteen protein subunits of the respiratory complexes to ultimately produce energy for the cell in the form of ATP. However additional roles of individual MRPs have been suggested (Koc et al., 2013; Koc et al., 2001c; Rackham and Filipovska, 2014). MRPS29, a GTPase also known as Death-Associated Protein 3 (DAP3) and MRPS30 (PDCD9) may be linked to roles in apoptosis (Kissil et al., 1999; Miyazaki et al., 2004; Sun et al., 1998; Tang et al., 2009). Some newer members of the mitoribosome may possess extra-ribosomal activities as well. MRPS39 (AURKAIP1) was first identified as a protein that binds to and regulates the activity of Aurora-A

Kinase 1 (Koc et al., 2013). MRPL38 (ICT1) has been characterized as a peptidyl-tRNA hydrolase that releases stalled ribosomes (Richter et al., 2010b). MRPL59 (CRIF1) functions to insert mitochondrial-synthesized OXPHOS subunits into the IMM (Kim et al., 2012), consistent with the close association of mitoribosomes with the IMM (Christian and Spremulli, 2010; Haque et al., 2010a; Haque et al., 2010b; Liu and Spremulli, 2000; Smits et al., 2010). Several non-ribosomal proteins co-sediment with ribosomal complexes in gradients and function in mitoribosome assembly (see below), yet interestingly proteomic studies have not identified them as MRPs, indicating that they may exist in a sub-stoichiometric abundance, have a dynamic association with the ribosome and/or will eventually be assigned as MRPs as with AURKAIP1, ICT1 and CRIF1, under the proposed guidelines (Koc et al., 2013). Mutations in MRPs and rRNAs (DiMauro and Schon, 2003; Galmiche et al., 2011; Haque et al., 2008; Miller et al., 2004; O'Brien et al., 2005; Papapetropoulos et al., 2006; Saada et al., 2007; Scheper et al., 2007) lead to severe disease phenotypes, emphasizing the importance of mitoribosome function.

2. Mitochondrial Translation

The process of mitoribosome translation is reviewed by several authors (Christian and Spremulli, 2012; Chrzanowska-Lightowlers et al., 2011; Kuzmenko et al., 2014; Smits et al., 2010; Watanabe, 2010). Mammalian mitoribosomes have evolved to preferentially recognize leaderless mRNA (Christian and Spremulli, 2010), as is the case for most mitochondrial transcripts. Currently, TACO1 is the only known translational activator in mammalian mitochondria (Weraarpachai et al., 2009). Several factors are known to be involved in the assembly of electron transport chain complexes: C12orf62 (COX14) (Weraarpachai et al., 2012), SURF1 (Zhu et al., 1998), c20orf7 (Sugiana et al., 2008), hCOA3 (Clemente et al., 2013),

FAM36A (Szklarczyk et al., 2013), CRIF1 (Kim et al., 2012) and the MITRAC complexes (Mick et al., 2012). Since all mtDNA-encoded products are hydrophobic core components of ETC complexes, it is also likely that translation is coupled to insertion of the proteins into the inner mitochondrial membrane. The mitoribosomal LSU may directly interact with the C-terminal tail of OXA1L to dock at the IMM and insert its newly synthesized protein into the IMM (Haque et al., 2010a; Haque et al., 2010b; Lightowlers et al., 2014; Liu and Spremulli, 2000). Alternatively, MRPL45 at the polypeptide exit tunnel of the mitoribosome may allow direct docking at the IMM and alignment of the polypeptide exit tunnel with OXA1L (Greber et al., 2014). Thus all of the molecular genetic processes in mitochondria appeared to be highly coordinated in a chain of events (**Frontispiece figure**). Mitochondrial translation may also dictate RNA and ribosome stability. In one case of a pathogenic mtDNA microdeletion, mRNA lacking a stop codon undergoes translation-dependent deadenylation and RNA decay (Temperley et al., 2003). Additionally, actinonin, an inhibitor of human peptide deformylase in mitochondria, induces mitoribosome stalling, initiating a ribosome and RNA decay pathway (Richter et al., 2013).

3. Mitochondrial Ribosome Assembly

The assembly of bacterial large and small ribosomal subunits has been completely reconstituted *in vitro* from its individual proteins and RNAs purified from bacterial cells, without accessory proteins or assembly factors. This culminated in the generation of the Nomura maps and classification of the ribosomal proteins as primary, secondary or tertiary RNA binding (Nomura, 1973; Nomura and Erdmann, 1970; Shajani et al., 2011). Reconstitution of bacterial ribosomes has also been successful with *in vitro*-synthesized unmodified RNA (Krzyzosiak et

al., 1987). Such an amazing feat has not been accomplished with mitoribosomes, largely due to the limited amounts of starting material and the complexity of mitoribosome assembly. Nevertheless, the kinetics of bacterial ribosome assembly is greatly enhanced by accessory factors. Bacterial ribosome assembly involves co-transcriptional rRNA processing and coordinated steps of rRNA folding (Woodson, 2008, 2011), rRNA modifications and protein-binding events that continually stabilize the complex, and these mechanisms are expected to be conserved in mitoribosome assembly. Many of the suspected mitochondrial ribosome assembly proteins are thought to resemble bacterial homologues. RNA chaperones, protein chaperones and GTPases are all crucial in the assembly process, thus ribosome assembly is an energy-demanding process. The requirement of GTPases suggests that the energetic state of the cell can dictate mitoribosome assembly based on the available amount of GTP. Mammalian mitoribosomes are unique in that they possess intrinsic GTPase activity, attributed to MRPS29 (DAP3), a cell death-associated protein that lacks a bacterial equivalent. It is unknown whether its GTPase activity contributes to mitoribosome assembly or function.

a. rRNA Methyltransferases Function in Ribosome Assembly

rRNA methyltransferases are a class of proteins that have significant roles in ribosome assembly and typically utilize S-adenosyl methionine (AdoMet, SAM) as the methyl donor substrate. Some rRNA methyltransferases have methyltransferase-independent roles in ribosome assembly, as demonstrated by catalytically-inactive mutants of bacterial KsgA (Connolly et al., 2008), yeast cytosolic Dim1p (Lafontaine et al., 1998) and yeast Pet56p (Lovgren and Wikstrom, 2001) can still support ribosome formation. Inactivation of the small ribosomal subunit rRNA methyltransferase KsgA in bacteria is non-lethal and provides resistance to the antibiotic

kasugamycin. Surprisingly, overexpression of catalytically-inactive KsgA in a KsgA-deleted background is deleterious. In strains lacking functional KsgA, intermediates in SSU assembly accumulate along with precursor rRNA (Connolly et al., 2008). Deletion of the mammalian homologue of KsgA in mice, TFB1M, is embryonic lethal, while a heart-specific TFB1M knockout leads to mitochondrial cardiomyopathy wherein SSU and monosome assembly is severely inhibited (Metodiev et al., 2009). In addition to the role of POLRMT in transcription and primer synthesis in TFB2M-containing complexes, POLRMT associates with TFB1M to enhance its rRNA methyltransferase activity and promote SSU and monosome assembly (Surovtseva and Shadel, 2013).

Surprisingly, depletion of NSUN4, a 12S rRNA methyltransferase, in mice, significantly increased SSU and LSU levels, but also depleted the steady state level of monosomes (Metodiev et al., 2014). NSUN4 exists as a stoichiometric complex with MTERF4. MTERF4 directs the complex to the LSU, promoting LSU assembly, while NSUN4 methyltransferase activity is specific for the SSU 12S rRNA (Camara et al., 2011; Metodiev et al., 2014; Spahr et al., 2012; Yakubovskaya et al., 2012). Thus, the MTERF4-NSUN4 complex most likely bridges the large and small subunits together to encourage monosome formation. Heart-specific knockout of MTERF4 in mice leads to embryonic lethality and a similar ribosomal phenotype as knockout of NSUN4, as there is an apparent upregulation of the individual ribosomal subunits but no corresponding increase in the levels of monosomes (Camara et al., 2011).

RlmB, the bacterial homologue of mammalian rRNA methyltransferase MRM1, is not necessary for ribosome assembly, as deletion of RlmB showed no altered ribosome sedimentation properties (Lovgren and Wikstrom, 2001). Deletion of the yeast homologue, Pet56p, causes a defect in the assembly of the LSU (Sirum-Connolly et al., 1995), however

Pet56p variants with mutations in the SAM-binding pocket that abolish methyltransferase activity were still able to support ribosome biogenesis *in vivo* (Lovgren and Wikstrom, 2001).

Deletion of RrmJ (FtsJ), the bacterial homologue of mammalian FtsJ2 (MRM2), leads to accumulation of the SSU and LSU at the expense of monosome abundance (Caldas et al., 2000b). RrmJ and MRM2 are rRNA methyltransferases that are active on LSU particles or intermediates of the LSU assembly, but not on free rRNA in bacteria (Caldas et al., 2000a) and yeast mitochondria (Pintard et al., 2002), respectively. Site-specific mutations in the substrate RNA-binding site or mutations that inactivate the methyltransferase activity independent of AdoMet-binding in RrmJ precludes the rescue of the ribosome assembly defect in RrmJ-deficient strains (Hager et al., 2002; Hager et al., 2004). After the acceptance of our first manuscript and during the review of our second manuscript, there was evidence that knockdown of MRM2 and RNMTL1 disrupts mitoribosome levels (Rorbach et al., 2014). It will be of interest to identify and study catalytically inactive mitochondrial 2'-O-ribose rRNA methyltransferase mutants. It is unclear whether all of the rRNA modifications will suffice for ribosome assembly or whether the methyltransferases have roles in the assembly process independent of or in addition to RNA modification.

b. GTPases Function in Ribosome Assembly

GTPases are another class of proteins important for ribosome assembly. In bacteria, some of the ribosome assembly GTPases (RA-GTPases) function in the assembly of either the SSU or LSU, and others function in the assembly of monosomes, while some may even have additional roles in non-ribosomal processes such as DNA replication and segregation, stress response, cell growth, cell division and cell morphology (Britton, 2009; Goto et al., 2013). The exact

mechanisms by which RA-GTPases function is unclear, but they are likely to recruit other assembly factors or to directly alter the RNA structure through RNA-binding events. Since GTPases utilize the high-energy molecule GTP, ribosome assembly can be regulated by the energetic status of mitochondria and the amount of nutrients in the extra-cellular environment. RA-GTPases may serve as checkpoints in the assembly process by loading or unloading proteins. Bacteria are remarkable for their ability to suppress temperature-sensitive RA-GTPase mutants or deficiencies by overexpressing compensatory proteins.

Currently, two GTPases are known to have roles in the assembly of the SSU: ERAL1 and MTG3 (Table 3). ERAL1, the mammalian mitochondrial homologue of bacterial Era, binds to a region of 12S rRNA encompassing the adenosines subject to TFB1M-mediated dimethylation and is suggested to assist the folding of the RNA (Dennerlein et al., 2010; Uchiumi et al., 2010). Era may not directly participate in bacterial ribosome assembly, but it is proposed to bind to the SSU at the subunit interface, blocking monosome formation until a signal abrogates this effect, thus serving as a checkpoint in the assembly process (Shajani et al., 2011). Era is also believed to have an extra-ribosomal function in regulating cell division, although ERAL1 is not known to function in cell division in human cells. siRNA-mediated depletion of ERAL1 severely reduced mitochondrial SSU and LSU levels (Uchiumi et al., 2010), causing a translation defect.

Depletion of YqeH in bacteria depletes SSU levels and leads to the accumulation of aberrant small subunit rRNAs, without affecting the levels of LSU (Britton, 2009). Depletion of MTG3, the yeast homologue of YqeH (MTG3 / hNOA1 / C4orf14 in humans), leads to a severe decrease in mitochondrial translation and depletion of mitoribosomes, consistent with decreased rRNA levels and accumulation of a precursor SSU rRNA species, indicating a link between ribosome formation and rRNA processing (Paul et al., 2012) . Overexpression of a large

ribosomal subunit protein MRPL4 partially rescues the MTG3 deficiency. Similarly, MTG3 in mammalian mitochondria is associated with the SSU via a GTP-dependent manner and is important for translation (He et al., 2012a; Kolanczyk et al., 2011). Inactivation of MTG3 in mice depletes monosome levels and thus is embryonic lethal (Kolanczyk et al., 2011). MTG3 can bind to DNA and RNA containing G-quadruplexes, possibly indicating an extra-ribosomal role in maintaining mtDNA and/or transcript levels (Al-Furoukh et al., 2013).

Two GTPases have been implicated in LSU assembly: MTG1 and MTG2. MTG1 (RbgA in bacteria, Mtg1p in yeast mitochondria) was first identified in a yeast screen for proteins that affect mitochondrial translation but are not directly involved in processes such as initiation, elongation or termination (Barrientos et al., 2003). A deficiency of RbgA in bacteria leads to reduced monosome levels and impaired LSU assembly, as an LSU intermediate accumulated. This LSU intermediate was deficient in ribosomal proteins that are crucial for the structure and function of the PTC (Britton, 2009). RbgA binds to the LSU rRNA near the A-site and P-site in both intermediate and fully assembled LSU stages. Yeast mutants with Mtg1p deficiency maintained mitochondrial rRNA expression and processing, but have a mitochondrial translation defect, as shown by radioactive pulse labeling (Barrientos et al., 2003). These mutants were partially rescued by expression of the human MTG1 gene or by mutating their LSU rRNA in Domain V, a region involved in the PTC. While yeast Mtg1p was found not to co-localize with mitoribosomes, human MTG1 was found associated with the LSU in a GTP-dependent manner (Barrientos et al., 2003; Kotani et al., 2013). Knockdown of MTG1 in HeLa cells did not significantly alter mitochondrial rRNA levels, but significantly decreased protein synthesis. The recombinant human MTG1 has no detectable intrinsic GTPase activity until stimulated by the presence of LSU or monosome particles (Kotani et al., 2013). It remains to be determined

whether MTG1 impacts ribosome assembly in yeast and mammalian mitochondria as it does in bacteria. Without a known mechanistic basis, the depletion of MTG1 was associated with an increase of all mitochondrial-encoded mRNAs except ND5 (Wolf and Mootha, 2014).

ObgE in bacteria (Mtg2p in yeast mitochondria, MTG2 or ObgH1 in mammalian mitochondria) also has both ribosome-assembly and extra-ribosomal functions, including the general stress response, sporulation, chromosome segregation and chromosome replication (Britton, 2009). Bacterial ObgE was found to interact with ribosomal protein L13 and to sustain monosome levels. A lack of ObgE leads to accumulation of the individual ribosomal subunits and an aberrant pattern of LSU sedimentation. Yeast Mtg2p is necessary for mitochondrial translation through association with the LSU. Mtg2p deficiency severely decreased both SSU and LSU levels (Datta et al., 2005). Similarly, mammalian MTG2 is also required for translation and associates with the LSU, but its effect on ribosome assembly remains to be determined. siRNA targeting MTG2 in HeLa cells did not reduce mitochondrial translation as drastically as siRNA targeting of MTG1 (Kotani et al., 2013). In contrast to recombinant MTG1, MTG2 has measurable intrinsic GTPase activity. Interestingly, overexpression of ObgE partially suppresses a temperature-sensitive RrmJ rRNA methyltransferase mutant in bacteria (Britton, 2009). A similar observation was made with the corresponding yeast mitochondrial proteins Mtg2p and MRM2 (Datta et al., 2005).

c. Other Assembly Factors

MTERF3 is a putative transcription termination factor that behaves as a negative regulator of mitochondrial DNA transcription initiation in mice (Park et al., 2007) and is required for embryonic development. MTERF3 can also bind to 16S rRNA and its loss is associated with

defective LSU assembly and a translation defect in both Drosophila and mice (Wredenberg et al., 2013).

C7orf30 (ybeB in bacteria) is a protein associated with the mitochondrial LSU (Rorbach et al., 2012; Wanschers et al., 2012), specifically with MRPL14, and may be minimally associated with the monosome (Fung et al., 2013). Knockdown of C7orf30 causes a defect in LSU and monosome assembly and thus a defect in translation. However, the mechanism by which C7orf30 operates is unclear, since C7orf30 belongs to the DUF143 family of proteins that may act as ribosome silencers (Fung et al., 2013). Overexpression of mutant C7orf30 at one of the conserved residues, H185A, disrupts the mitoribosome profile on a sucrose gradient, producing a dominant negative effect, possibly by outcompeting the endogenous C7orf30 protein (Rorbach et al., 2012).

The m-AAA protease consisting of Afg3l2 and paraplegin subunits are required for the maturation of MRPL32 by cleaving its precursor form upon import into mitochondria (Almajan et al., 2012; Nolden et al., 2005). The inability to process the precursor protein results in an inability to properly incorporate MRPL32 into the ribosome, as seen in hereditary spastic paraplegia.

C1qR, also known as p32, binds to all mitochondrial mRNAs and interacts with ribosomal proteins (Yagi et al., 2012). Mitochondrial ribosome stability and translation were perturbed when p32 was deleted in MEFs, thus mitoribosome formation may be among the multiple functions of p32.

Although the function of MPV17L2 is unknown, it associates with the LSU and monosome in mammalian mitochondria and has a role in ribosome assembly (Rosa et al., 2014). siRNA targeting MPV17L2 disrupted assembly of the SSU, LSU and monosome complexes.

GRSF1 has been implicated in ribosome assembly and recruitment of RNA into the ribosomal complexes (Antonicka et al., 2013). The mechanism by which GRSF1 promotes ribosome assembly is unclear. Studies have proposed that GRSF1 preferentially binds to G-rich RNA sequences, particularly “GGG” (Kash et al., 2002; Schaub et al., 2007; Ufer et al., 2008), which is found in 22 of the 37 mitochondrial transcripts, including the 12S and 16S rRNAs. Since we have identified GRSF1 at the nucleoid (Bogenhagen et al., 2008), it is possible that GRSF1 functions as an RNA chaperone assisting the incorporation of the rRNAs into the ribosomes. Alternatively, GRSF1 may have an indirect role in mitoribosome assembly or stability by assisting in RNA processing (Jourdain et al., 2013), however 13 of the 15 mitochondrial transcripts that lack “GGG” are tRNAs. Further studies are needed to resolve this discrepancy.

RNA helicases are expected to be crucial at multiple steps of the RNA folding and ribosome assembly pathway, although none have been well characterized in mammalian mitochondria. DEAD-box RNA helicases in *E. coli* have RNA-dependent ATPase activity, and 4 of the 5 are directly involved in ribosome assembly (Shajani et al., 2011). While DEAD-box helicases are sometimes dispensable in bacteria, they are essential in eukaryotic cytoplasmic ribosome biogenesis (Martin et al., 2013; Peil et al., 2008; Shajani et al., 2011). Mrh4, a DEAD-box helicase in yeast mitochondria interacts with the large ribosomal subunit rRNA, intermediates in LSU assembly and monosomes, and is essential for translation (De Silva et al., 2013). Deletion of Mrh4 leads to an accumulation of a LSU assembly intermediate. Since Mrh4 is most closely related to DDX28, an uncharacterized putative helicase that we have co-immunoprecipitated with RNMTL1 (Lee et al., 2013) and is associated with nucleoids

(Bogenhagen et al., 2008), it will be of interest to determine if DDX28 functions in ribosome assembly.

d. Mitoribosome Assembly Begins at the Mitochondrial Nucleoid

Since mitochondria originate from an α-proteobacteria, their ribosome assembly pathways are expected to have some similarities. In bacteria, transcription of a polycistronic precursor RNA at the nucleoid is processed almost immediately by RNases and folded by helicases, while translated ribosomal proteins assemble onto the rRNAs with the help of assembly factors (Shajani et al., 2011). Coupling of steps in the ribosome assembly pathway is likely designed for efficiency and regulatory control. Prior to recent work in the Bogenhagen laboratory, little attention has been devoted to investigating where mitoribosomes are assembled in mitochondria. Based on our initial observation of ribosomal proteins and other factors in nucleoid preparations, we developed the hypothesis that early steps in mitoribosome assembly occur at the nucleoid. This hypothesis has been confirmed by the presence of RNA processing proteins (RNase P and RNase Z), mitoribosomal protein subunits, rRNA methyltransferases and mitoribosome assembly factors (MTG3, MPV17L2, GRSF1, ERAL1) in nucleoid preparations (Bogenhagen et al., 2008; He et al., 2012a; Lee et al., 2013; Rosa et al., 2014). Confocal microscopy revealed that RNase P subunits, RNase Z, and rRNA methyltransferases are localized in foci next to nucleoids. Additionally, they remain in stable complexes with nucleoids after centrifugation through isokinetic and isopycnic gradients. While these RNA processing enzymes are diffusible in mitochondria, we used a stable isotope labeling by amino acids in cell culture (SILAC) approach and found that certain newly-synthesized mitoribosomal proteins were enriched at the nucleoid compared to ribosome complexes (Bogenhagen et al., 2014). Thus,

MRPs translated in the cytosol are imported into mitochondria and gather at the nucleoid, then move into ribosomal complexes. Transcription inhibition in mitochondria with 2'-C-methyladenosine severely blunted the enrichment of newly-synthesized mitoribosomal proteins at the nucleoid relative to the ribosomal complexes, indicating that mitoribosome assembly is a co-transcriptional process. Mitochondrial ribosome biogenesis also begins at the nucleoid in plants (Bohne, 2014), consistent with plant mitochondria having the same ancestral roots as mammalian mitochondria.

Since mitoribosome biogenesis is crucial for mitochondrial biogenesis, it is of interest to study factors that contribute to the assembly, stability and/or function of mitoribosomes. MRM1, MRM2 and RNMTL1 were previously uncharacterized proteins that likely contribute to the grand scheme of biogenesis. My contribution to this body of work is the initial characterization of three novel mitochondrial rRNA methyltransferases (Chapter 3) and the assignment of these proteins to their specific substrate sites on 16S rRNA (Chapter 4).

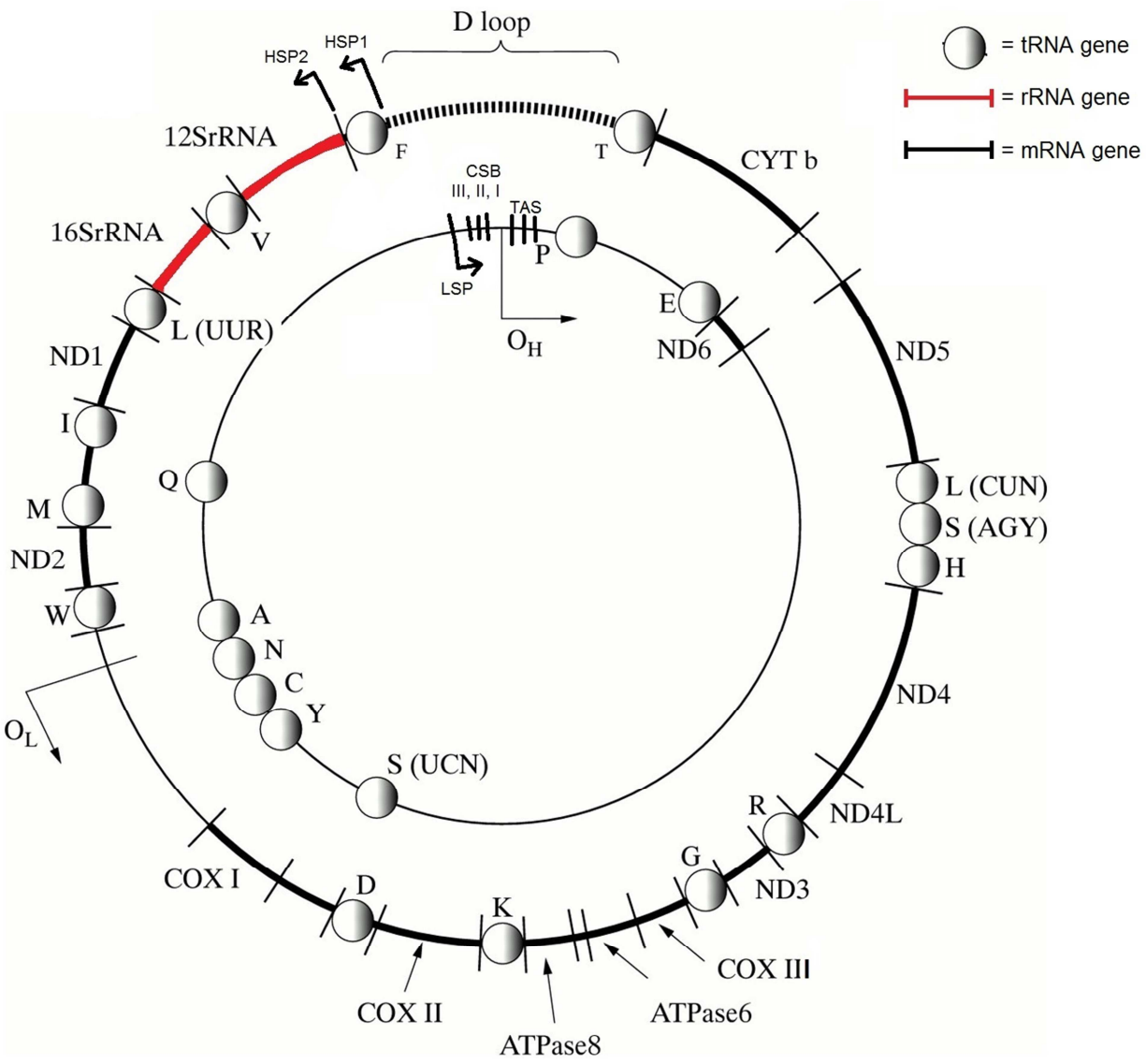

Figure 1 – Map of the human mitochondrial genome, modified from (Chinnery et al., 1999). The mRNAs (bold lines), rRNAs (red lines) and tRNAs (circles) are emphasized. HSP1, heavy-strand promoter 1; HSP2, heavy-strand promoter 2; LSP, light-strand promoter; CSB, conserved sequence box; TAS, termination-associated sequence.

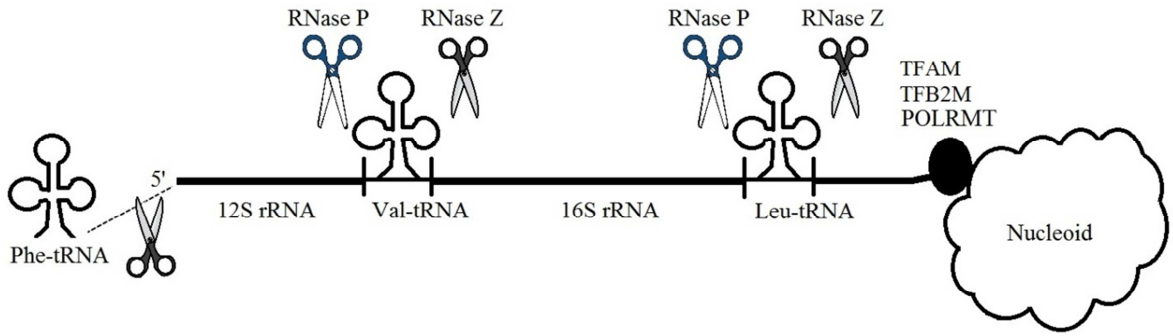

Figure 2 – tRNA punctuation model. RNase P recognizes and cleaves at the 5' end of tRNAs in a polycistronic precursor RNA, followed by subsequent RNase Z cleavage at the 3' end of tRNAs.

	E. coli	Yeast mitochondria	Mammalian mitochondria
SSU	**16S rRNA**	**15S rRNA**	**12S rRNA**
	Not modified	Not modified	m^5U^{429} – ?
	m^4Cm^{1402} RsmH RmsI	Not modified	m^4C^{839} NSUN4
	Not modified	Not modified	m^5C^{841} NSUN4
	$m^6{}_2A^{1518}$ KsgA	Not modified	$m^6{}_2A^{936}$ TFB1M
	$m^6{}_2A^{1519}$ KsgA	Not modified	$m^6{}_2A^{937}$ TFB1M
LSU	**23S rRNA**	**21S rRNA**	**16S rRNA**
	Gm^{2251} RlmB/YjfH/RrmA	Gm^{2270} Pet56p	Gm^{1145} – ?
	Cm^{2498} RlmM/YgdE	Not modified	Not modified
	Um^{2552} RlmE/RrmJ/FtsJ/Yg1136c	Um^{2791} MRM2	Um^{1369} – ?
	Not modified	Not modified	Gm^{1370} – ?
	Ψ^{2580} - RluC	Ψ^{2819} – ?	Ψ^{1397} – ?

Table 1 – Mammalian mitochondrial rRNA modifications and their corresponding sites in bacteria (*E. coli*) and yeast (*S. cerevisiae*) mitochondria. (Note: not all of the bacterial rRNA modifications are shown). Red, data for the proteins involved in the methylation of these sites are provided in this thesis.

	Bacteria (E. coli)	**Yeast cytosolic**	**Yeast mitochondria**	**Mammalian cytosolic**	**Mammalian mitochondria**
2'-O-methyl	4	55	2	105	3
Ψ	11	45	1	95	1
Base mod.	21	10	0	10	5
Other	2	0	0	0	0
Total	**38**	**110**	**3**	**210**	**9**

Table 2 – rRNA modifications across various species, sorted by type of modification (Decatur and Fournier, 2002; Maden and Hughes, 1997; Pintard et al., 2002; Purta et al., 2009; Rorbach and Minczuk, 2012).

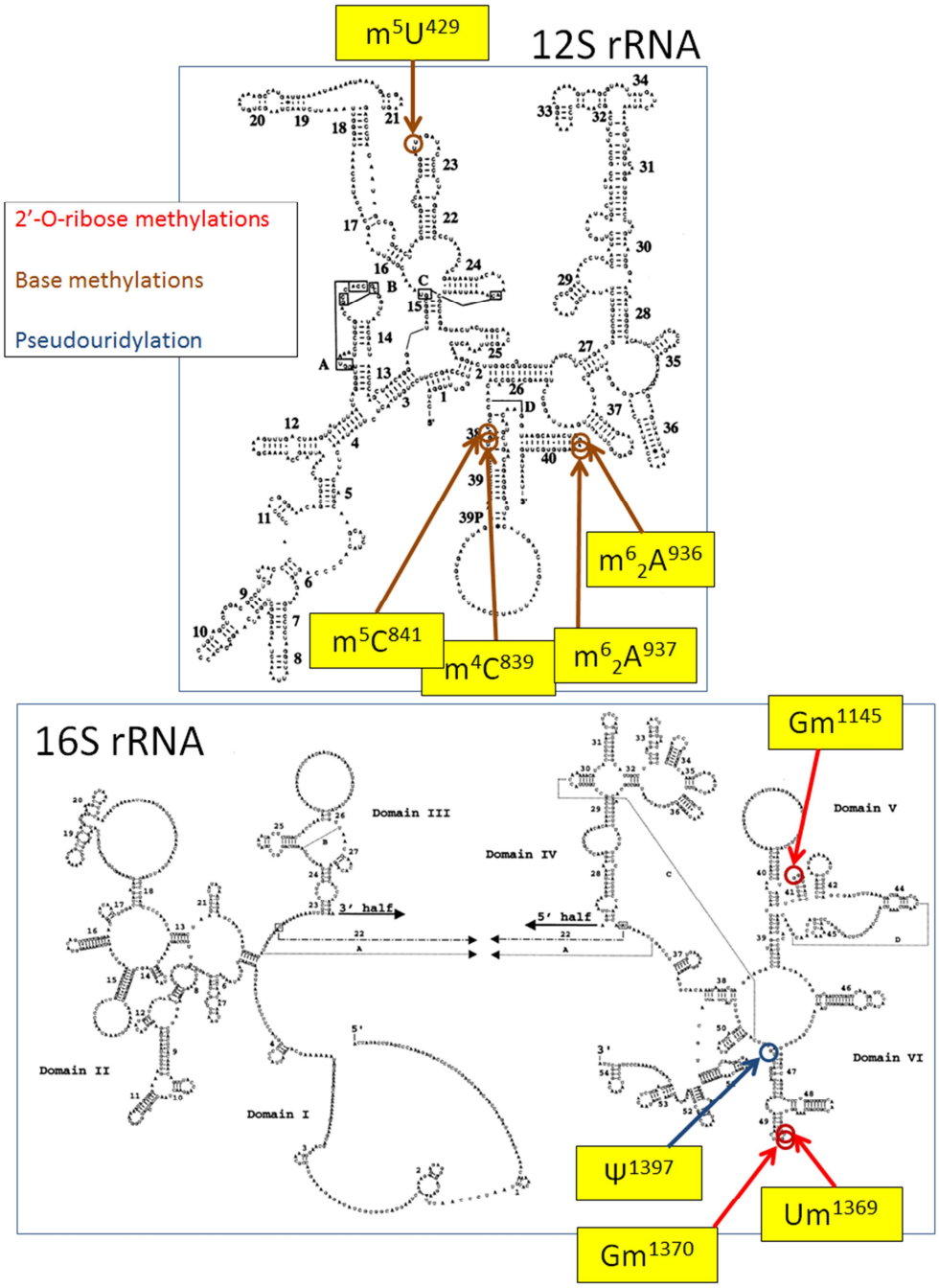

Figure 3 – The secondary structure of human mitochondrial 12S and 16S rRNAs and their modifications, modified from (Burk et al., 2002; Springer and Douzery, 1996). Evidence for the substrate sites of MRM1, MRM2 and RNMTL1 is provided in this thesis.

Species	Protein	Role in ribosome assembly?
Bacterial	RbgA	Yes – Deletion causes reduction of monosome and lack of free LSU.
Yeast (mito)	Mtg1p	Unknown – Deletion causes a translation defect.
Mammalian (mito)	MTG1	Unknown – Knockdown causes decreased translation.
Bacterial	ObgE	Yes – Deficiency causes lack of monosomes and accumulation of an atypical LSU. Overexpression rescues RrmJ mutant.
Yeast (mito)	Mtg2p	Yes – Deficiency caused decreased levels of both SSU and LSU. Overexpression rescues MRM2 mutant.
Mammalian (mito)	MTG2	Yes – Deficiency leads to decreased levels of SSU and LSU.
Bacterial	Era	Unknown – Possibly acts as a checkpoint.
Mammalian (mito)	ERAL1	Yes – Knockdown caused decreased SSU assembly.
Bacterial	YqeH	Yes – Deficiency eliminated detectable amounts of SSU.
Yeast (mito)	MTG3	Yes – Deficiency causes no detectable SSU.
Mammalian (mito)	MTG3 / hNOA1/ C4orf14	Yes – Knockout in mice depleted monosomes and altered the subunit sedimentation profiles.
Mammalian (mito)	MRPS29 / DAP3	Unknown – Ribosomal protein with intrinsic GTPase and tied to extra-ribosomal functions.

Table 3 – GTPases involved in ribosome assembly among different species.

Chapter 2 – Materials and Methods

Oligonucleotides and Reagents – Oligonucleotides were purchased from Operon and the sequences are shown in **Table 1**. Chemicals used are listed with their suppliers: DMEM, mifepristone, zeocin (Invitrogen); hygromycin B, Fugene 6 (Roche); 60% Iodixanol (Optiprep), DNase I Type II, and others chemicals (Sigma-Aldrich); TurboNuclease (Accelagen); Amplify™ (Amersham Biosciences); Restriction enzymes (New England Biolabs); 10% Triton X-100 (Fisher); [γ-^{32}P]ATP, S-[^{3}H]-adenosylmethionine (MP Biochemicals); [^{35}S]methionine/cysteine (Perkin Elmer Life Sciences); HisTrap^{TM}, Heparin-Sepharose HiTrap^{TM}, Superose 6 chromatography columns (GE Healthcare). Antibodies against antigens are listed with their providers and dilutions: SDHA (MitoSciences; 1:10,000), FLAG (Sigma-Aldrich; 1:1,500), MRM1 (Sigma-Aldrich; 1:500), MRM2 (Abcam; 1:1,000), MRPS15 (Proteintech; 1:1,500), RNMTL1 (Proteintech; 1:5,000), DNA (Chemicon; 1:12,000), TFAM (Bogenhagen laboratory; 1:5,000), MRPL13 (Spremulli Laboratory, 1:1,500 to 1:4,000). Other antibodies include fluorescent goat-anti-rabbit or goat-anti-mouse antibodies (Molecular Probes; 1:1,000), and alkaline phosphatase- or HRP-conjugated goat-anti-rabbit or goat-anti-mouse antibodies (KPL or Thermo Scientific, respectively; 1:5,000). Biotin-CTP (Invitrogen), T7 RNA Polymerase (Ambion T7 Megascript), Hybond N+ membrane (GE Healthcare); Ultrahyb and Brightstar® BioDetect Kit (Ambion).

Oligo	**Sequence (5' to 3')**	**Purpose**
mmRNMTL1 AscI (Fwd)	CGGCGCGCCAGTAATGGCAGCGCCGG	Cloning mouse RNMTL1 into pGS vector
mmRNMTL1 NotI (Rv)	TGCGGCCGCAGTGGTAACTCCTG	Cloning mouse RNMTL1 into pGS vector
mmMRM1 AscI (Fwd)	CGGCGCGCCAGAAATGCGGCGACTCTG	Cloning mouse MRM1 into pGS vector
mmMRM1	TGCGGCCGCAGGAGTCTTGGAGAAG	Cloning mouse MRM1

NotI (Rv)		into pGS vector
mmMRM2 AscI (Fwd)	CGGCGCGCCAGAAATGGCCGGGCATCTG	Cloning mouse MRM2 into pGS vector
mmMRM2 NotI (Rv)	TGCGGCCGCACGGCCTCCTGGTG	Cloning mouse MRM2 into pGS vector
hsRNMTL1 NdeI (Fwd)	GACATATGGTGCGACCGTTGCTG	Cloning human RNMTL1 into pET22b+ vector, lacking the MLS
hsRNMTL1 NotI (Rv)	ATGCGGCCGCGTGGTAACTCCTGTC	Cloning human RNMTL1 into pET22b+ vector
mmMRM1 NdeI (Fwd)	CCATATGGGAGAACGGCCTGGCG	Cloning human MRM1 into pET22b+ vector
mmMRM2 NdeI (Fwd)	ACATATGGGCGCTGAGCACCTG	Cloning human MRM2 into pET22b+ vector
h12SF (Fwd)	TAGATACCCCACTATGCTTAGC	RT-PCR for h12s rRNA
h12SR (Rv)	CGATTACAGAACAGGCTCC	RT-PCR for h12s rRNA
h16SF (Fwd)	CCAAACCCACTCCACCTTAC	RT-PCR for h16S rRNA
h16SR (Rv)	TCATCTTTCCCTTGCGGTAC	RT-PCR for h16S rRNA
ND1F (Fwd)	TCAAACTCAAACTACGCCCTG	RT-PCR for ND1 mRNA
ND1R (Rv)	GTTGTGATAAGGGTGGAGAGG	RT-PCR for ND1 mRNA
ND2F (Fwd)	CTACTCCACCTCAATCACACTAC	RT-PCR for ND2 mRNA
ND2R (Rv)	AGGTAGGAGTAGCGTGGTAAG	RT-PCR for ND2 mRNA
ND5F (Fwd)	GTCCATCATAGAATTCTCAC	RT-PCR for ND5 mRNA
ND5R (Rv)	GCCCTCTCAGCCGATGAAC	RT-PCR for ND5 mRNA
ND6F (Fwd)	CCACAACCACCACCCCATC	RT-PCR for ND6 mRNA
ND6R (Rv)	GGTTGAGGTCTTGGTGAGT	RT-PCR for ND6 mRNA
COXIF (Fwd)	ACACGAGCATATTTCACCTC	RT-PCR for COXI mRNA
COXIR (Rv)	CCTAGGGCTCAGAGCACTGC	RT-PCR for COXI mRNA
siRNMTL1-A (dsRNA)	GGAGCAACGAGAGAAACAA	siRNA against RNMTL1
siRNMTL1-B (dsRNA)	GGAUUGGUCCGACCUCGUA	siRNA against RNMTL1
siMRM1-A (dsRNA)	CCAGGCCCAUGUUUAUUGA	siRNA against MRM1
siMRM1-B (dsRNA)	GGAAGUUGAGGGAAAGUUU	siRNA against MRM1
siMRM2-A (dsRNA)	ACAUCUCAGGGACCCAUUU	siRNA against MRM2
siMRM2-B (dsRNA)	GAAUGUAAGGAUCAUCAAA	siRNA against MRM2

D5 Primer	GGTTGGGTTCTGCTCCGAGG	Domain 5 Methylation analysis
D6 Primer	GATCACGTAGGACTTTAATCG	Domain 6 Methylation analysis
8-17 hG1144	TCCGAGGTCGCCTATTAGCAATACGAA AACCGAAATTTTT	DNAzyme targeting G1144 on 16S rRNA
8-17 hG1145	CTCCGAGGTCGCTATTAGCAATACGAA CAACCGAAATTTT	DNAzyme targeting G1145 on 16S rRNA
8-17 hU1369	TTAATCGTTGAATATTAGCAATACGAA AACGAACCTTTAA	DNAzyme targeting U1369 on 16S rRNA
10-23 hG1370	TTTAATCGTTGAAGGCTAGCTACAACGA AAACGAACCTTTA	DNAzyme targeting G1370 on 16S rRNA
hs16S Probe (EcoRI Fwd)	GAATTCCTAGTGTCCAAAGAGCTG	Probe for 16S rRNA
hs16S Probe (Hind III Rv)	AAGCTTCCAAGCATAATATAGCAAG	Probe for 16S rRNA

Table 4 – DNA oligonucleotides used in this thesis.

Tissue Cell Culture – HeLa adherent cells, HEK293T cells and mouse 3T3 fibroblasts were grown on tissue culture plates (Corning or BD Falcon) in DMEM supplemented with 10% fetal bovine serum (FBS), 100 units/ml penicillin and 100 μg/ml streptomycin in an incubator at 37°C, with 5% CO_2. HeLa suspension cells were grown in SMEM supplemented with calf serum, penicillin, and streptomycin as with adherent cells, in spinner flasks at 37°C. When indicated, the growth medium was supplemented with 1 mM sodium pyruvate and 50 μg/ml uridine. Cells were transfected with Fugene 6 according to manufacturer instructions and stable transfectants were isolated on selective media.

Cloning of plasmids – pGS-mmRNMTL1, pGS-mmMRM1, and pGS-mmMRM2 were cloned by ligation of PCR-amplified genes into an AscI/NotI-digested pGS vector (pGeneSwitch) designed by D.F.B. (Brown et al., 2011). Genes were amplified using primers with restriction site overhangs such that an AscI site was added upstream of the start codon and a

NotI site replaced the stop codon, allowing a transcript to code for a fusion protein with a C-terminal Eos tag. pET22b^{+}-hsRNMTL1, pET22b^{+}-mmMRM1 and pET22b^{+}-mmMRM2 were similarly cloned but with NdeI and NotI restriction sites, producing a 6X-His-tag fusion protein. pBSKII^{+}-hs16SrRNA was kindly provided by the Miguel Garcia-Diaz lab. pBS^{-}-hs16S-probe was cloned by using pBSKII^{+}-h16SrRNA as a template and primers that orient 317 base pairs of 16S rRNA complementary sequence downstream of the pBS^{-} plasmid T7 promoter in between EcoRI and HindIII restriction sites. Thus, the probe anneals to nucleotides 142 to 458 of 16S rRNA. Ligation products were transformed into OneShot Top10 chemically competent E. coli for amplification and then plasmids were isolated by MidiPrep (Qiagen).

Isolation of Purified Mitochondria – This method is scaled for approximately 2 x 10^{8} cells or about twelve 150 mm x 25 mm tissue culture plates, however volumes can be adjusted for as little as half of a 100 mm x 20 mm tissue culture plate of cells. All buffers were supplemented with 2 mM DTT and protease inhibitors (0.2 mM PMSF, 5 μg/ml leupeptin, and 1 μM pepstatin A) and all centrifugation steps were performed at 4°C unless otherwise stated. Adherent cells were trypsinized and neutralized in DMEM containing FBS, or suspension cells were pelleted at 500*g* for 5 min, 4°C, then resuspended in PBS and pelleted again. The cells were resuspended in 5 ml MIB (1X MSH (210 mM mannitol, 70 mM sucrose, 20 mM Hepes pH 8.0, 2 mM EDTA), 0.2 mg/ml BSA, DTT and protease inhibitors), then pelleted and resuspended in 3 ml MIB. The cells were transferred to a 15 ml-conical tube and 12 μl were used for counting in a hematocytometer. 8 μl of 10% digitonin in DMSO (50% inert) were added and the tube was gently inverted several times. A 1 μl sample of cells was used to assess permeability to trypan blue as an indication that the diluted digitonin has weakened the cell membranewithout causing cell lysis. If over 90% of the cells appeared susceptible to trypan blue, 7 ml MIB was added to

further dilute the digitonin and then the cells were centrifuged at 1,200*g* for 5 min. If >10% of the cells were refractory to trypan blue, digitonin was added in increments of 2 μl. The pelleted cells were resuspended in 5 ml MIB and forcibly passed through a 25-gauge needle ten times. A 1 μl sample was inspected under the microscope for cell lysis indicated by a significant decrease in the density of organelles localized at the cytoplasmic side of the nuclei. 5 ml of MIB was added to the lysate and nuclei were removed by three successive centrifugations at 900*g* for 5 min. The supernatant was then spun at 16,000*g* for 15 min either in an HB-6 swinging bucket rotor or in microfuge tubes. The pellet containing crude mitochondria was then resuspended in 3 ml KIB (MIB supplemented with 1 M KCl) to remove cytosolic contaminants, and the mitochondria were pelleted again, then resuspended in 1 ml Energy Mix (1 mM ADP, 5 mM glutamic acid, 5 mM sodium malate, 1X MSH with 2 mM $MgCl_2$ (instead of EDTA), 1 mM K_2HPO_4, DTT, and protease inhibitors) supplemented with 40 μg DNase I and 1 μl TurboNuclease. The DNase treatment of crude mitochondria was carried out at 37°C for 20 min in a closed container. The DNase was inactivated with 100 μl of 0.25 M EDTA and the mitochondria were pelleted again. The mitochondria were resuspended in 1 ml MSH supplemented with DTT and protease inhibitors, and then spun through a sucrose step gradient (1.7 M and 1 M sucrose buffered in 20 mM Hepes, pH 8.0, 2 mM EDTA, DTT, and protease inhibitors) at 112,000*g* for 25 min. The mitochondrial layer was transferred to a clean tube and diluted in three volumes of 0.5X MSH, then centrifuged at 10,000*g* for 10 min. For experiments that did not require the mitochondria to be highly purified, some steps were skipped for practical purposes as indicated.

Immunoblotting – The concentration of proteins in cell fractions were determined by BioRad assays and samples were loaded onto 12% or 14% SDS-PAGE with sample loading

buffer. Proteins were transferred onto PVDF membranes, blocked in 5% (w/v) non-fat milk powder dissolved in PBS containing 0.5% (v/v) Tween-20. Blots were probed with antibodies specified and developed with secondary antibody conjugated to either alkaline phosphatase for colorimetric detection or horseradish peroxidase for chemiluminescence.

Confocal Microscopy – 3.5-cm diameter MatTek dishes were coated with 15 μg/ml fibronectin for 2 h, then blocked with FBS-containing DMEM for 20 min. 80,000 cells were plated and incubated overnight. In some cases, cells were incubated with 50 nM MitoTracker Red for 90 min prior to a PBS wash and were fixed with 4% paraformaldehyde. Cells were permeabilized with 0.25% Triton X-100 in PBS and blocked with MaxBlock (Active Motif) over night at 4°C, then in 5% (v/v) horse serum, 3% (w/v) BSA, 0.2% Triton X-100 in PBS for 30 min at room temperature. Antibodies were applied at specified dilutions.

Sedimentation Analysis on Glycerol Gradient – Purified mitochondria were resuspended in lysis buffer (20 mM Hepes, pH 8.0, 20 mM NaCl, 2 mM EDTA, 2 mM DTT with protease inhibitors, 2% Triton X-100). Insoluble material was removed by centrifugation at 5,000*g* for 5 min, 4°C. The soluble supernatant was layered over a 10-ml 15-40% glycerol gradient prepared in gradient buffer (same as the lysis buffer, except with 0.2% Triton X-100), layered on top of a pad consisting of 30% iodixanol, 30% glycerol in gradient buffer in a 14 x 29-mm tube. The gradient was centrifuged at 210,000*g* for 4 h, 4°C. Fractions were collected from the bottom of the gradient and analyzed by SYBR Green II RNA staining and immunoblotting.

Sedimentation Analysis on Iodixanol Gradient – Ribosome-containing fractions were concentrated by ultrafiltration using a Vivaspin 50-kDa concentrator. The nucleoid- and ribosome-containing fractions from the glycerol gradient were individually pooled and separately layered on top of a 20-40% iodixanol gradient containing 0.2% Triton X-100 and 2 mM EDTA,

then centrifuged at 140,000*g* overnight, 4°C. Fractions were collected from the bottom of the gradient.

Sedimentation Analysis on Sucrose Gradient – Purified mitochondria were resuspended in 10 mM Tris, pH 7.5, 100 mM KCl, 2% Triton X-100, 5 mM β-mercaptoethanol, 20 mM $MgCl_2$. The soluble material was separated by centrifugation at 3,000*g* for 5 min, 4°C, then layered over a 10-ml 10-30% sucrose gradient prepared in the lysis buffer, but with 0.02% Triton X-100, over a pad of 30% iodixanol, 30% glycerol. The gradient was centrifuged at 70,000*g* for 17 h, 4°C and fractions were collected from the bottom.

Real Time-Polymerase Chain Reaction (RT-PCR) – RNA isolated by using TRIzol (Invitrogen) was used as a template for first-strand cDNA synthesis with reverse transcriptase and random primers (Invitrogen). cDNA was amplified with primers specific for human 12S, 16S, ND1, ND2, ND5, ND6 and COXI, using 2X SYBR Green DNA Polymerase Mix and a Step One Plus instrument (Applied Biosystems).

Immunoprecipitation of RNMTL1-interacting proteins – 3T3-Sw mouse fibroblasts (integrated the pSwitch vector, coding for a chimeric mifepristone-activated promoter activation domain) were stably transfected with pGS-RNMTL1-3FH, encoding mouse RNMTL1 with a $FLAG_3$-His_6 tag at the C-terminus. Twelve 150 mm x 25 mm plates of cells were grown for two days and then expression of RNMTL1-3FH was induced by incubating with 50 pM mifepristone for 16 h. Mitochondria were purified and resuspended in 150 μl of FLAG column wash buffer (provided by Sigma) supplemented with Triton X-100 (50 mM Tris, pH 7.4, 150 mM NaCl, 0.02% Triton X-100, protease inhibitors). An equal volume of 2X lysis buffer (100 mM Hepes, pH 7.5, 200 mM NaCl, 4% Triton X-100 and protease inhibitors) was added and the solution was gently mixed by pipetting. The insoluble material was removed by centrifugation at 15,000*g* for

5 min, 4°C, and then the soluble fraction was incubated with pre-washed FLAG M resin (FLAG antibody-conjugated beads) (Sigma) for 3 h, 4°C while rotating. The mixture was centrifuged at 1,000*g* for 1 min, 4°C and the supernatant (flowthrough) was collected. The resin was washed six times with wash buffer and proteins were removed from the resin by incubating with 200 µl of 150 µg/ml $FLAG_3$ peptide diluted in wash buffer. Samples were separated by 12% SDS-PAGE and silver-stained for visualization of all protein bands.

Proteomics – A 20 µl of sample of FLAG resin-eluted proteins were loaded and briefly electrophoresed into a polyacrylamide gel by standard SDS-PAGE techniques. The gel was submitted to the Proteomics Center at Stony Brook University. Tryptic peptide fragments were analyzed by LC-MS/MS using a Thermo Fisher Scientific LTQ Orbitrap XL ETD mass spectrometer by matching collision-induced dissociation spectra against a library of known peptide spectra derived from the Swiss-Prot/Trembl database.

Purification of Recombinant Proteins – Codon optimized RIPL DE3 *E. coli* transformed with pET22b$^+$-hsRNMTL1, pET22b$^+$-mmMRM1 or pET22b$^+$-mmMRM2 were grown to approximately OD_{600} = 0.3, and then expression was induced with 1 mM isopropyl 1-thio-β-D-galactopyranoside (IPTG) for 3 hours at 37°C, with shaking. Bacteria were pelleted by centrifugation and resuspended in lysis buffer (20 mM Hepes, pH 7.5, 1 M KCl, 5% glycerol, 0.5% Triton X-100, 1 mM β-mercaptoethanol, protease inhibitors). The cells were lysed by sonication on an ice water bath. The soluble fraction was separated by centrifugation at 25,000*g* for 30 min, 4°C and then passed through a 0.45 µm PVDF filter. Lysate from cells expressing hsRNMTL1 were loaded onto a HisTrap^{TM} column at 95% Buffer A (20 mM Hepes, pH 7.5, 1 M KCl, 5% (v/v) glycerol, 3 mM β-mercaptoethanol, 0.02% (v/v) Triton X-100, 0.2 mM PMSF), 5% Buffer B (same as Buffer A, except supplemented with 50 mM KCl and 500 mM imidazole,

pH 8.3). The column was washed with 15 column volumes of 95% Buffer A, 5% Buffer B, and then with 15 column volumes of 85% Buffer A, 15% Buffer B. Proteins were eluted using a 15-100% Buffer B gradient and fractions were collected. The elution fractions containing the highest concentration of RNMTL1 (peak fractions), as determined by SDS-PAGE and Coomassie Blue staining, corresponded to approximately 50% Buffer A, 50% Buffer B. These fractions were pooled and loaded onto a heparin HiTrap™ column at 95% Buffer C (20 mM Hepes, pH 7.5, 5% glycerol, 7 mM β-mercaptoethanol, 0.02% Triton X-100, 1 mM EDTA, 0.2 mM PMSF), 5% Buffer D (same as Buffer C, except supplemented with 1 M KCl). The column was washed with 5 ml of 95% Buffer C, 5% Buffer D. Proteins were eluted using a 5-100% Buffer D gradient. The peak elution fractions corresponded to approximately 70% Buffer D. The peak elution fractions were pooled and diluted with an equal volume of enzyme storage buffer (77.3% glycerol, 20 mM Tris pH 8.0, 5 mM DTT, 0.02% Triton X-100, protease inhibitors) and stored at -80°C. Purification of mmMRM1 was performed similarly to hsRNMTL1 with minor changes. Cell lysate was bound to HisTrap™ column and the column was washed with 10 column volumes of Buffer A, followed by 10 column volumes of 95% Buffer E (20 mM Hepes, pH 7.5, 5% glycerol, 3 mM β-mercaptoethanol, 0.02% Triton X-100, 0.2 mM PMSF, 200 mM KCl), 5% Buffer F (same as Buffer E, except supplemented with 500 mM imidazole, pH 8.3) and 15 column volumes of 85% Buffer E, 15% Buffer F. Peak fractions corresponded to approximately 55% Buffer F. These fractions were pooled and diluted in an equal volume of Buffer C, and then loaded onto a heparin HiTrap™ column. The column was washed with 5 column volumes of 90% Buffer C, 10% Buffer D. Proteins were eluted in a 10-100% Buffer D gradient. The peak fraction corresponded to approximately 62% Buffer D. mmMRM2 was purified as with mmMRM1, except the peak elution of mmMRM2 from the HisTrap™ column

corresponded to approximately 70% Buffer B and from the HiTrap™ column at approximately 45% Buffer D.

Analysis of a potential interaction between recombinant human MTERF3 and hsRNMTL1. Recombinant human MTERF3 lacking a His-tag was kindly provided by the Miguel Garcia-Diaz lab. 70 pmol of hsRNMTL1 was incubated with 70 pmol of MTERF3 in a final volume of 50 µl and a final concentration of 1X Wash Buffer (5X Wash Buffer = 100 mM Hepes, pH 7.5, 500 mM NaCl, 10 mM β-mercaptoethanol, 125 mM imidazole, pH 8.3, 0.1% Triton X-100), on ice for 5 min. The low concentration of imidazole in the Wash Buffer is used to prevent non-specific protein binding to the Dynabeads®. 20 µl of Dynabeads® slurry was thoroughly washed with 1X Wash Buffer and incubated with the proteins on a rotator for 15 min, 4°C. The unbound proteins were collected and the beads were washed three times with 200 µl of 1X Wash Buffer. Bound proteins were eluted from the beads in 50 µl of Elution Buffer (1 M imidazole, pH 8.3, 2% SDS).

siRNA Treatment of Tissue Culture Cells – HeLa adherent cells and HEK293T cells were reverse-transfected with 3 nM or 6 nM siRNA by first diluting the siRNA in OptiMEM and adding 10 µl (for 3 nM siRNA) or 20 µl (for 6 nM siRNA) RNAiMax and 800,000 cells. The mixture was plated on a 10-cm diameter culture plate and incubated for 3 days.

Radioactive Pulse-labeling of Mitochondrial Proteins – HeLa cells were transfected with siRNA targeting a negative control (scrambled, Scr) sequence or gene of interest for the indicated lengths of time. Cells were rinsed in Hanks' balanced salt solution for 5 min, DMEM lacking cysteine and methionine for 5 min, and then DMEM with dialyzed FBS and 100 µg/ml emetine also lacking cysteine and methionine for 5 min. 8 µl (~80 µCi) of [^{35}S]cysteine/methionine was added to 4 ml of medium for 1 h of labeling. The medium was then

changed to DMEM with FBS and emetine for a 30-min chase. Partially purified mitochondria were analyzed by SDS-PAGE and Coomassie Blue stain and destain. The gel was dried and exposed to a phosphor storage screen, and then the screen was scanned by a Typhoon 9000 (GE).

Crosslinking of [^{3}H]AdoMet to Recombinant Proteins – Purified recombinant proteins (14.5 pmol BSA, 14.2 pmol hsRNMTL1, 51 pmol mmMRM1, 49 pmol mmMRM2) were diluted in 50 mM Tris, pH 8.0, 40 mM NaCl, 2 mM DTT, 2 mM EDTA and 1.1 μCi of [^{3}H]AdoMet and incubated on ice for 10 min. The mixtures were then spotted onto a siliconized microscope slide, placed on top of ice, exposed to 254-nm UV light for the indicated lengths of time and subjected to SDS-PAGE, Coomassie blue staining and destaining. Radioactivity was detected by soaking the gel in Amplify™ (Amersham Biosciences), drying onto 3MM Whatman paper and exposure of the dried gel to X-ray film at -80°C.

Gel filtration – A Superose 6 (GE) gel filtration column was prepared by washing in several column volumes of running buffer (20 mM Hepes, pH 7.5, 300 mM NaCl, 5% glycerol, 2 mM DTT, 0.02% Triton X-100). 250 μg of BSA (66 kDa) and 250 μg of carbonic anhydrase (29 kDa) were mixed in 300 μl and loaded onto the column to provide a standard elution profile for two proteins of known sizes that exist as monomers. Similarly, approximately 100 μg of hsRNMTL1 (26 kDa), 265 μg of mmMRM1 (32 kDa) and 250 μg of mmMRM2 (24 kDa) were individually analyzed by Superose 6 gel filtration. Fractions were analyzed by standard SDS-PAGE and Coomassie Blue staining, and in the case of hsRNMTL1 immunoblotting.

In vitro methylation assays – 5 pmol of proteins were incubated with 5 pmol of *in vitro*-synthesized 16S rRNA and 70 pmol [^{3}H]AdoMet in a final concentration of 1X Buffer (2X Buffer = 50 mM Hepes, pH 8.0, 100 mM KCl, 2 mM DTT, 2% glycerol, and 10 mM $MgCl_2$ or 4 mM EDTA, pH 8.0) in a volume of 100 μl for 30 min, 30°C. The RNA was extracted by TRIzol

and a subsequent phenol-chloroform extraction. The RNA was resuspended in 0.3 M sodium acetate in TE (DEPC-treated), and subjected to scintillation counting in OptiFluor for 5 min per sample. The counts for ^{3}H are reported as counts per minute (CPM).

Primer Extension Assays with Reverse Transcriptase – RNA from partially purified mitochondria were isolated from cells transfected with siRNA targeting Scr or RNMTL1 by using TRIzol. A control, unmodified RNA was generated by T7 RNA polymerase transcription from EcoRI-linearized pBSKII^{+}-hs16SrRNA plasmid. Primers were designed to anneal to 16S rRNA with their 3' termini 4 or 5 nucleotides upstream of the known 2'-O-ribose modified residues. Primers were labeled at the 5' termini with [γ-^{32}P]ATP and polynucleotide kinase, and then purified on urea-14% polyacrylamide gel. Labeled primers were annealed to 500 ng of RNA and extended with Superscript 3 reverse transcriptase in the presence of RNasin RNase inhibitor, DTT and various concentrations of dNTPs for 30 min at 37°C. Reactions were terminated by adding 0.3 M sodium acetate, 20 mM EDTA and 10 μg glycogen, followed by ethanol precipitation and analysis on urea-14% polyacrylamide DNA sequencing gel. Radioactivity was detected by exposure to phosphor storage screen and detection with Typhoon 9000.

DNAzyme Analysis of RNA – 8-17 DNAzyme reactions to cleave unmodified 16S rRNA at G1144, G1145 and U1369 were performed by annealing RNA (750 ng – 2 μg) from *in vitro* transcription or from cells treated with siRNA to DNAzyme (400 pmol) and DEPC-treated water in 16 μl at 95°C for 2 min. The reaction was cooled to room temperature (~25°C) for 10 min, followed by addition of 16 μl 2X Buffer (200 mM KCl, 800 mM NaCl, 100 mM Hepes, pH 7.5, 15 mM $MgCl_2$, 15 mM $MnCl_2$), and then incubated at 37°C for 1 h. Reactions were stopped by addition of 3 μl of 0.25 M EDTA, pH 8.0 (DEPC-treated), 100 μl of 0.3 M sodium acetate (DEPC-treated) and 10 μg glycogen, followed by ethanol precipitation and a wash with 70%

ethanol. 10-23 DNAzyme reactions (G1370) were performed by annealing RNA with DNAzyme in 12 μl and adding 12 μl of 2X Buffer (30 mM NaCl), 8 mM Tris, pH 8.0). The reaction was heated at 95°C for 3 min, cooled on ice for 5 min and then incubated at room temperature for 10 min. 6 μl of 5X Buffer (750 mM NaCl, 200 mM Tris, pH 8.0) and 2 μl of 0.3 M $MgCl_2$ was added and the reaction was incubated at 37°C for 1 h. Reactions were stopped as with 8-17 DNAzyme reactions. Control reactions were performed with DEPC-treated water in place of DNAzymes.

Northern Blotting – DNAzyme-treated RNA samples were dried and resuspended in 6 μl DEPC-treated TE (10 mM Tris, pH 7.5, 1 mM EDTA). 9 μl of RNA loading solution (80% (v/v) de-ionized formamide, 5% (v/v) formaldehyde, 20 mM EDTA, pH 8.0, 40 μg/ml ethidium bromide, 0.05% (w/v) bromophenol blue and 0.05% (w/v) xylene cyanol) was added to the samples and heated at 65°C for 5 min. The samples were loaded onto a MOPS-2% Agarose gel and electrophoresed at 83V for ~2.5 hours in MOPS Buffer (20 mM MOPS, pH 7.0, 2 mM sodium acetate, 1 mM EDTA, pH 8.0) with a buffer exchange system. The gel was imaged with UV for ethidium bromide detection and then soaked in 10X SSC (1.5 M sodium chloride, 150 mM sodium citrate) for 10 min. The RNA was transferred to HyBond N+ (GE) nitrocellulose membrane overnight by capillary action in 10X SSC. The membrane was auto-crosslinked by a UV Stratalinker (Stratagene) and baked in a vacuum at 80°C for 2 hours. Ultrahyb pre-hybridization buffer (Ambion) was applied according to manufacturer instructions and a biotinylated RNA probe was hybridized overnight at 68°C. The biotinylated probe was generated by *in vitro* T7 RNA polymerase transcription of pBS^--hs16S-probe in the presence of biotinylated-CTP. The membrane was then washed two times in 2X SSC, 0.5% SDS and then two times in 0.2X SSC, 0.5% SDS for 10 min each at 65°C and RNA was detected by

streptavidin linked to alkaline phosphatase (Brightstar® BioDetect Kit; Ambion) according to manufacturer instructions. Blots were exposed to X-ray film and the developed scan was digitized by a Typhoon 9000. Bands were quantified with Image Quant TL Analysis Toolbox and the percent of RNA cleavage was calculated by:

$$Percent\ cleavage = \frac{Pixel\ density\ of\ cleaved\ band}{(Pixel\ density\ of\ cleaved + Pixel\ density\ of\ uncleaved\ bands)}\ x\ 100\%$$

Chapter 3 – Initial Characterization of Three Novel Mitochondrial rRNA Methyltransferases

A. RNMTL1, MRM1 and MRM2 are mitochondrial proteins

The Bogenhagen lab has identified many novel mammalian mitochondrial nucleoid proteins by proteomic analysis (Bogenhagen et al., 2008; Wang and Bogenhagen, 2006). We were particularly interested in RNMTL1, since neither RNMTL1 nor any of its homologues have been previously characterized. A search for possibly related RNA methyltransferases in the mitochondrial proteomic databases revealed MRM1 and MRM2, which have homologues in lower organisms, but were not characterized in vertebrates. RNMTL1, MRM1 and MRM2 have all been identified in mitochondrial preparations (Pagliarini et al., 2008) and in a study of the human "methyltransferasome" (Petrossian and Clarke, 2011). We started with an analysis of the mouse genes, which are well conserved in humans. Human and mouse MRM1, MRM2 and RNMTL1 are 73%, 79% and 81% identical, respectively. The amino acid sequence of mouse RNMTL1 and MRM1 reveal structural domains that are similar to a 2'-O-ribose binding domain and SpoU-methylase domain, while MRM2 has an FtsJ-like domain (**Fig 4A**). MitoProt II predicts an N-terminal mitochondrial targeting signal (MTS) that is cleaved after import in each of the three proteins (**Table 5**). Vector NTI was used to compare the sequence homologies to other characterized methyltransferases: bacterial KsgA and RlmE (FtsJ/RrmJ), yeast Pet56 (MRM1) and MRM2, and mouse TFB1M, TFB2M, NSUN4 and MRPP1. A dendrogram grouping the proteins by degree of relation is shown in **Fig 4B**. RNMTL1 is more closely related to MRM1 than it is to MRM2. From these indications that MRM1, MRM2 and RNMTL1 are novel putative RNA methyltransferases in mammalian mitochondria, we began to study them more in depth.

We first performed subcellular fractionation of HeLa cells and immunoblotting to confirm our nucleoid proteomic data. Equal amounts of protein from whole cell homogenate (Hom), post-nuclear supernatant (PNS), post-mitochondrial supernatant (PMS), crude mitochondria (CM) or purified mitochondria (PM) were loaded per lane and immunoblotting revealed that the three putative RNA methyltransferases are enriched in the mitochondria, along with a positive control, SDHA, a 70 kDa protein subunit of Complex II that resides within the inner mitochondrial membrane (**Fig 4C-E**).

B. RNMTL1, MRM1 and MRM2 are associated with mitochondrial nucleoids and ribosomal complexes

We were interested in the localization of RNMTL1, MRM1 and MRM2 within mitochondria. We stably transfected 3T3-Sw cells with the mouse genes tagged with a photoactivatable fluorescent protein, Eos, at the 3' terminus and prepared the cells for confocal microscopy. These fusion proteins are expressed under the control of a mifepristone-inducible promoter and the Eos tag fluoresces as a green signal. Mitochondria were stained with MitoTracker Red (**Fig 5A,C**), which is a dye that is oxidized and thereby contained within the mitochondrial matrix, or with anti-SDHA antibody and a secondary antibody conjugated to Alexa 568 (red) (**Fig 5E**). We observe a mitochondrial localization of these proteins, consistent with the subcellular fractionation data. In each case, the Eos fluorescence did not fill the interior of the mitochondria. Since RNMTL1 was detected in a proteomic analysis of nucleoids (Bogenhagen et al., 2008), we were interested in the sub-mitochondrial localization of these proteins. Mitochondrial DNA was probed with an anti-DNA antibody and an Alexa 568-

conjugated secondary antibody (**Fig 5B,D,F**). The Eos signal appears in distinct foci in close proximity to the nucleoids.

In our experience, despite preserving the natural mitochondrial targeting signal at the N-terminus, fusion with an Eos tag at the C-terminus of mitochondrial proteins can sometimes alter mitochondrial morphology and protein localization. This may be the result of the tag disrupting the natural folding of the protein or disrupting its interactions. The expression level of the fusion protein may also not be the same as the endogenous expression. We therefore directed an antibody against endogenous RNMTL1 in HeLa cells and counterstained with MitoTracker Red (**Fig 6A**) or anti-DNA antibody (**Fig 6B**). We observe a localization pattern similar to that of Eos-tagged RNMTL1. Thus both expression of a fluorescently tagged RNMTL1 and an antibody targeting endogenous RNMTL1 reveal that RNMTL1 exists in a punctate pattern adjacent to mitochondrial nucleoids (**Fig 5E,F**).

We sought additional evidence for RNMTL1, MRM1 and MRM2 existing in nucleoid complexes by solubilizing purified mitochondria from HeLa S3 spinner cells in non-denaturing conditions such that complexes are preserved. The soluble lysate was layered onto a non-denaturing 15-40% glycerol gradient and separated by isokinetic centrifugation such that species are separated by their sedimentation coefficient. The massive nucleoid complexes are observed to sediment to the bottom of the gradient. Fractions were collected from the bottom of the gradient and probed for RNMTL1, MRM1 and MRM2 proteins, as well as a ribosomal subunit protein, MRPL13, by immunoblotting (**Fig 7**). 16S rRNA levels were determined by TRIzol extraction of RNA from the fractions and RT-PCR (**Fig 7A**). Relative amounts of RNMTL1 and MRPL13 were determined by densitometry analysis of the immunoblot and are shown on the graph (**Fig 7A**). RNMTL1 and MRM1 were found in the nucleoid fraction and also in a more

slowly sedimenting complex with MRPL13, although most of the non-nucleoid MRM1 remained at the top of the gradient with the free pool of proteins. MRM2 was not abundant in the nucleoid fraction, but existed in a lower-density complex. The nucleoid fraction was identified by SYBR Green I fluorescence and TFAM immunoblotting (data not shown). The protein complexes that sedimented more slowly in the center of the gradient contained mitoribosomal complexes (see below). It should be noted that incompletely processed mitochondrial RNAs and possibly incompletely assembled mitoribosome complexes also sediment in this region of the gradient (Bogenhagen et al., 2014).

To validate the co-sedimentation of RNMTL1 and MRM1 with nucleoids, the nucleoid fraction from the glycerol gradient was layered on top of a 20-40% iodixanol (OptiPrep) gradient and separated by isopycnic centrifugation, such that species are separated by their buoyant density. Fractions were collected from the bottom of the gradient and mitochondrial DNA content was detected by SYBR Green I fluorescence. DNA was extracted from several fractions and digested with HindIII, and then electrophoresed through an agarose gel and stained with ethidium bromide to confirm the identity and purity (**Fig 8A**). Fractions were also probed for TFAM, RNMTL1 and MRM1 proteins (**Fig 8B**). TFAM is a nucleoid marker and is found in the same fraction as the peak of mtDNA along with RNMTL1 and MRM1. Thus, RNMTL1 and MRM1 are indeed tightly associated with nucleoids and remain in a complex after centrifugation through two types of media.

To explore the association of RNA methyltransferases with ribosomal complexes, fractions 8-11 from the glycerol gradient generated in **Fig 7** were pooled and concentrated, then layered onto a 20-40% iodixanol gradient and separated by isopycnic centrifugation. Fractions were collected from the bottom and the relative RNA abundance was measured by SYBR Green

II fluorescence (**Fig 9A**). Control experiments corroborated that the deproteinized RNA in the fractions with the peak SYBR Green II fluorescence was rRNA. Fractions were also probed for MRPS15 (a member of the mitochondrial SSU), MRPL13 (a member of the mitochondrial LSU), RNMTL1 and MRM2 proteins by immunoblotting (**Fig 9B**). RNMTL1 and MRM2 remain tightly associated with the ribosomal complex after centrifugation through two types of media, as indicated by MRPS15- and MRPL13-containing fractions.

Our first report focused more on the characterization of RNMTL1, since it is a novel protein (Lee et al., 2013). We have established that RNMTL1 exists in two relatively stable complexes: nucleoids and ribosomes, while MRM1 is mostly found in the nucleoid and free floating protein fractions and MRM2 is predominantly in the ribosome complexes. As noted above, the apparent ribosome association of these proteins might reflect their presence in assembly intermediates rather than mature ribosomal subunits. Conventional procedures for isolation of mitoribosome complexes employ sucrose gradients with higher salt and $MgCl_2$ concentrations (O'Brien, 1971). To determine whether RNMTL1 was specifically associated with the LSU, SSU or monosome, we applied soluble HeLa S3 mitochondrial lysate onto a non-denaturing 10-30% sucrose gradient supplemented with 20 mM $MgCl_2$ to preserve the monosomes, over a pad of glycerol and iodixanol. Fractions were collected from the bottom of the gradient and probed for proteins (**Fig 10A**) or 12S rRNA and 16S rRNA (**Fig 10B**). RNMTL1 was found in the 39S LSU fractions and at the top of the gradient, but not in the monosome or SSU fractions. Analysis of the same fractions for MRM1 revealed that both proteins remained at the top of the gradient in the low molecular weight region. Upon very long exposure, a trace amount of MRM1 was found associated with higher molecular weight complexes (**Fig 10A**). We conclude that the higher salt concentrations in the sucrose gradient

compared to the glycerol and iodixanol gradients displace a majority of the rRNA methyltransferases from ribosomal complexes.

C. Murine RNMTL1 interacts with mitochondrial LSU components and other proteins

We next investigated the proteins that interact with murine RNMTL1. We expressed $FLAG_3$-His_6-tagged mouse RNMTL1 (RNMTL1-3FH) from a mifepristone-inducible promoter in 3T3-Sw mouse fibroblasts. The protein is imported into mitochondria, similarly to the Eos-tagged proteins (data not shown). Mitochondria were purified from mifepristone-induced cells by two methods, either with or without 1 M KCl in the MIB buffer prior to sedimentation in between the 1.7 M / 1 M sucrose layers (see Methods). Mitochondria were then lysed in non-denaturing conditions. The soluble fraction was incubated with FLAG M resin, and then the resin was washed and RNMTL1-interacting proteins were eluted in a batch-wise manner by competition with $FLAG_3$ peptide. Samples of the washes and elutions were subject to SDS-PAGE, followed by immunoblotting (**Fig 11A**) or silver staining (**Fig 11B**). The three elutions were pooled and the proteins were partially electrophoresed into a polyacrylamide gel by standard SDS-PAGE techniques. The gel was subjected to proteomic analysis. A large fraction of spectral counts were attributed to mitochondrial large ribosomal subunit proteins (39% of counts), and small subunit proteins were detected at a lower abundance (8%). The well-represented non-ribosomal mitochondrial proteins that co-immunoprecipitated with RNMTL1-3FH are listed (36%) (**Table 6**). In the second experiment, washing mitochondria with MIB containing 1 M KCl efficiently reduced the cytosolic contaminants. It is possible that many of the RNMTL1-protein interactions are RNA-dependent and analysis of RNA-independent interactions have yet to be performed.

One of the proteins that immunoprecipitated with murine RNMTL1-3FH was MTERF3. This potential interaction was particularly interesting because, as mentioned above, MTERF3 is involved in mitochondrial LSU biogenesis (Wredenberg et al., 2013). We considered that MTERF3 may direct RNMTL1 and its rRNA methyltransferase activity to 16S rRNA or a partially assembled LSU intermediate, much like MTERF4 directs NSUN4 to the LSU, although the RNA substrate of NSUN4 is 12S rRNA (Camara et al., 2011; Metodiev et al., 2014). We first performed a negative control experiment to test if recombinant human MTERF3 lacking a His-tag (kindly provided by the Miguel Garcia-Diaz lab) can bind to magnetic Dynabeads®, which bind to His-tagged proteins. We performed this experiment in a batch-wise format. We incubated the protein with the beads and collected the unbound material. The beads were then washed three times and the bound proteins were eluted with 1 M imidazole, pH 8.3 and 2% SDS. Samples of the load, unbound proteins, washes and elutions were analyzed by standard SDS-PAGE and Coomassie Blue staining. As expected, nearly all of the MTERF3 protein was in the unbound fraction (fractions on the left of the pre-stained marker (PSM) in **Fig 12**). We then applied recombinant His_6-tagged hsRNMTL1 protein to magnetic Dynabeads® and incubated it with MTERF3 (fractions on the right of the PSM in **Fig 12**). hsRNMTL1 bound and eluted from the Dynabeads®, but MTERF3 was almost completely found in the unbound fraction. Thus, we did not observe MTERF3 to co-elute with RNMTL1. However, we have not ruled out the possibility that recombinant hsRNMTL1 was non-functional (see below) or that the His-tag interferes with the potential interaction between RNMTL1 and MTERF3. It remains to be determined whether there is a direct interaction in mitochondria.

D. RNMTL1 is involved in mitochondrial protein synthesis

Since RNMTL1 was tightly associated with mitoribosomes and is a putative RNA methyltransferase, it is likely to have an important role in ribosome assembly, stability and/or function. We tested several commercial siRNA constructs for their efficiency to deplete RNMTL1 protein levels. HeLa cells were reverse-transfected with siRNA and mitochondria were purified for immunoblotting. Equal amounts of protein were loaded per lane and probed for either RNMTL1 or the control, MRPL13. siRNA reduced RNMTL1 levels by ~90%, but "R1" was slightly more effective (**Fig 13A**). We did not detect drastic changes in the abundance of several mitochondrial transcripts due to treatment of HeLa cells with 6 nM siRNA (**Fig 13B**). The relative abundance of the 16S rRNA transcript compared to 12S rRNA was not affected by siRNA against RNMTL1. Thus, despite depletion of a putative rRNA methyltransferase, mitochondrial rRNAs remain relatively stable without complete methylation. siRNA targeting RNMTL1 caused HeLa cells to grow more slowly than cells treated with siRNA targeting a scrambled sequence (Scr), but mitochondrial transcripts were not affected, suggesting a phenotype at the protein level. To test whether mitochondrial translation was affected, we transfected HeLa cells with siRNA for 3 days and depleted the medium of cysteine and methionine, while simultaneously administering an inhibitor of the cytosolic ribosomes, emetine, prior to protein analysis. The medium was supplemented with radioactive [^{35}S]cysteine/methionine for 1 h to label newly synthesized proteins. Purified mitochondria from treated cells were subject to SDS-PAGE and autoradiography. R1 siRNA decreased mitochondrial translation by ~40% (**Fig 13C**).

E. Analysis of activity in recombinant RNA methyltransferase family members

To further characterize the RNA methyltransferase family members, we expressed recombinant human RNMTL1 (hsRNMTL1) and mouse MRM1 (mmMRM1) and MRM2 (mmMRM2) without their predicted mitochondrial localization signals, which are expected to be cleaved immediately after protein import into mitochondria, using codon-optimized RIPL DE3 *E. coli*. We purified the proteins on nickel (HisTrap^{TM}) columns, followed by heparin HiTrap^{TM} columns. We found that 1 M KCl was needed to disrupt binding to bacterial nucleic acids. The purity of the proteins is shown in a Coomassie Blue-stained gel (**Fig 14A)**. We experienced some difficulty in working with recombinant hsRNMTL1. In the process of purifying the protein, we noticed that only approximately 20% of the total protein was soluble after bacterial cell lysis. We attempted to increase the solubility of the protein by expressing it with a proteolytically excisable N-terminal maltose-binding protein domain to encourage protein folding and expressing at temperatures below 37°C. However, the solubility of the protein did not improve. We also experienced precipitation of hsRNMTL1 in enzyme storage conditions after several weeks at -20°C, despite the presence of approximately 350 mM KCl.

To determine whether the recombinant proteins can bind to AdoMet, we utilized a cross-linking protocol. Proteins were incubated with [^{3}H]AdoMet on ice and exposed to UV light for several minutes, then separated by SDS-PAGE and subjected to fluorography. BSA, the negative control, did not crosslink to AdoMet, whereas NSUN4, the positive control did, as expected. mmMRM2 also crosslinked to AdoMet, but not hsRNMTL1 or mmMRM1 (**Fig 14B,C**). It is possible that recombinant hsRNMTL1 and mmMRM1 may not have been properly folded or may require post-translational modifications that are not provided by expression in a bacterial system.

RNMTL1 and MRM1 contain domains resembling the SpoU-methylase sequence and thus are classified as SPOUT-family methyltransferases (Petrossian and Clarke, 2011). All currently known SPOUT-family members exist as dimers (Tkaczuk et al., 2007), thus we determined whether our recombinant proteins behaved as such. We used a Superose 6 gel filtration column, which separates species by their Stokes radius, such that larger particles elute first and smaller particles enter the pores of the column resin and elute later. Calibration of the Superose 6 gel filtration column revealed that BSA, a 66 kDa monomeric protein, eluted mainly in fractions 26-27, while carbonic anhydrase, a 29 kDa monomeric protein, eluted mainly in fractions 33-35. hsRNMTL1 eluted in fractions 34-35, mmMRM1 eluted in fractions 34-36 and mmMRM2 eluted in fractions 38-41. Since all of the methyltransferase proteins eluted near the position of carbonic anhydrase, we conclude that our recombinant proteins behaved as monomers (**Fig 15**). Perhaps the recombinant proteins are not behaving as they would endogenously in mitochondria, consistent with the lack of ability to crosslink to AdoMet. (**Fig 14B,C**).

In attempt to provide direct evidence that these proteins methylate 16S rRNA, we incubated the recombinant proteins with [^{3}H]AdoMet and *in vitro*-synthesized 16S rRNA, and then ethanol-precipitated the RNA for analysis by scintillation counting. Reactions were performed in the presence of magnesium or EDTA, since some methyltransferases require magnesium while others do not (Motorin and Helm, 2011). We did not observe any enhanced methylation of the RNA in the presence of the recombinant hsRNMTL1, mmMRM1 or mmMRM2 (**Table 7**). The positive control MTERF4-NSUN4 complex showed slightly enhanced RNA methylation, consistent with the findings that NSUN4 has been demonstrated to have $m^{5}C$ methyltransferase activity (Metodiev et al., 2014) and the recombinant protein

complex has loose substrate specificity, *in vitro* (Yakubovskaya et al., 2012). RNA methylation is a spontaneous reaction (Motorin and Helm, 2011), possibly accounting for the level of radioactivity retained by the precipitated RNA without the presence of active methyltransferase protein. In our experiment, it may even have been possible that the recombinant proteins bound to the RNA and inhibited spontaneous *in vitro* methylation, as marked by the lower CPM's compared to RNA-only samples. In addition to the potential problems of purifying these proteins from bacteria as discussed above, the lack of *in vitro* methyltransferase activity was not unexpected, since RrmJ and MRM2 methylate partially assembled ribosomal intermediates and not naked RNA (Caldas et al., 2000a; Pintard et al., 2002). In addition, the lack of activity for mmMRM1 and mmMRM2 may also be due to the species-specific substrate recognition, although the 16S rRNA genes are 74% identical and the 2'-O-ribose methylation sites are conserved.

Protein	Species	Reference	Amino acids	pI	Molecular Weight (kDa)	Probability imported into mito (%)	Cleavage site
MRM1	Human	NP_079140.2	353	8.15	38.6	98.8	27
	Mouse	NP_663408.2	320	9.17	34.8	98.9	25
MRM2	Human	NP_037525.1	246	9.60	27.4	29.7	14
	Mouse	NP_080786.1	246	9.75	27.1	75.7	27
RNMTL1	Human	NP_060616.1	420	8.89	47.0	56.5	11
	Mouse	NP_899086.2	418	9.45	46.8	99.7	49

Table 5 – Predicted attributes of MRM1, MRM2 and RNMTL1.

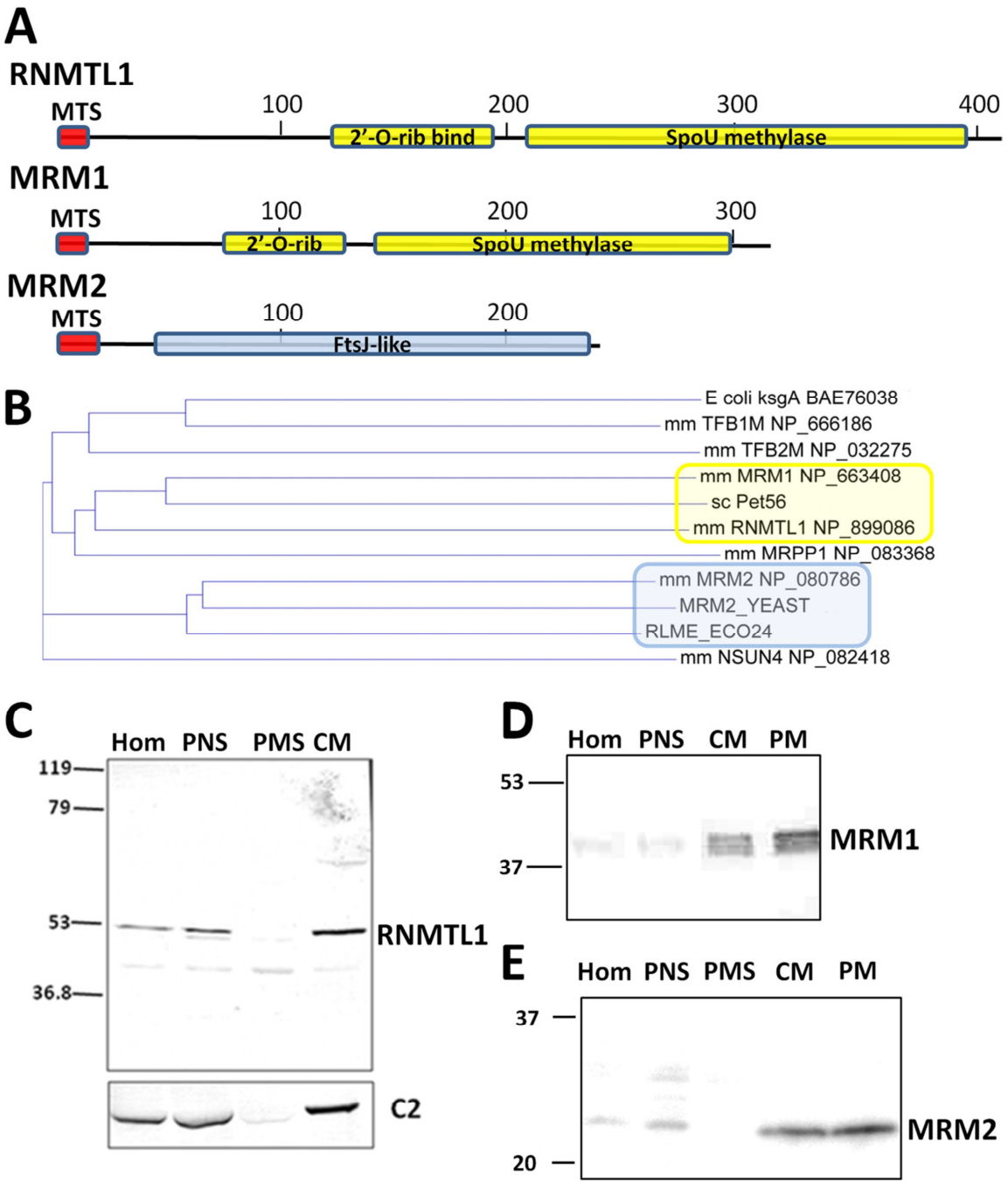

Figure 4 – RNMTL1, MRM1 and MRM2 are members of the methyltransferase family. **A)** Amino acid sequence analysis of mouse RNMTL1, MRM1 and MRM2. **B)** Dendrogram of known and putative RNA methyltransferases. HeLa subcellular fractions were immunoblotted for RNMTL1 (**C**), MRM1 (**D**) and MRM2 (**E**) and compared to a positive control, C2, a subunit of the succinate dehydrogenase complex. (**Figures 4A** and **4B** were produced by D.F.B.).

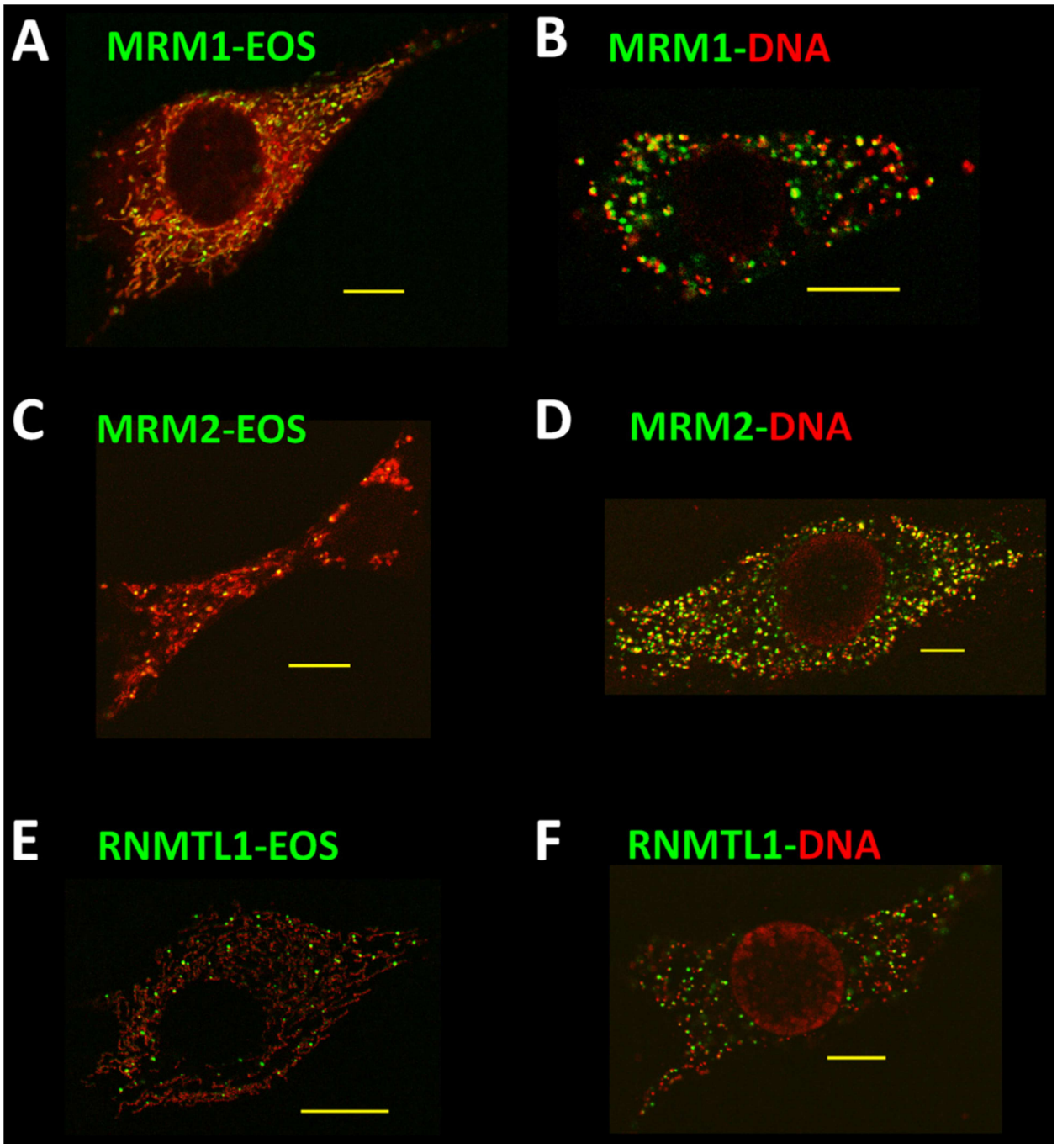

Figure 5 – MRM1, MRM2 and RNMTL1 tagged with Eos localize to foci in the vicinity of nucleoids. Confocal microscopy imaging of Eos-tagged proteins (green) counterstained with MitoTracker Red (red) (**A,C**) or anti-SDHA antibody (red) (**E**), or for mitochondrial DNA with anti-DNA antibody (red) (**B,D,F**). Scale bars, 10 μm.

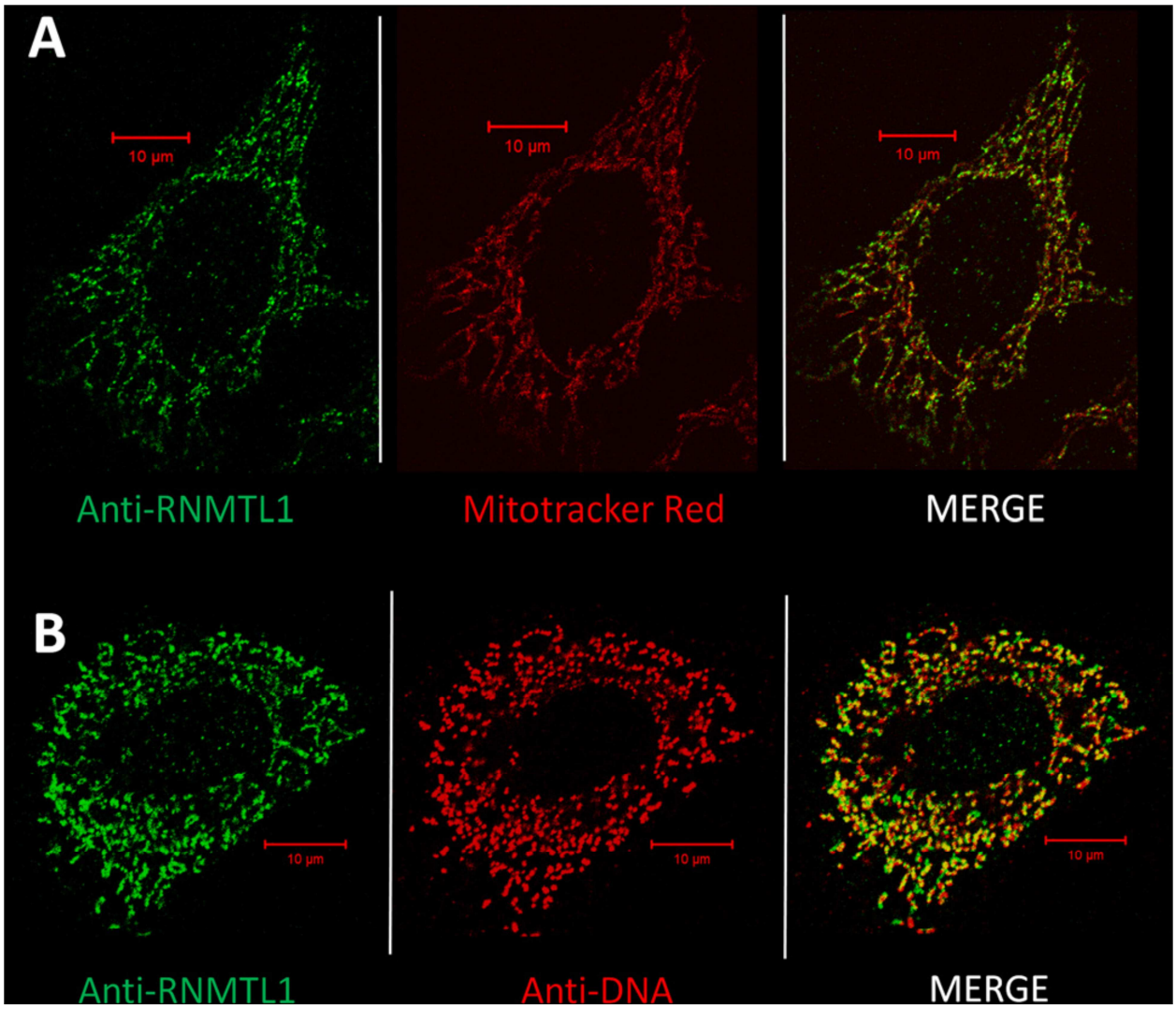

Figure 6 – Endogenous RNMTL1 is localized in foci in the vicinity of mitochondrial nucleoids. Anti-RNMTL1 antibody (green) was applied to HeLa cells and mitochondria were stained with MitoTracker Red (red) (**A**) or mitochondrial nucleoids were stained with anti-DNA antibody (red) (**B**).

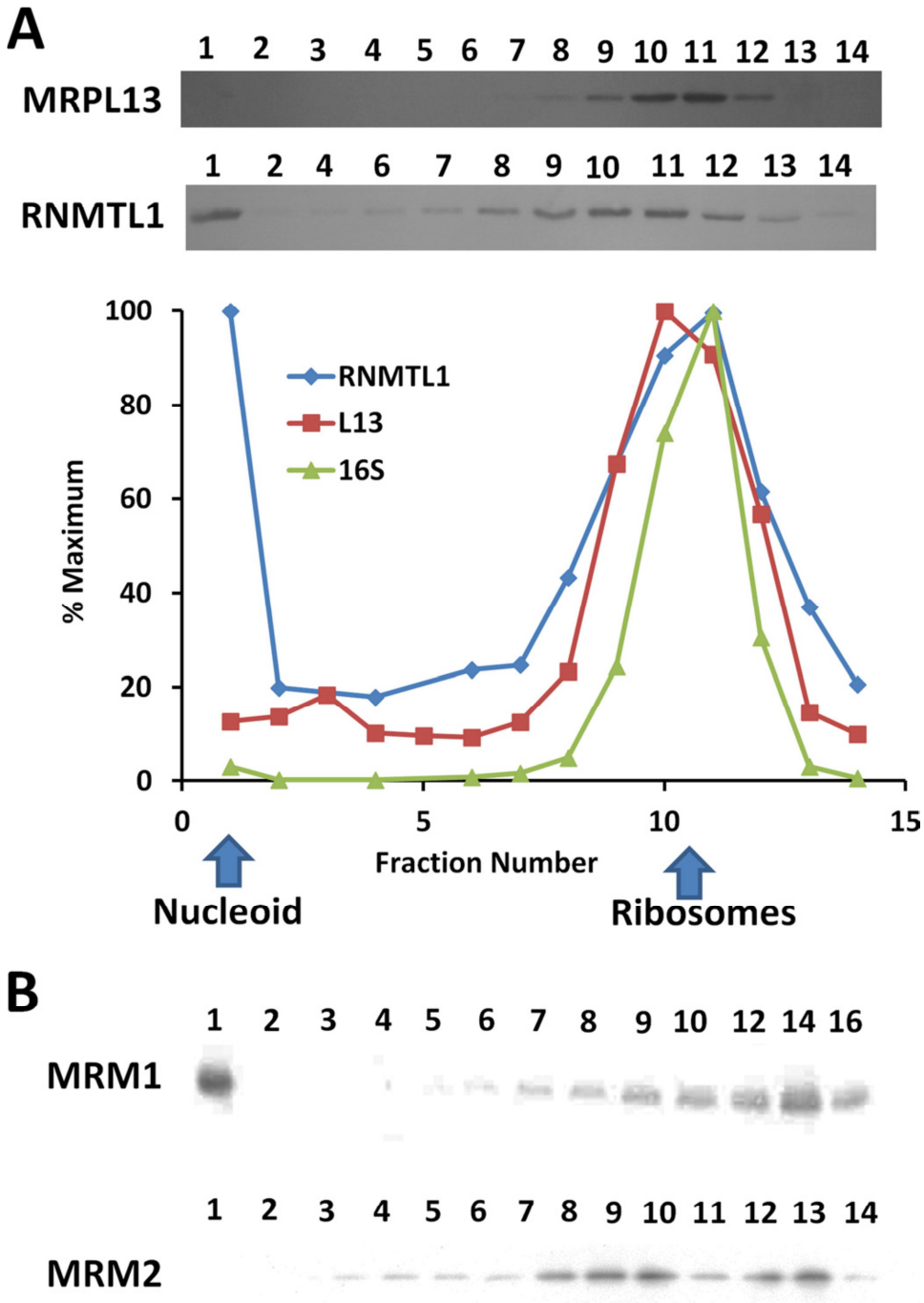

Figure 7 – RNMTL1 and MRM1 sediment with nucleoid and ribosomal complexes on a non-denaturing glycerol gradient, while MRM2 only sediments with ribosomal complexes. Proteins in the fractions were detected by immunoblotting, while 16S rRNA was detected by RNA extraction and RT-PCR. Relative amounts of RNMTL1 and MRPL13 proteins and 16S rRNA are graphed. (This experiment was conducted by D.F.B.).

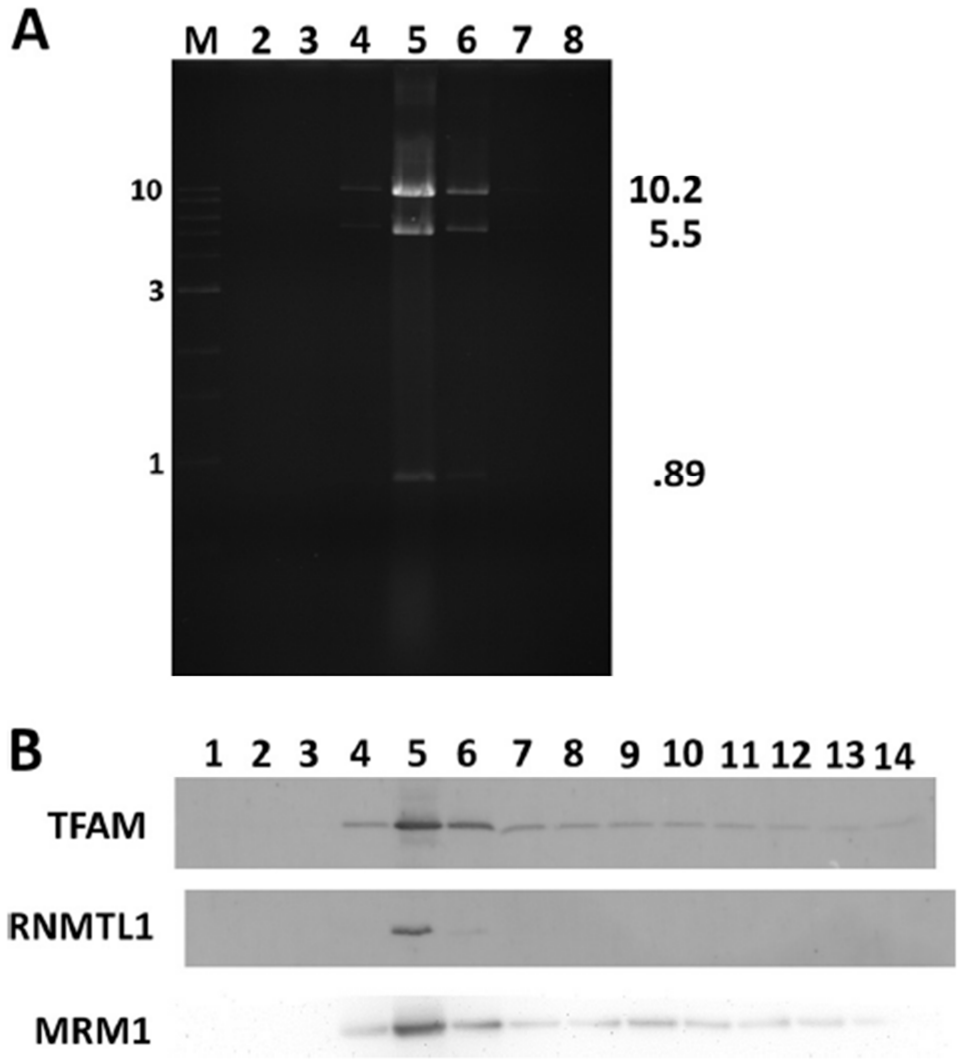

Figure 8 – RNMTL1 and MRM1 sedimenting with the nucleoid fraction remains associated with nucleoids after centrifugation through an iodixanol (OptiPrep) gradient. **A)** The nucleoid fraction from the glycerol gradient generated in **Fig 7** was loaded onto a 20-40% iodixanol gradient. Fractions were collected from the bottom and analyzed for mtDNA content by SYBR Green I fluorescence and HindIII restriction digest. Digested samples were run on agarose gel and stained with ethidium bromide. Sizes of DNA fragments are indicated on the right. M, 1 kb marker, with sizes indicated on the left. **B)** Fractions were probed for TFAM, RNMTL1 and MRM1 protein by immunoblotting. (This experiment was conducted by D.F.B.).

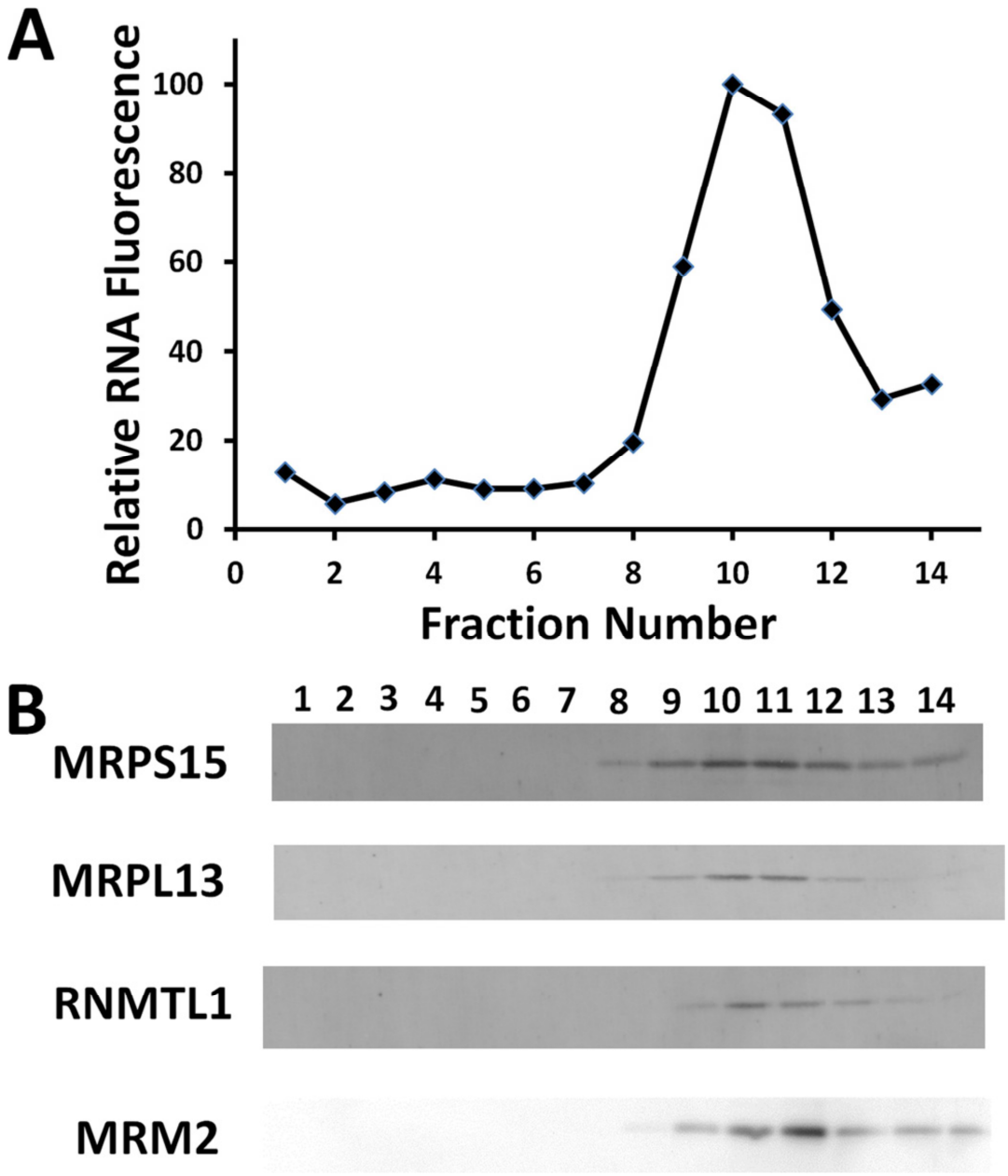

Figure 9 – RNMTL1 and MRM2 sedimenting with ribosomes in glycerol gradient fractions remain associated with ribosomes after centrifugation through an iodixanol gradient. Fractions 8-11 from the glycerol gradient produced in **Fig 7** were pooled and concentrated then separated on a 20-40% iodixanol gradient. Fractions were collected from the bottom and analyzed for RNA with SYBR Green II fluorescence (**A**) and for proteins by immunoblotting (**B**). (This experiment was conducted by D.F.B.).

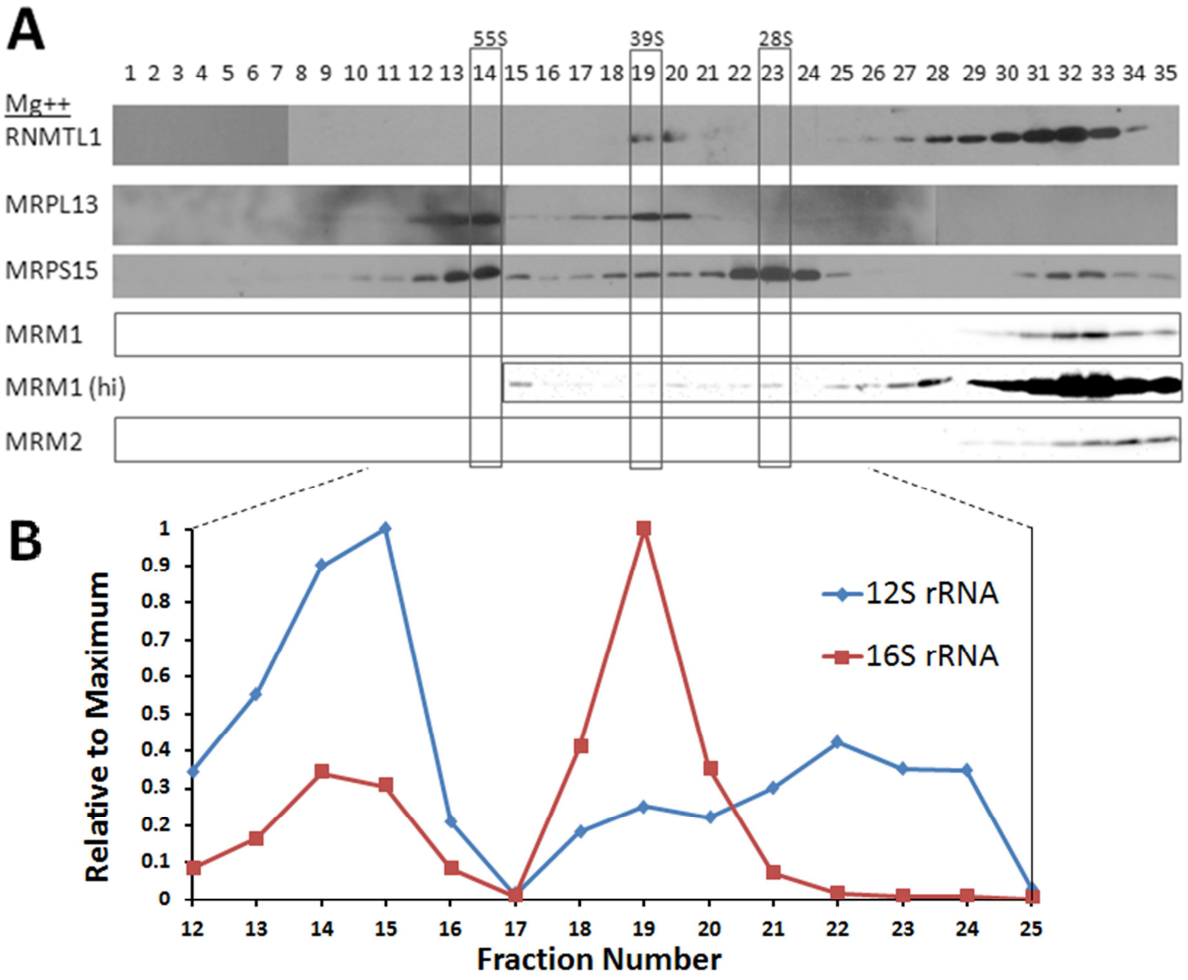

Figure 10 – RNMTL1 is associated with the LSU on a sucrose gradient supplemented with $MgCl_2$. Purified HeLa S3 mitochondria were lysed in non-denaturing conditions and the soluble fraction was layered onto a 10-30% sucrose gradient. Fractions were probed for LSU marker MRPL13, SSU marker MRPS15, RNMTL1, MRM1 and MRM2 proteins by immunoblotting (**A**) and fractions 12-25 were analyzed for relative quantities of 12S and 16S rRNA by RT-PCR (**B**). The immunoblot for MRM1 was overexposed to reveal a small proportion of protein migrating with denser complexes (MRM1 (hi)).

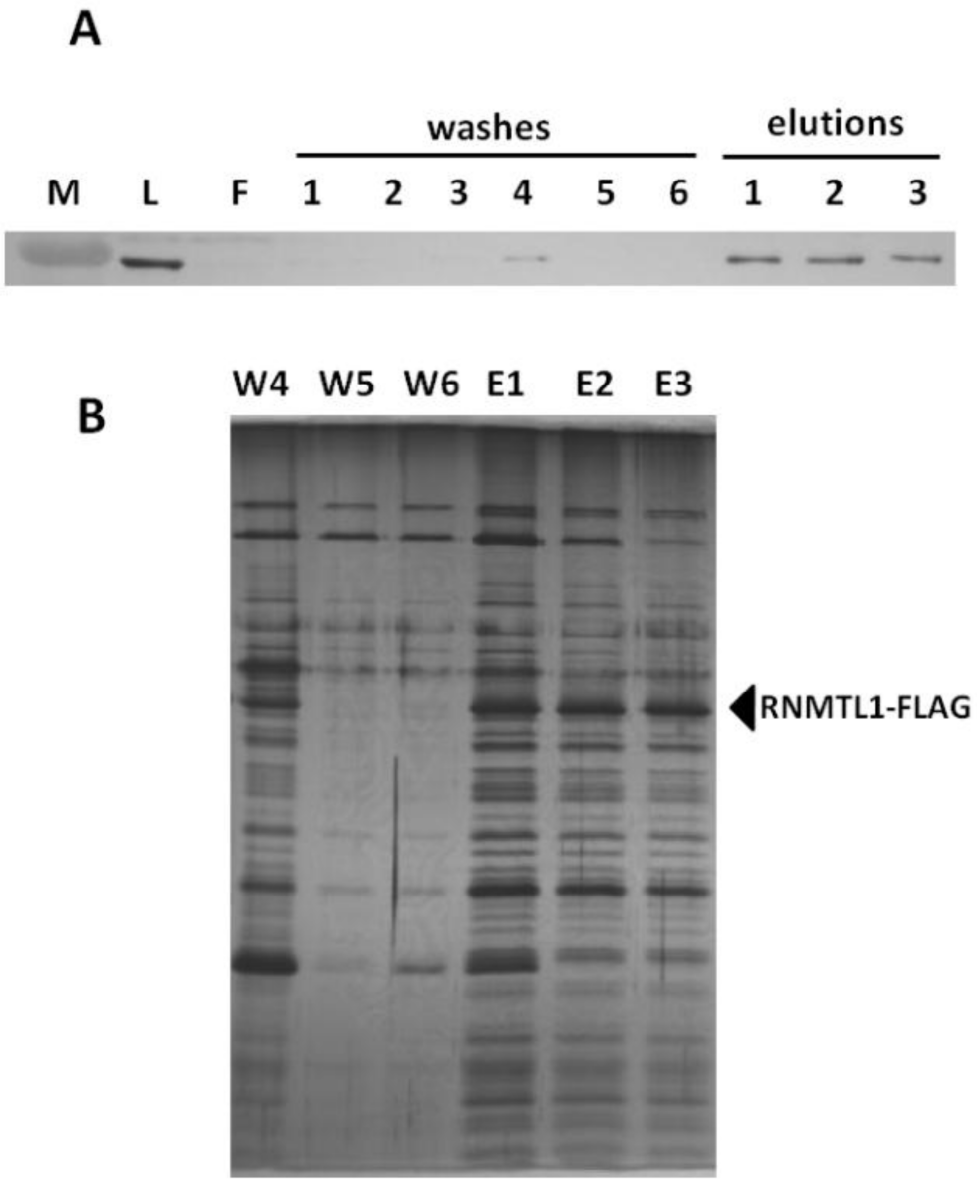

Figure 11 – Affinity chromatography purification of RNMTL1-3FH and associated proteins. Samples of the FLAG M resin washes and elutions were subject to SDS-PAGE and immunoblotting for FLAG (**A**) or silver staining (**B**). M, pre-stained protein marker, L, mitochondrial lysate loaded onto FLAG M resin.

Protein Name	Molecular mass (kDa)	Experiment 1 Spectral counts	Experiment 2 Spectral counts
RNMTL1	47	44	28
LRPPRC	157	11	18
DDX28	60	14	8
HSP60 (Hspd1)	61	3	18
HSP75 (GRP75)	73	1	19
p32 (C1qbp)	31	2	10
RPUSD4	42	7	3
PTCD3	78	0	9
GRSF1	42	2	6
SQRDL	50	4	4
MTERF3 (Mterfd1)	47	0	7
POLRMT	128	3	2
LRRC59	35	3	2

Table 6 – Well-represented non-ribosomal mitochondrial proteins that were co-immunoprecipitated by RNMTL1-3FH.

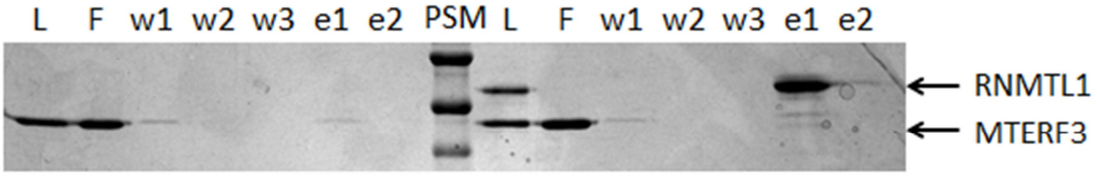

Figure 12 – Recombinant hsRNMTL1 does not interact with MTERF3. The fractions on the left of the pre-stained protein marker (PSM) correspond to a negative control experiment in which recombinant human MTERF3, which lacks a His-tag, was applied to Dynabeads. The beads were washed and bound proteins were removed by an elution buffer containing 1 M imidazole, pH 8.3 and 2% SDS. The fractions on the right of the marker correspond to an experiment testing whether recombinant His_6-tagged hsRNMTL1 bound to Dynabeads® can retain recombinant human MTERF3 on the beads. MTERF3 did not bind to hsRNMTL1 and did not remain indirectly bound to the beads. L, load; F, flowthrough (unbound); w1/w2/w3, bead washes; e1/e2, bead elutions.

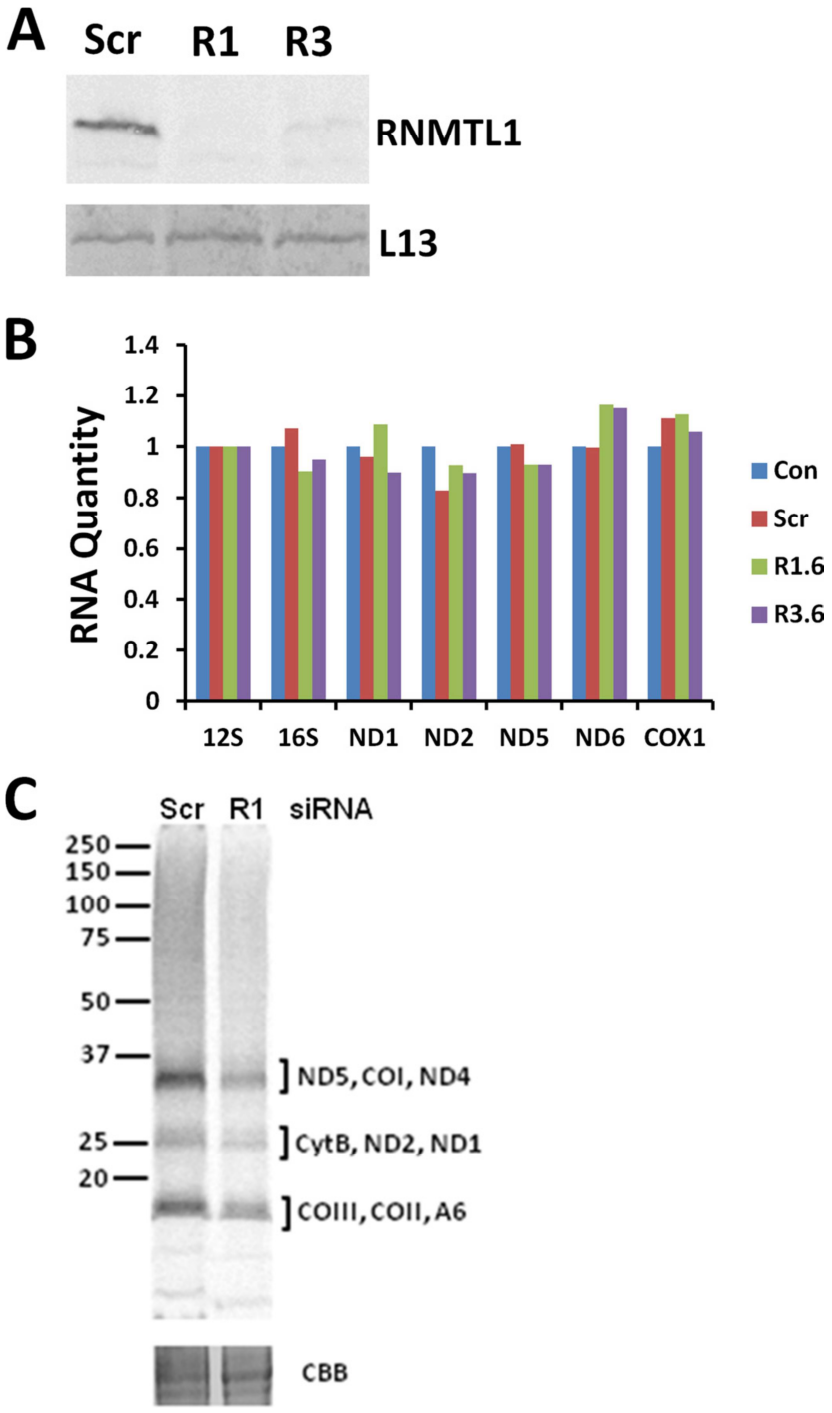
A
Scr
R1
R3
RNMTL1
L13
B
RNA Quantity
1.4
1.2
1
0.8
0.6
0.4
0.2
0
12S
16S
ND1
ND2
ND5
ND6
COX1
Con
Scr
R1.6
R3.6
C
Scr
R1
siRNA
250
150
100
75
50
37
25
20
ND5, COI, ND4
CytB, ND2, ND1
COIII, COII, A6
CBB

Figure 13

Figure 13 – siRNA-mediated depletion of RNMTL1 in HeLa cells decreased mitochondrial translation without drastically affecting mitochondrial transcript levels. **A)** HeLa cells were transfected with siRNA targeting a negative control, scrambled sequence (Scr) or siRNA targeting RNMTL1 (R1, R3). Purified mitochondria were probed for RNMTL1 and a loading control, MRPL13 by immunoblotting. **B)** RT-PCR analysis of mitochondrial transcripts after siRNA treatment normalized to 12S rRNA levels. Con, non-transfected, Scr, transfected with scrambled sequence, R1.6 and R3.6, two different siRNAs targeting RNMTL1 used at 6 nM. **C)** Autoradiograph of [^{35}S]cysteine/methionine labeled mitochondrial proteins after siRNA treatment. CBB, Coomassie Blue staining as a protein loading control. (This experiment was conducted by D.F.B.).

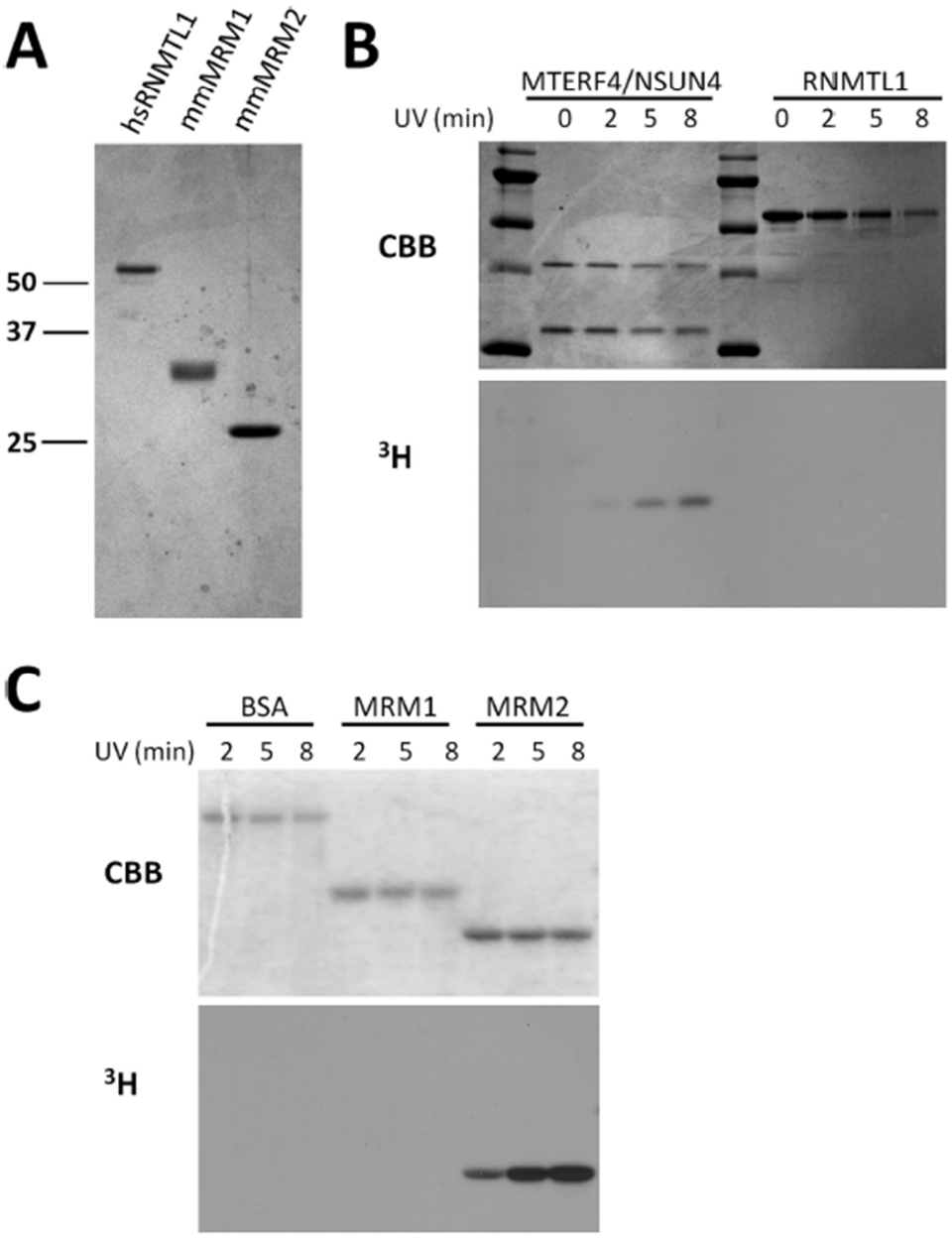

Figure 14 – Recombinant RNMTL1 and MRM1 do not cross-link to [^{3}H]AdoMet under conditions that permit cross-linking for NSUN4 and MRM2. **A)** 500 ng of recombinant proteins, human RNMTL1 (hsRNMTL1), mouse MRM1 (mmMRM1) and mouse MRM2 (mmMRM2) lacking their predicted mitochondrial localization signals were purified from *E. coli* and separated on SDS-12% polyacrylamide and visualized by Coomassie Blue staining. **B,C)** Human MTERF4/NSUN4 (3.48 pmol) (provided by the Miguel Garcia Diaz lab at Stony Brook University), RNMTL1 (14 pmol), BSA (14.5 pmol), MRM1 (51 pmol) and MRM2 (49 pmol) were incubated with [^{3}H]AdoMet, exposed to UV light for 0, 2, 5 or 8 min and separated by SDS-PAGE for Coomassie Blue staining (CBB), followed by fluorography (^{3}H).

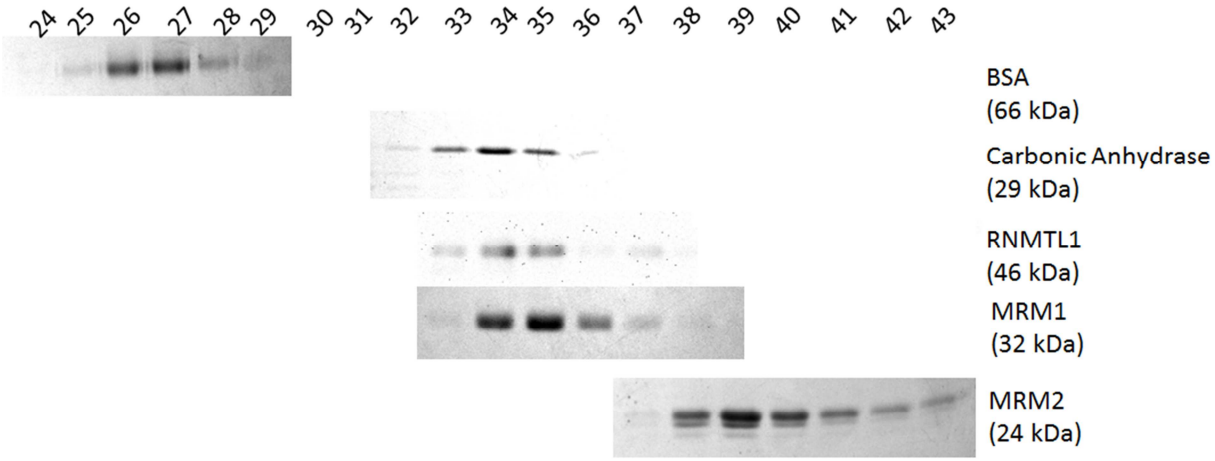

Figure 15 – Recombinant hsRNMTL1, mmMRM1 and mmMRM2 behave as monomeric proteins. The recombinant proteins were flowed through a Superose 6 gel filtration column and fractions were collected. Fractions were separated on standard SDS-PAGE and Coomassie Blue staining or immunoblotting in the case of hsRNMTL1. The BSA and carbonic anhydrase standards were run separately from the recombinant proteins.

Protein	Conditions	CPM
RNA only	+ $MgCl_2$	159
hsRNMTL1	+ $MgCl_2$	74
mmMRM1	+ $MgCl_2$	56
mmMRM2	+ $MgCl_2$	52
hsMTERF4-NSUN4	+ $MgCl_2$	166
RNA only	+ EDTA	87
hsRNMTL1	+ EDTA	42
mmMRM1	+ EDTA	63
mmMRM2	+ EDTA	43
hsMTERF4-NSUN4	+ EDTA	422

Table 7 – hsRNMTL1, mmMRM1 and mmMRM2 do not catalyze *in vitro* methylation of 16S rRNA. This experiment was conducted once under these conditions.

Chapter 4 – Assignment of Three Mitochondrial rRNA Methyltransferases to their Substrate Sites

There were several indications for the involvement of MRM1, MRM2 and RNMTL1 in the 2'-O-ribose methylation of G^{1145}, U^{1369} and G^{1370} sites on human 16S rRNA, respectively. 1) MRM1 (RlmB in bacteria, Pet56p in yeast mitochondria) and MRM2 (RrmJ/FtsJ in bacteria, Mrm2p in yeast mitochondria), and their equivalent rRNA methylation sites are evolutionarily conserved in bacteria and yeast mitochondria. 2) Analysis of the amino acid sequences revealed that MRM1 and RNMTL1 are predicted to have 2'-O-methyltransferase domains, and MRM2 has a FtsJ-like domain (FtsJ is a bacterial 2'-O-methyltransferase). 3) Human mitochondrial 16S rRNA contains a unique G^{1370} 2'-O-methylation site, whereas mitochondrial mRNAs and tRNAs are not known to possess a 2'-O-ribose methylation. 4) We found RNMTL1 weakly associated with the mitochondrial LSU, which may be mediated by interactions with 16S rRNA. The 2'-O-methylation of G^{1145}, U^{1369} and G^{1370} are likely important for ribosome assembly, stability, and/or function because their bacterial counterparts exist within regions that fold into a secondary structure participating in the peptidyltransferase center of the large ribosomal subunit. The secondary structure of human 16S rRNA that encompasses the 2'-O-ribose methylation sites is shown in **Fig 16A**. The G^{1145} site within the P-loop and the U^{1369} and G^{1370} sites within the A-loop of human 16S rRNA is compared to their corresponding sites in bacterial rRNA (**Fig 16B**). In bacteria, G^{2251} in the P-loop is crucial for tRNA binding and peptidyl transferase activity (Green et al., 1997). This site may mediate a long-range interaction with sites over 300 nucleotides away in sequence (Green et al., 1997). In bacteria, U^{2552}, which corresponds to U^{1369} in human 16S rRNA, is base-paired to C^{2556}. While 2'-O-methylation of U^{2552} does not have a

major effect on the A-loop fold, it has an impact on the conformation of U^{2555} and C^{2556} residues, which may mediate tertiary interactions in the ribosome, by shifting the sugar pucker of C^{2556} into a specific conformation (Blanchard and Puglisi, 2001).

A. Mapping the site of modification attributable to RNMTL1 using primer extension

We proceeded to use a common method of mapping 2'-O-ribose methylation sites to study RNMTL1. Reverse transcriptase is inhibited by a 2'-O-ribose site at low dNTP concentrations, but can bypass the modification site at high dNTP concentrations (Maden, 2001). Thus reverse transcriptase-mediated extension of a DNA primer on a RNA template would stall at 2'-O-methylation sites. We designed a primer that anneals four nucleotides downstream of the G^{1145} site and a primer that anneals downstream of the G^{1370} site on 16S rRNA (**Fig 17A**). The primers were radioactively 5' end-labeled by polynucleotide kinase and γ-[^{32}P]ATP, and annealed to 500 ng of *in vitro*-synthesized 16S rRNA or RNA from crude mitochondria from HeLa cells treated with siRNA targeting a scrambled sequence or RNMTL1 for three days. The reaction proceeded with Superscript 3 reverse transcriptase and 2, 4 or 6 nM dNTPs. Separation of the primer extension products on sequencing gels revealed no effect of R1 siRNA on reverse transcriptase read-through of the G^{1145} site relative to control siRNA (**Fig 17B**), whereas it caused an increased read-through of G^{1370} (**Fig 17C**). From this, we conclude that RNMTL1 is involved in the methylation of G^{1370} and not G^{1145}. This experiment also revealed subtle problems in interpreting primer extension results. G^{1145} is situated in the middle of a G-rich equence, which is known to inhibit primer extension. Also, the juxtaposition of U^{1369} and G^{1370} modifications presents a challenge in determining the extent of primer extension past each site.

B. Mapping the 2'-O-methylation sites on 16S rRNA with DNAzymes

We sought to develop an alternative method to confirm the assignment of RNMTL1 to methylation of G^{1370} and to map the methylation sites of MRM1 and MRM2. We reviewed the literature for alternative methods of detecting 2'-O-ribose methylation. These methods include resistance to RNase H when hybridized to a chimeric oligonucleotide (Yu et al., 1997), splint ligation (Saikia et al., 2006), reverse transcription coupled to PCR (Dong et al., 2012), mass spectrometry, two-dimensional thin layer chromatography of nuclear digests, and boronate affinity chromatography, among other techniques (Behm-Ansmant et al., 2004). A simple, low-cost and definitive method that has not received much attention is the use of DNAzymes (Buchhaupt et al., 2007; Cruz et al., 2004), which are single-stranded deoxy-oligonucleotides that consist of two annealing arms flanking a "catalytic bubble" (**Fig 18A**). The arms direct the DNAzyme to a specific di-nucleotide junction of the RNA and the catalytic bubble directs a divalent metal ion (magnesium or manganese) to promote the RNA to undergo self-cleavage at the targeted site. The mechanism of DNAzyme-mediated RNA self-cleavage is shown by Buchhaupt et al (Buchhaupt et al., 2007). The ribose 2'-OH of the RNA undergoes a nucleophilic attack on its own 3'-phosphodiester bond. If the RNA is methylated at the 2'-OH, then it cannot undergo self-cleavage in the presence of a targeted DNAzyme. We designed Type 8-17 and Type 10-23 DNAzymes to target the cleavage of G^{1144}, a control site that is known to be unmethylated, and the three methylated sites G^{1145}, U^{1369} and G^{1370}. We tested the efficiency of these DNAzymes on unmodified, *in vitro*-synthesized 16S rRNA and observed that the RNA is cleaved to near completion for each of the targeted sites (**Fig 18B**) (Lee and Bogenhagen, 2014).

We tested the efficacy of two siRNAs targeting each of human MRM1 (siMRM1-A and siMRM1-B) and MRM2 (siMRM2-A and siMRM2-B). HeLa cells were transfected with 3 nM

siRNA for 3 days and crude mitochondria were isolated. Equal amounts of mitochondrial protein from treated cells were immunoblotted and compared to the Scr control. siMRM1-B and siMRM2-B were more effective at depleting the cells of MRM1 and MRM2, respectively (**Fig 19A,B**). We have also previously validated the efficacy of siRNA "R1" in depleting human cells of RNMTL1 protein (**Fig 12A**).

Having three known 16S rRNA methylation sites and three putative mitochondrial 2'-O-ribose rRNA methyltransferase proteins, we then utilized DNAzymes in combination with siRNA and Northern blotting as tools to assign the methyltransferases to their substrate sites (**Fig 20**). We tested whether knockdown of the methyltransferases would increase the susceptibility of 16S rRNA to DNAzyme-mediated cleavage at the known methylation sites. After 3 nM siRNA treatment for 3 days, the cells were trypsinized and washed in PBS, and then whole cell RNA was extracted by TRIzol®. We performed a subsequent phenol-chloroform extraction and ether extraction prior to ethanol precipitation to obtain highly purified RNA. This step was necessary as some contaminants remain associated with the RNA after TRIzol extraction. 2 μg of RNA were treated with a stoichiometric excess of DNAzyme (400 pmol). The RNA was separated on a denaturing agarose gel and the ethidium bromide staining was imaged with UV light. The bands in the lower panels correspond to cytosolic rRNAs, which are estimated to be 100 times more abundant than the mitochondrial rRNAs (King and Attardi, 1993), and serve as loading controls (**Fig 21A**). Somewhat surprisingly, 16S rRNA from cells treated with the negative control siRNA had an observable level of accessibility to DNAzymes targeting cleavage at G^{1145} and U^{1369} (**Fig 21A**). Quantification of the extent of cleavage (see Materials and Methods) revealed approximately 34% cleavage at G^{1145} (n=3), approximately 30% cleavage at U^{1369} (n=5), and approximately 9% cleavage at G^{1370} (n=5) in the Scr control samples. Since

DNAzymes cannot direct RNA self-cleavage at sites that have a 2'-O-methyl group, this indicates that 16S rRNA is not completely modified under normal cell growth conditions. However, there are several caveats to the absolute quantification of DNAzyme-mediated RNA cleavage: 1) despite careful handling, the RNA loaded per lane has slight variability, 2) the intensity of bands detected on X-ray film follows a non-linear response, 3) the level of background detected by X-ray film is variable and sometimes a smear may appear to indicate intensity from a band, and 4) different cell lines may have different levels of steady-state methylation on 16S rRNA. Nonetheless, we consistently observed a significant increase in cleavage at G^{1145} when MRM1 was knocked down in HeLa cells, and a significant increase in G^{1370} cleavage when RNMTL1 was knocked down (**Fig 21A**). However, when we analyzed the RNA from cells treated with siRNA targeting MRM2 under these conditions, we did not observe an obvious change in cleavage at U^{1369} with siRNA targeting any of the methyltransferases (data not shown).

We reasoned that the significant level of unmodified 16S rRNA at U^{1369} in HeLa cells complicated our effort to document an increase in accessibility of this site to DNAzymes after depletion of MRM2. Therefore, we tested whether some level of unmodified 16S rRNA at U^{1369} is observed in another human cell line. We treated HEK293T cells with siRNA as we had HeLa cells. HEK293T cells have a higher level of 16S rRNA unmethylated at G^{1145} than HeLa cells, whereas HeLa cells have a higher level of unmethylated U^{1369}. These experiments in HEK293T cells confirmed that knockdown of MRM1 and RNMTL1 causes increased cleavage at G^{1145} and G^{1370}, respectively (**Fig 21B**). There was a slight improvement in 16S rRNA cleavage at U^{1369} due to depletion of MRM2 relative to the negative control compared to HeLa cells (**Fig 21B**). We then doubled the amount of siRNA targeting MRM2 to 6 nM and the corresponding amount

of RNAiMax in HEK293T cells, and supplemented the media with 1 mM sodium pyruvate and 50 μg/ml uridine. This produced a much more significant effect, clearly indicating that knockdown of MRM2 causes increased cleavage at U^{1369} (**Fig 21C**). A summary combining the results of HeLa and HEK293T data reveals the effects of depleting each of the methyltransferase proteins on each methylation site (n≥3 for each set), (**Table 8**). On average, siRNA targeting MRM1 increased DNAzyme-mediated 16S rRNA cleavage at G^{1145} compared to the negative Scr control by ~1.7-fold. The effect of siRNA targeting MRM2 increased cleavage at U^{1369} by ~1.4-fold, compared to the control, and the effect of siRNA targeting RNMTL1 increased cleavage at G^{1370} by ~2.5-fold, compared to the control. While the quantification of RNA cleavage is subject to variability, we consistently see that siRNA targeting MRM1, MRM2 and RNMTL1 leads to obvious increases in the susceptibility of 16S rRNA to DNAzyme-mediated cleavage at G^{1145}, U^{1369} and G^{1370}, respectively. Although we have not yet ruled out an indirect mechanism of action, we have provided convincing data that allows the assignment of MRM1, MRM2 and RNMTL1 as 2'-O-methyltransferases specific to G^{1145}, U^{1369} and G^{1370} sites, respectively.

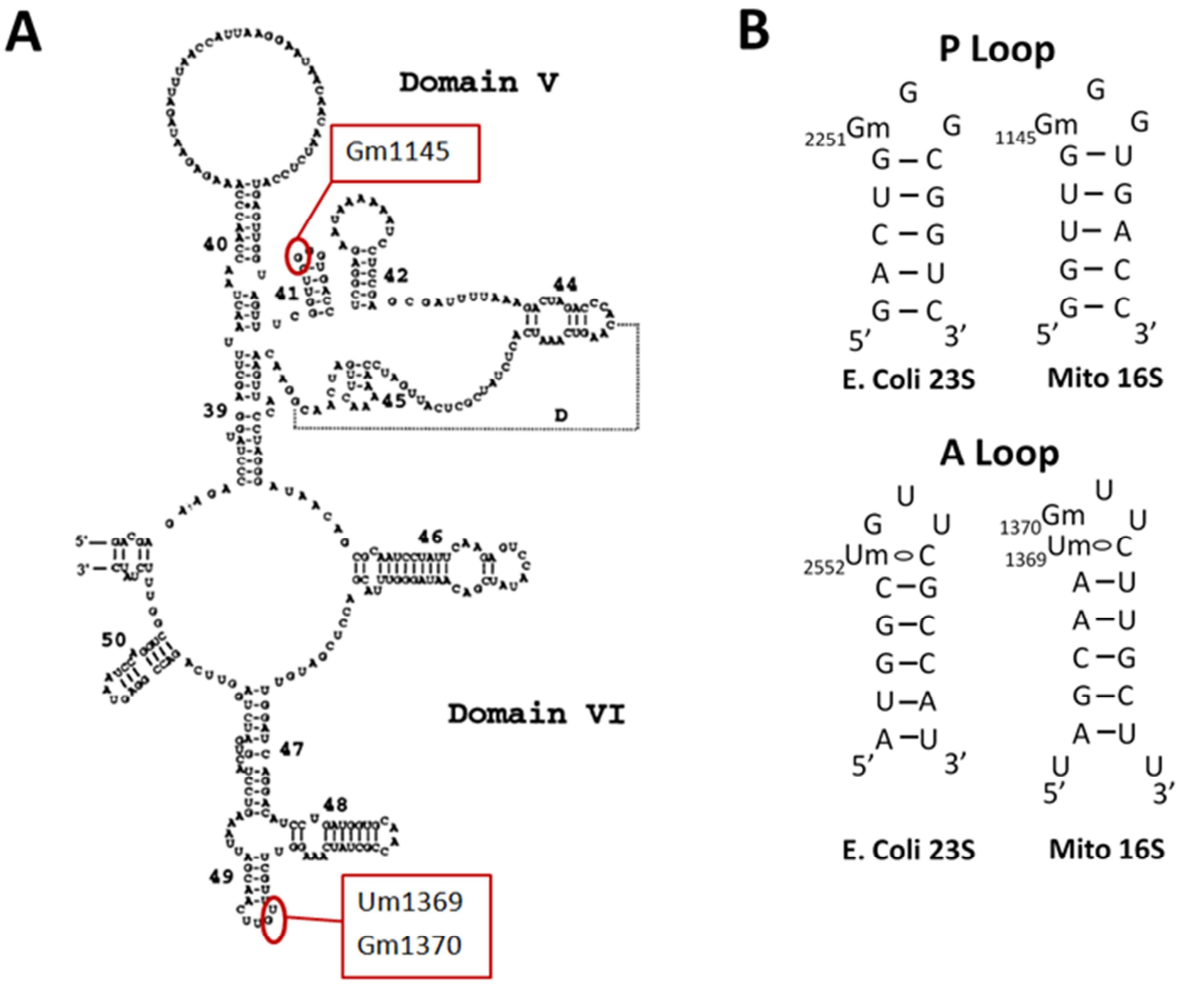

Figure 16 – The methylation sites on mitochondrial 16S rRNA that are conserved in bacteria contribute to secondary structures in the P-loop and A-loop, which participate in the peptidyl transferase center. **A)** The 2'-O-ribose methylations located in human mitochondrial 16S rRNA. **B)** Comparison of the secondary structure encompassing the conserved methylation sites on mitochondrial and bacterial large ribosomal subunit rRNA.

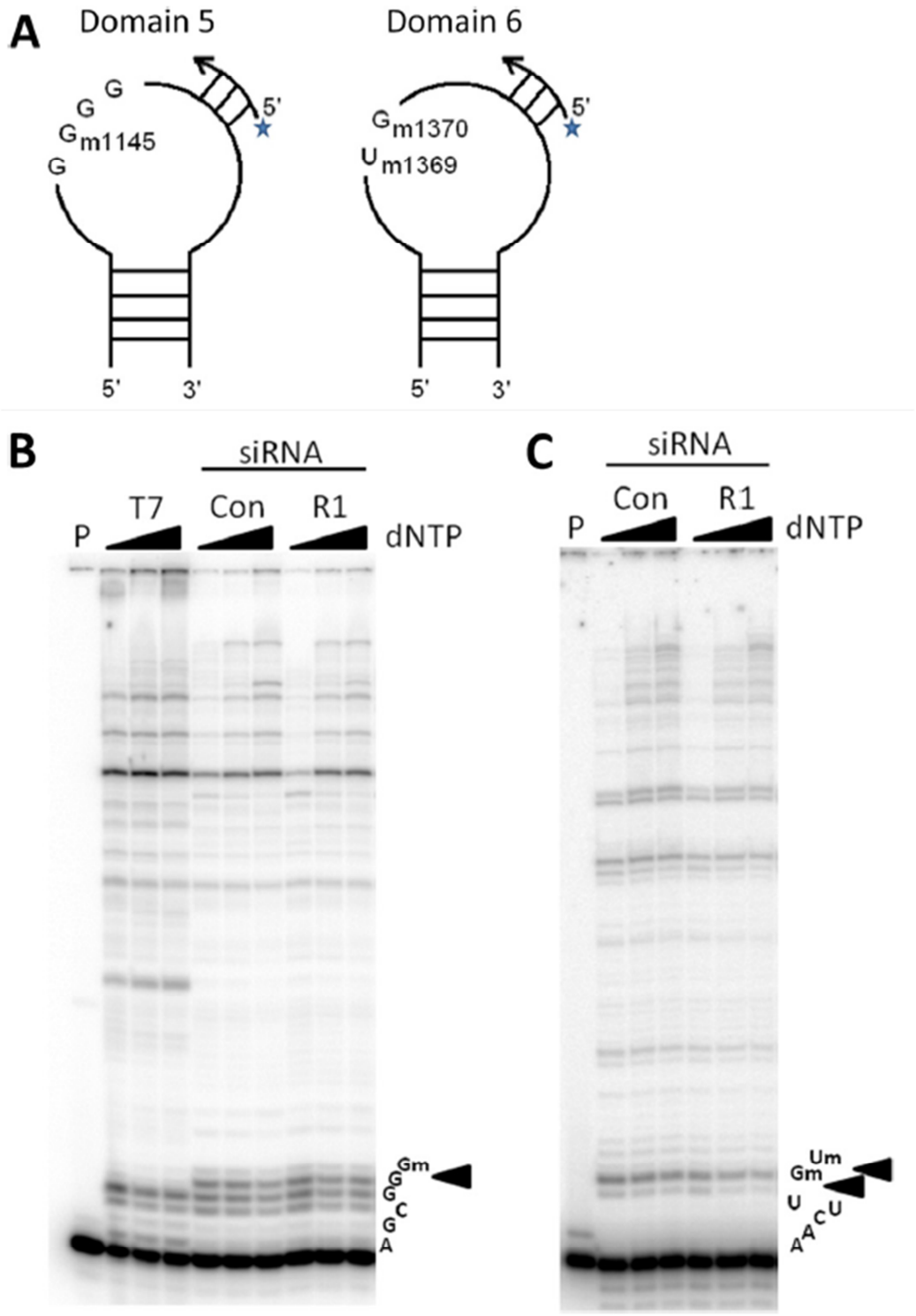
A
Domain 5
Domain 6
G
G
Gm1145
G
5'
5'
3'
Gm1370
Um1369
5'
5'
3'
B
siRNA
T7
Con
R1
P
dNTP
Gm
G
G
C
G
A
C
siRNA
Con
R1
P
dNTP
Um
Gm
U
A
A
C
U

Figure 17

Figure 17 – Depletion of RNMTL1 increases reverse transcriptase extension past G^{1370} in domain 6 of 16S rRNA. **A)** Primers were designed to anneal to 4 or 5 nucleotides upstream of known methylation sites in domain 5 or domain 6. RNA was isolated from HeLa cells treated with Scr (Con) or R1 siRNA, or from *in vitro* transcription of the 16S rRNA gene by T7 RNA polymerase. Primers targeting domain 5 (**B**) or domain 6 (**C**) were radioactively 5' end labeled and annealed to 500 ng RNA, then incubated with reverse transcriptase and 2, 4 or 6 nM dNTPs. Reactions were electrophoresed through a urea-14% polyacrylamide DNA sequencing gel and radioactivity was detected by a phosphor storage screen. The sequence of RNA extended by reverse transcriptase is shown on the right of the gel image. P, primer, T7, primer extension through unmodified RNA, arrows, bands of interest due to methylated nucleotides. (This experiment was conducted by D.F.B.).

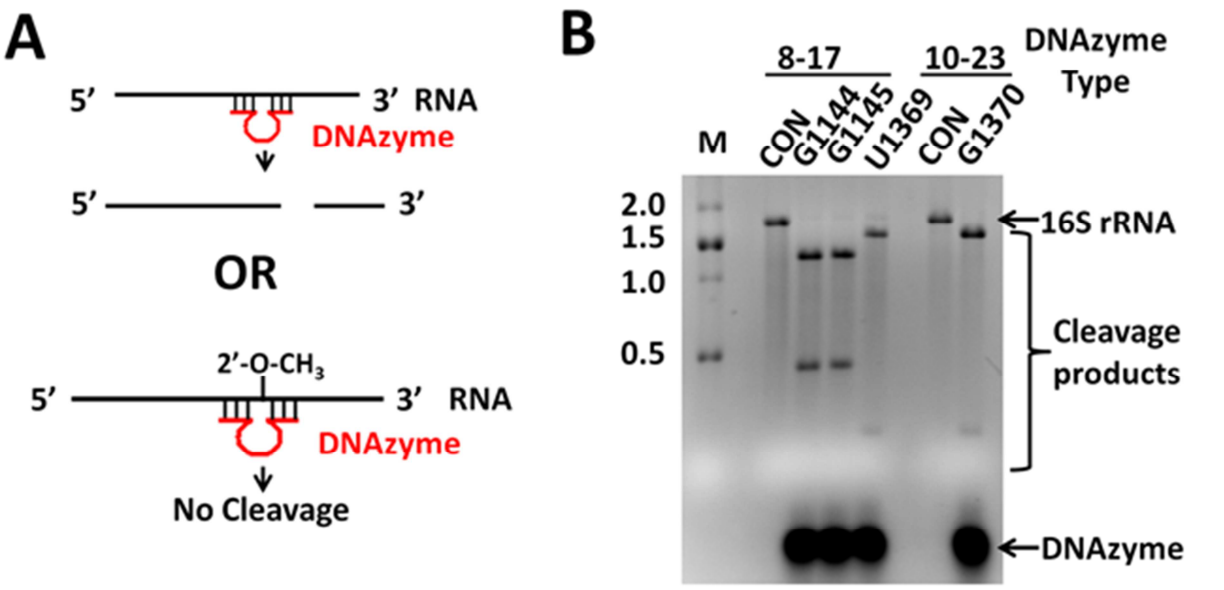

Figure 18 – DNAzymes effectively cleave unmodified RNA and are an effective tool for studying 2'-O-ribose methylation of RNA. **A)** Approach to determining whether RNA is 2'-O-methylated or unmodified. DNAzyme (red) anneals to unmodified RNA (black) and promotes site-specific RNA self-cleavage. **B)** 0.75 μg of *in vitro*-synthesized 16S rRNA were treated with DNAzymes targeting G^{1144} and the three methylation sites and separated on a 2% agarose gel. M, 1 kb marker.

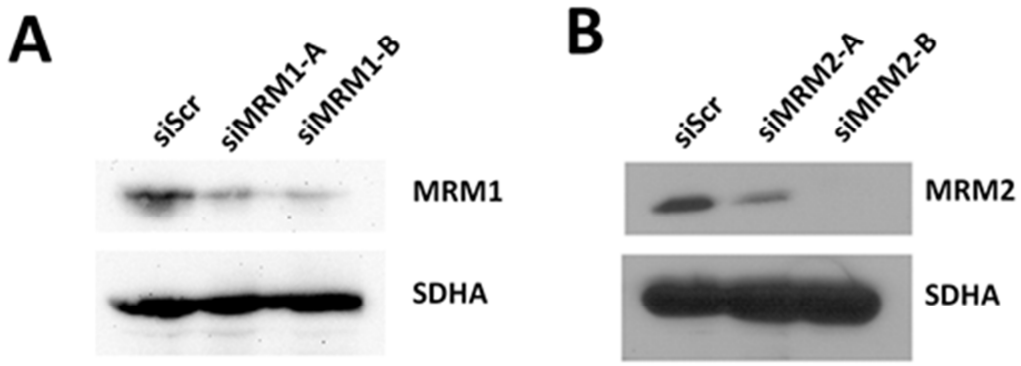

Figure 19 – siRNA effectively depletes MRM1 and MRM2 protein levels in HeLa cells. Crude mitochondria isolated from HeLa cells were treated with 3 nM siRNA for 3 days. Mitochondria were analyzed by SDS-PAGE and immunoblotting. siMRM1-B (**A**) and siMRM2-B (**B**) were more effective than siMRM1-A and siMRM2-A, respectively. SDHA, mitochondrial succinate dehydrogenase subunit A, serving as a loading control.

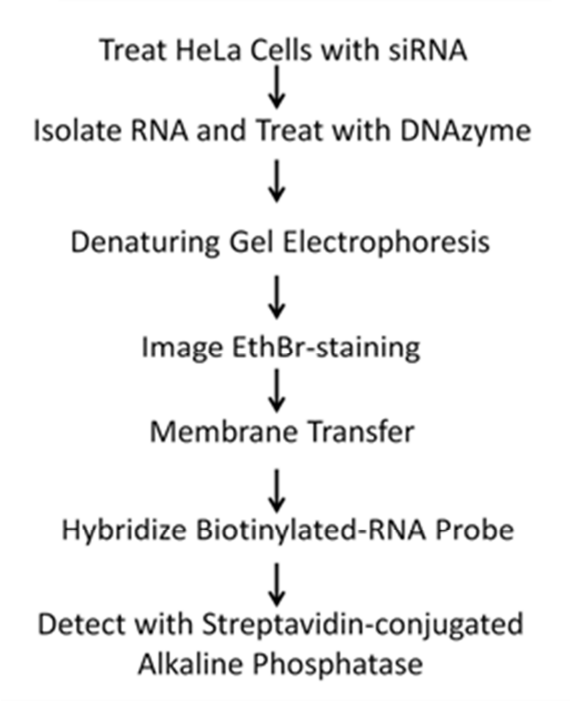

Figure 20 – Schematic of the application of siRNA and DNAzymes to assign 2'-O-methyltransferases to their substrate sites.

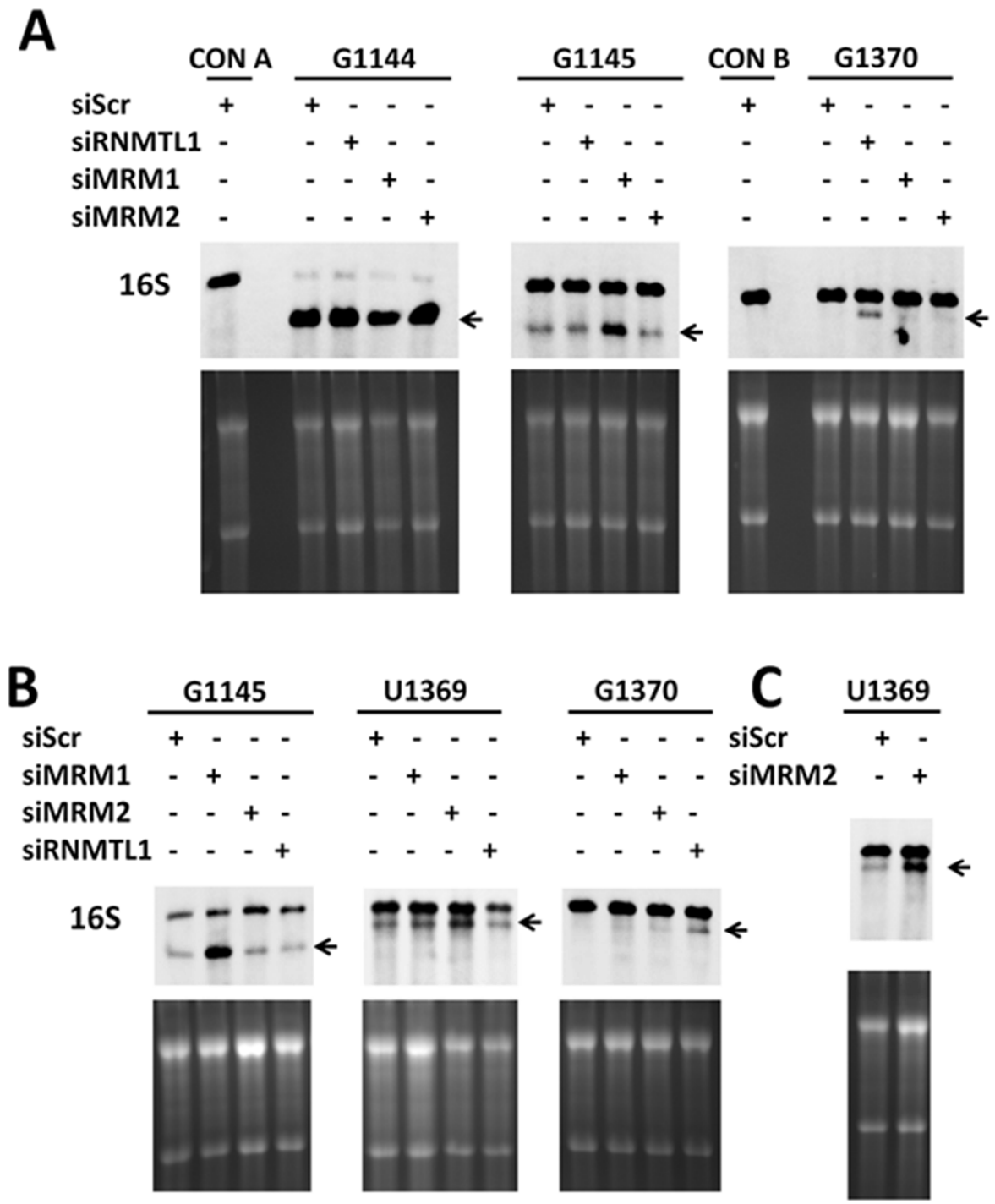
A
CON A
G1144
G1145
CON B
G1370
siScr
siRNMTL1
siMRM1
siMRM2
16S
B
G1145
U1369
G1370
siScr
siMRM1
siMRM2
siRNMTL1
16S
C
U1369
siScr
siMRM2

Figure 21

Figure 21 – DNAzymes allow the assignment of 2'-O-methyltransferases to their substrate sites. 2 μg of whole cell RNA was isolated from HeLa (**A**) and HEK293T (**B**) cells treated with 3 nM siRNA for 3 days, and analyzed by DNAzymes and Northern blotting. DNAzyme-mediated G^{1144} cleavage was robust in all conditions tested, as expected. siRNA targeting MRM1 and RNMTL1 significantly enhanced the cleavage of 16S rRNA at G^{1145} and G^{1370}, respectively, compared to the control siRNA targeting a scrambled sequence (**A,B**). siRNA targeting MRM2 slightly increased the cleavage at U^{1369} compared to the control siRNA (**B**), but when HEK293T cells were treated with 6 nM siRNA, the effect was much more significant (**C**).

Condition	% Cleavage at G1145	% Cleavage at U1369	% Cleavage at G1370
siScr	19.17	39.26	2.55
	50.66	30.99	11.81
	34.27	34.12	13.80
		22.12	6.13
		22.90	11.00
Average	34.70	29.88	9.06
Stdev	15.75	7.35	4.60
SEM	9.09	3.29	2.06
siMRM1	35.95	39.59	9.58
	70.04	36.71	7.90
	72.32	20.80	10.41
			11.60
Average	59.44	32.37	9.87
Stdev	20.37	10.12	1.55
SEM	11.76	5.84	0.78

Condition	% Cleavage at G1145	% Cleavage at U1369	% Cleavage at G1370
siMRM2	13.83	48.24	8.30
	40.27	34.90	9.46
	24.95	44.30	14.20
		39.95	9.09
		41.40	9.00
Average	26.35	41.76	10.01
Stdev	13.28	4.97	2.38
SEM	7.66	2.22	1.06
siRNMTL1	18.89	42.31	14.63
	37.83	26.75	32.59
	23.57	34.62	30.10
		22.20	19.75
			17.10
Average	26.76	31.47	22.83
Stdev	9.87	8.86	8.03
SEM	5.70	4.43	3.59

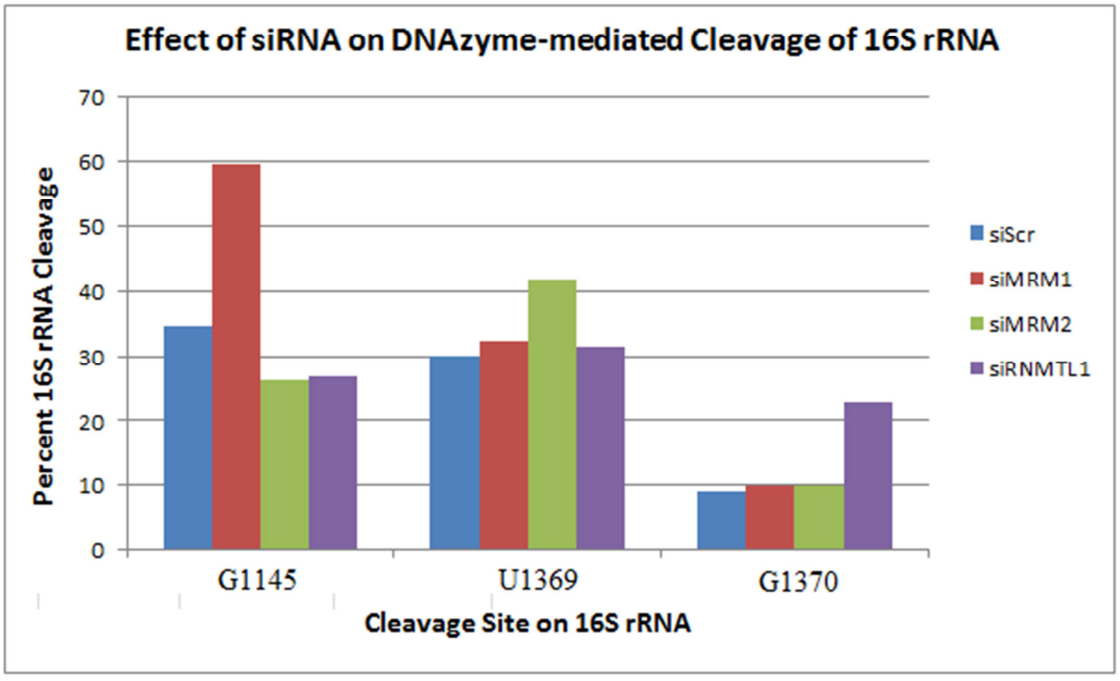

Table 8 – Quantification of the effects of siRNA on DNAzyme-mediated 16S rRNA cleavage. This table combines data from HeLa and HEK293T cells treated with siRNA for 3 days and the average data is graphed.

Chapter 5 – Conclusion and Perspectives

I have presented data produced by subcellular fractionation, confocal microscopy, sedimentation through different gradients and immunoprecipitation combined with mass spectrometry demonstrating that the three novel mammalian proteins MRM1, MRM2 and RNMTL1 are localized to mitochondria and are tightly associated with mtDNA nucleoids. In gradients with relatively low salt concentrations and in the presence of EDTA, a large proportion of MRM1 was found associated with the nucleoid complex or as a free protein, and although MRM2 did not have much presence in the nucleoid complexes, a significant proportion of MRM2 was found in fractions that contained both mitoribosomal subunits and incompletely processed mitochondrial RNAs that have retained some tRNA junctions (Bogenhagen et al., 2014). This indicates that not all of the ribosomes in these fractions are fully assembled. RNMTL1 was found to be associated with both nucleoid and ribosomal complexes. It is possible that MRM1, MRM2 and RNMTL1 are associated with incompletely assembled ribosomal intermediates and may modify nascent rRNA or rRNA that is being assembled into the ribosome. These proteins may also have methyltransferase-independent roles in ribosome assembly and other processes, such as serving as checkpoints for ribosome assembly. Perhaps the methyltransferases do not catalyze the methyl transfer reaction until the ribosome subunits have reached a particular stage in assembly or until mitochondria have received the proper signals to complete ribosome assembly. This would be consistent with the levels of unmethylated 16S rRNA detected in our RNA analysis. Under higher salt conditions (100 mM KCl) and in the presence of 20 mM $MgCl_2$ used in the sucrose gradient, RNMTL1 was the only one of the three proteins to have maintained a significant association with the LSU, while MRM1 and MRM2 behaved essentially as free proteins. The sequence of events involving RNA processing, RNA

modification and RNA incorporation into mitoribosomes is still unclear. It will be important in the future to understand the exact substrate of the RNA methyltransferases and the timing of their function.

RNMTL1 is important for mitochondrial translation, as its depletion over 3 days did not significantly alter mitochondrial transcript levels, but severely decreased mitochondrial protein synthesis. Knockdown of MRM2 in human cells has also been demonstrated to cause a significant reduction in mitochondrial translation (Rorbach et al., 2014). It will be of interest to determine whether depletion of MRM1 will produce a similar effect. Nonetheless, siRNAs did not completely abolish mitochondrial translation, suggesting that: 1) the activity of the residual proteins is sufficient to maintain a low level of translation, 2) the pre-existing translation machinery is stabilized, and/or 3) there is a compensation mechanism in mitochondria similar to that in bacteria and yeast mitochondria, for example, by overexpression of a RA-GTPase.

I purified recombinant mouse MRM1, mouse MRM2 and human RNMTL1 proteins from *E. coli*. hsRNMTL1 and mmMRM1 did not bind and crosslink to AdoMet in the same conditions that NSUN4 and mmMRM2 were able to. I was not able to observe RNA methyltransferase activity with naked 16S rRNA, *in vitro*. These proteins behaved as monomers, despite the fact that all other known members of SPOUT family proteins that include RNMTL1 and MRM1 exist as dimers (Tkaczuk et al., 2007). It is also possible that in the purification process, the exposure of proteins to the low salt concentrations may have caused protein aggregation and subsequent loss of activity. Alternatively, expression of recombinant proteins in bacteria dismisses the possible requirements for post-translational modifications and/or protein folding with certain chaperones. Perhaps purification of recombinant proteins from an insect cell line or rabbit reticulocyte lysate would generate functional proteins. Endogenous proteins may also be isolated

from large-scale mitochondrial preparations from cells by ion exchange, size exclusion, and/or immuno-purification. The inability to observe RNA methylation *in vitro* may be due to the requirement of a protein partner, as in the case of MTERF4-NSUN4 (Yakubovskaya et al., 2014), although methylation of the NSUN4 substrate site was independent of MTERF4 *in vivo* (Metodiev et al., 2014). I identified endogenous MTERF3 among other proteins that co-immunoprecipitate with murine RNMTL1-3FH, and since MTERF3 is a mitoribosomal LSU biogenesis factor (Wredenberg et al., 2013), we considered whether MTERF3 and RNMTL1 behaved like the MTERF4-NSUN4 complex. However, I was not able to provide evidence that recombinant human MTERF3, can interact with hsRNMTL1 *in vitro*. The native Stokes radii of the mitochondrial rRNA methyltransferases can be studied in further detail by analyzing mitochondrial lysates by gel filtration, similar to our analysis of the recombinant proteins. This method would provide a different resolution than sedimentation gradients and would give insight on whether the endogenous proteins in the low molecular weight pool exist as monomers, dimers or multimers. Additionally, MRM1- and MRM2-interacting proteins can be identified by immunoprecipitation and mass spectrometry as conducted for RNMTL1. It will be important to compare the set of proteins that interact with the methyltransferases on an RNA-dependent manner to those that interact on an RNA-independent manner. This can be accomplished by treating the mitochondrial lysate with RNase A prior to co-immunoprecipitation.

MRM1, MRM2 and RNMTL1 were putatively identified as 2'-O-ribose rRNA methyltransferases based on their amino acid sequence homology to known methyltransferase domains. Additionally, MRM1 and MRM2 have bacterial and yeast mitochondrial counterparts that methylate sites corresponding to human 16S rRNA at G^{1145} and U^{1369}, respectively. Mitochondrial RNMTL1 and G^{1370} methylation appear to be exclusive to higher eukaryotes, thus

we speculated that RNMTL1 catalyzes 2'-O-ribose methylation of G^{1370}. Primer extension assays with reverse transcriptase indicated that RNMTL1 is indeed involved in the methylation of 16S rRNA at G^{1370}. However, the reverse transcriptase-mediated primer extension assay would not have been a good approach to assess methylation at G^{1145} and U^{1369} since the assay depends on a reduced probability of bypassing the methylation sites at low dNTP concentrations. G^{1145} is immersed in a G-rich sequence and reverse transcriptase encounters an adjacent methylation site prior to U^{1369}. Both situations present problems for the primer extension assay. Instead, DNAzyme analysis was applied to confirm that RNMTL1 is involved in the 2'-O-ribose methylation of G^{1370}, and to provide the first set of data to assign MRM1 and MRM2 to the methylation of G^{1145} and U^{1369}, respectively. Although an indirect mechanism of methylation has not been ruled out, MRM1 and MRM2 appear to be bona fide rRNA 2'-O-methyltransferases, much like their bacterial and yeast mitochondrial counterparts.

There are other future experiments that could be undertaken to improve understanding of the roles of these three rRNA methyltransferases and how they fit into the broader picture of ribosome biogenesis and function, and even in mitochondrial biogenesis. One may consider generating cell lines with a knock-out of each of the rRNA methyltransferases and combinations of them. Recent developments in genome engineering are providing affordable methods of specific gene manipulation (Gaj et al., 2013). Knock-out cells may need to be cultured in media supplemented with sodium pyruvate and uridine if they are deficient in mitochondrial function. If there is an overlap in substrate specificity amongst the rRNA methyltransferases, one may assess the ability to rescue possible defects in the knock-out cells by overexpressing combinations of the mitochondrial rRNA methyltransferases. It will also be of interest to identify rRNA methyltransferase mutations that inactivate the RNA-binding domain or AdoMet-binding

domain, or mutations of residues directly involved in the methyltransferase reaction. One may assess the methyltransferase-independent activity of these proteins in mitoribosome assembly and whether they are able to partially rescue possible defects in the knockout cells. Bacteria and yeast mitochondria have compensation mechanisms for deficiencies in rRNA methyltransferases proteins. For example, overexpression of RA-GTPases ObgE in bacteria or Mtg2p in yeast mitochondria can rescue deficiency of RrmJ or MRM2 methyltransferases, respectively. The details of these compensation mechanisms are unknown. If the purpose of rRNA methylation in ribosome assembly and/or stability is to encourage a specific RNA conformation or to recruit proteins, and if RA-GTPases function in a similar manner, then this may offer a plausible explanation. Nonetheless, compensation mechanisms for deficiencies in rRNA methyltransferases have not yet been studied in mammalian mitochondria.

Since the three methyltransferases are generally associated with nucleoids, it will be of interest to determine when and where the rRNA methylation events occur. rRNA can be isolated from different complexes separated in sedimentation gradients and tested for susceptibility to DNAzyme-mediated cleavage at the three different methylation sites. It will be of interest to determine whether unmodified rRNA can be incorporated into mitoribosomes, as this appears to occur in bacteria with a deletion in RlmB (analogous to MRM1) (Lovgren and Wikstrom, 2001). Yeast mitochondria with a deficiency in Mrm2p (analogous to MRM2) are able to incorporate rRNA into ribosome assembly intermediate particles that are substrates for the methyltransferase reaction, *in vitro* (Pintard et al., 2002). Intermediates in mammalian mitoribosome assembly have not been well-defined, but mass spectrometry of sucrose gradient fractions may help distinguish intermediates from fully assembled LSU and SSU. The use of siRNA targeting genes in the mitoribosomal assembly pathway may enhance the accumulation of assembly intermediate

complexes. If ribosomal assembly intermediates can be isolated, cryo-EM images may shed light on the mitoribosome assembly process, although this may be very difficult to do, since it will require relatively homogenous samples. In addition, if these intermediates can be isolated, perhaps the incompletely assembled complexes can be used as substrates for a methyltransferase reaction with recombinant proteins or proteins immuno-purified from mitochondria. Endogenous rRNA methyltransferase proteins can also be purified from a large scale mitochondrial preparation to analyze their activity on *in vitro*-synthesized 16S rRNA or on ribosome assembly intermediate complexes. Such experiments could provide an informative contrast to our inability to demonstrate methylation of naked 16S rRNA with recombinant proteins, *in vitro*. This would be consistent with certain methyltransferases requiring a protein-RNA complex as a substrate. The SILAC approach to studying nucleoid and ribosome components separated in glycerol gradients (Bogenhagen et al., 2014) can also be combined with siRNA targeting the methyltransferases to better understand the relationship between rRNA methylation and ribosome assembly.

References

Agrawal, R.K., and Sharma, M.R. (2012). Structural aspects of mitochondrial translational apparatus. Current opinion in structural biology *22*, 797-803.

Al-Furoukh, N., Goffart, S., Szibor, M., Wanrooij, S., and Braun, T. (2013). Binding to G-quadruplex RNA activates the mitochondrial GTPase NOA1. Biochimica et biophysica acta *1833*, 2933-2942.

Albring, M., Griffith, J., and Attardi, G. (1977). Association of a protein structure of probable membrane derivation with HeLa cell mitochondrial DNA near its origin of replication. Proceedings of the National Academy of Sciences of the United States of America *74*, 1348-1352.

Almajan, E.R., Richter, R., Paeger, L., Martinelli, P., Barth, E., Decker, T., Larsson, N.G., Kloppenburg, P., Langer, T., and Rugarli, E.I. (2012). AFG3L2 supports mitochondrial protein synthesis and Purkinje cell survival. The Journal of clinical investigation *122*, 4048-4058.

Amato, P., Tachibana, M., Sparman, M., and Mitalipov, S. (2014). Three-parent in vitro fertilization: gene replacement for the prevention of inherited mitochondrial diseases. Fertility and sterility *101*, 31-35.

Anderson, L. (1981). Identification of mitochondrial proteins and some of their precursors in two-dimensional electrophoretic maps of human cells. Proceedings of the National Academy of Sciences of the United States of America *78*, 2407-2411.

Anderson, S., Bankier, A.T., Barrell, B.G., de Bruijn, M.H., Coulson, A.R., Drouin, J., Eperon, I.C., Nierlich, D.P., Roe, B.A., Sanger, F., *et al.* (1981). Sequence and organization of the human mitochondrial genome. Nature *290*, 457-465.

Antonicka, H., Sasarman, F., Nishimura, T., Paupe, V., and Shoubridge, E.A. (2013). The mitochondrial RNA-binding protein GRSF1 localizes to RNA granules and is required for posttranscriptional mitochondrial gene expression. Cell metabolism *17*, 386-398.

Attardi, G., and Schatz, G. (1988). Biogenesis of mitochondria. Annual review of cell biology *4*, 289-333.

Baer, R.J., and Dubin, D.T. (1981). Methylated regions of hamster mitochondrial ribosomal RNA: structural and functional correlates. Nucleic acids research *9*, 323-337.

Bai, Y., Shakeley, R.M., and Attardi, G. (2000). Tight control of respiration by NADH dehydrogenase ND5 subunit gene expression in mouse mitochondria. Molecular and cellular biology *20*, 805-815.

Barrell, B.G., Anderson, S., Bankier, A.T., de Bruijn, M.H., Chen, E., Coulson, A.R., Drouin, J., Eperon, I.C., Nierlich, D.P., Roe, B.A., *et al.* (1980). Different pattern of codon recognition by mammalian mitochondrial tRNAs. Proceedings of the National Academy of Sciences of the United States of America *77*, 3164-3166.

Barrell, B.G., Bankier, A.T., and Drouin, J. (1979). A different genetic code in human mitochondria. Nature *282*, 189-194.

Barrientos, A., Korr, D., Barwell, K.J., Sjulsen, C., Gajewski, C.D., Manfredi, G., Ackerman, S., and Tzagoloff, A. (2003). MTG1 codes for a conserved protein required for mitochondrial translation. Molecular biology of the cell *14*, 2292-2302.

Battey, J., and Clayton, D.A. (1980). The transcription map of human mitochondrial DNA implicates transfer RNA excision as a major processing event. The Journal of biological chemistry *255*, 11599-11606.

Behm-Ansmant, I., Grosjean, H., Massenet, S., Motorin, Y., and Branlant, C. (2004). Pseudouridylation at position 32 of mitochondrial and cytoplasmic tRNAs requires two distinct enzymes in Saccharomyces cerevisiae. The Journal of biological chemistry *279*, 52998-53006.
Beilschmidt, L.K., and Puccio, H.M. (2014). Mammalian Fe-S cluster biogenesis and its implication in disease. Biochimie *100*, 48-60.
Bereiter-Hahn, J., and Voth, M. (1996). Distribution and dynamics of mitochondrial nucleoids in animal cells in culture. Exp Biol Online *1*, 17.
Blanchard, S.C., and Puglisi, J.D. (2001). Solution structure of the A loop of 23S ribosomal RNA. Proceedings of the National Academy of Sciences of the United States of America *98*, 3720-3725.
Bogenhagen, D.F. (1999). Repair of mtDNA in vertebrates. American journal of human genetics *64*, 1276-1281.
Bogenhagen, D.F. (2010). Does mtDNA nucleoid organization impact aging? Experimental gerontology *45*, 473-477.
Bogenhagen, D.F. (2012). Mitochondrial DNA nucleoid structure. Biochimica et biophysica acta *1819*, 914-920.
Bogenhagen, D.F., Martin, D.W., and Koller, A. (2014). Initial steps in RNA processing and ribosome assembly occur at mitochondrial DNA nucleoids. Cell metabolism *19*, 618-629.
Bogenhagen, D.F., Rousseau, D., and Burke, S. (2008). The layered structure of human mitochondrial DNA nucleoids. The Journal of biological chemistry *283*, 3665-3675.
Bogenhagen, D.F., Wang, Y., Shen, E.L., and Kobayashi, R. (2003). Protein components of mitochondrial DNA nucleoids in higher eukaryotes. Molecular & cellular proteomics : MCP *2*, 1205-1216.
Bohne, A.V. (2014). The nucleoid as a site of rRNA processing and ribosome assembly. Frontiers in plant science *5*, 257.
Borowski, L.S., Dziembowski, A., Hejnowicz, M.S., Stepien, P.P., and Szczesny, R.J. (2013). Human mitochondrial RNA decay mediated by PNPase-hSuv3 complex takes place in distinct foci. Nucleic acids research *41*, 1223-1240.
Bratic, A., and Larsson, N.G. (2013). The role of mitochondria in aging. The Journal of clinical investigation *123*, 951-957.
Britton, R.A. (2009). Role of GTPases in bacterial ribosome assembly. Annual review of microbiology *63*, 155-176.
Brown, T.A., Tkachuk, A.N., Shtengel, G., Kopek, B.G., Bogenhagen, D.F., Hess, H.F., and Clayton, D.A. (2011). Superresolution fluorescence imaging of mitochondrial nucleoids reveals their spatial range, limits, and membrane interaction. Molecular and cellular biology *31*, 4994-5010.
Brown, W.M., George, M., Jr., and Wilson, A.C. (1979). Rapid evolution of animal mitochondrial DNA. Proceedings of the National Academy of Sciences of the United States of America *76*, 1967-1971.
Buchhaupt, M., Peifer, C., and Entian, K.D. (2007). Analysis of 2'-O-methylated nucleosides and pseudouridines in ribosomal RNAs using DNAzymes. Analytical biochemistry *361*, 102-108.
Burk, A., Douzery, E., and Springer, M.S. (2002). The secondary structure of mammalian mitochondrial 16S rRNA molecules: Refinements based on a comparative phylogenetic approach. Journal of Mammalian Evolution *9*, 225-252.

Caldas, T., Binet, E., Bouloc, P., Costa, A., Desgres, J., and Richarme, G. (2000a). The FtsJ/RrmJ heat shock protein of Escherichia coli is a 23 S ribosomal RNA methyltransferase. The Journal of biological chemistry *275*, 16414-16419.
Caldas, T., Binet, E., Bouloc, P., and Richarme, G. (2000b). Translational defects of Escherichia coli mutants deficient in the Um(2552) 23S ribosomal RNA methyltransferase RrmJ/FTSJ. Biochemical and biophysical research communications *271*, 714-718.
Calvo, S.E., and Mootha, V.K. (2010). The mitochondrial proteome and human disease. Annual review of genomics and human genetics *11*, 25-44.
Camara, Y., Asin-Cayuela, J., Park, C.B., Metodiev, M.D., Shi, Y., Ruzzenente, B., Kukat, C., Habermann, B., Wibom, R., Hultenby, K., *et al.* (2011). MTERF4 regulates translation by targeting the methyltransferase NSUN4 to the mammalian mitochondrial ribosome. Cell metabolism *13*, 527-539.
Cech, T.R. (2000). Structural biology. The ribosome is a ribozyme. Science *289*, 878-879.
Chang, J.H., and Tong, L. (2012). Mitochondrial poly(A) polymerase and polyadenylation. Biochimica et biophysica acta *1819*, 992-997.
Chen, H.W., Rainey, R.N., Balatoni, C.E., Dawson, D.W., Troke, J.J., Wasiak, S., Hong, J.S., McBride, H.M., Koehler, C.M., Teitell, M.A., *et al.* (2006). Mammalian polynucleotide phosphorylase is an intermembrane space RNase that maintains mitochondrial homeostasis. Molecular and cellular biology *26*, 8475-8487.
Chen, X.J., and Butow, R.A. (2005). The organization and inheritance of the mitochondrial genome. Nature reviews Genetics *6*, 815-825.
Chinnery, P.F., Howell, N., Andrews, R.M., and Turnbull, D.M. (1999). Clinical mitochondrial genetics. Journal of medical genetics *36*, 425-436.
Chinnery, P.F., and Hudson, G. (2013). Mitochondrial genetics. British medical bulletin *106*, 135-159.
Christian, B.E., and Spremulli, L.L. (2010). Preferential selection of the 5'-terminal start codon on leaderless mRNAs by mammalian mitochondrial ribosomes. The Journal of biological chemistry *285*, 28379-28386.
Christian, B.E., and Spremulli, L.L. (2012). Mechanism of protein biosynthesis in mammalian mitochondria. Biochimica et biophysica acta *1819*, 1035-1054.
Chrzanowska-Lightowlers, Z.M., Pajak, A., and Lightowlers, R.N. (2011). Termination of protein synthesis in mammalian mitochondria. The Journal of biological chemistry *286*, 34479-34485.
Chujo, T., Ohira, T., Sakaguchi, Y., Goshima, N., Nomura, N., Nagao, A., and Suzuki, T. (2012). LRPPRC/SLIRP suppresses PNPase-mediated mRNA decay and promotes polyadenylation in human mitochondria. Nucleic acids research *40*, 8033-8047.
Clayton, D.A. (1982). Replication of animal mitochondrial DNA. Cell *28*, 693-705.
Clayton, D.A. (1991). Replication and transcription of vertebrate mitochondrial DNA. Annual review of cell biology *7*, 453-478.
Clayton, D.A. (2003). Mitochondrial DNA replication: what we know. IUBMB life *55*, 213-217.
Clemente, P., Peralta, S., Cruz-Bermudez, A., Echevarria, L., Fontanesi, F., Barrientos, A., Fernandez-Moreno, M.A., and Garesse, R. (2013). hCOA3 stabilizes cytochrome c oxidase 1 (COX1) and promotes cytochrome c oxidase assembly in human mitochondria. The Journal of biological chemistry *288*, 8321-8331.
Connolly, K., Rife, J.P., and Culver, G. (2008). Mechanistic insight into the ribosome biogenesis functions of the ancient protein KsgA. Molecular microbiology *70*, 1062-1075.

Cotney, J., McKay, S.E., and Shadel, G.S. (2009). Elucidation of separate, but collaborative functions of the rRNA methyltransferase-related human mitochondrial transcription factors B1 and B2 in mitochondrial biogenesis reveals new insight into maternally inherited deafness. Human molecular genetics *18*, 2670-2682.
Craven, L., Tuppen, H.A., Greggains, G.D., Harbottle, S.J., Murphy, J.L., Cree, L.M., Murdoch, A.P., Chinnery, P.F., Taylor, R.W., Lightowlers, R.N., *et al.* (2010). Pronuclear transfer in human embryos to prevent transmission of mitochondrial DNA disease. Nature *465*, 82-85.
Cruz, R.P., Withers, J.B., and Li, Y. (2004). Dinucleotide junction cleavage versatility of 8-17 deoxyribozyme. Chemistry & biology *11*, 57-67.
Datta, K., Fuentes, J.L., and Maddock, J.R. (2005). The yeast GTPase Mtg2p is required for mitochondrial translation and partially suppresses an rRNA methyltransferase mutant, mrm2. Molecular biology of the cell *16*, 954-963.
De Silva, D., Fontanesi, F., and Barrientos, A. (2013). The DEAD box protein Mrh4 functions in the assembly of the mitochondrial large ribosomal subunit. Cell metabolism *18*, 712-725.
Decatur, W.A., and Fournier, M.J. (2002). rRNA modifications and ribosome function. Trends in biochemical sciences *27*, 344-351.
Dennerlein, S., Rozanska, A., Wydro, M., Chrzanowska-Lightowlers, Z.M., and Lightowlers, R.N. (2010). Human ERAL1 is a mitochondrial RNA chaperone involved in the assembly of the 28S small mitochondrial ribosomal subunit. The Biochemical journal *430*, 551-558.
Desjardins, P., Frost, E., and Morais, R. (1985). Ethidium bromide-induced loss of mitochondrial DNA from primary chicken embryo fibroblasts. Molecular and cellular biology *5*, 1163-1169.
Detmer, S.A., and Chan, D.C. (2007). Functions and dysfunctions of mitochondrial dynamics. Nature reviews Molecular cell biology *8*, 870-879.
DiMauro, S., and Schon, E.A. (2003). Mitochondrial respiratory-chain diseases. The New England journal of medicine *348*, 2656-2668.
Dong, Z.W., Shao, P., Diao, L.T., Zhou, H., Yu, C.H., and Qu, L.H. (2012). RTL-P: a sensitive approach for detecting sites of 2'-O-methylation in RNA molecules. Nucleic acids research *40*, e157.
Dyall, S.D., Brown, M.T., and Johnson, P.J. (2004). Ancient invasions: from endosymbionts to organelles. Science *304*, 253-257.
Ernster, L., and Schatz, G. (1981). Mitochondria: a historical review. The Journal of cell biology *91*, 227s-255s.
Falkenberg, M., Larsson, N.G., and Gustafsson, C.M. (2007). DNA replication and transcription in mammalian mitochondria. Annual review of biochemistry *76*, 679-699.
Filee, J., Forterre, P., Sen-Lin, T., and Laurent, J. (2002). Evolution of DNA polymerase families: evidences for multiple gene exchange between cellular and viral proteins. Journal of molecular evolution *54*, 763-773.
Finkel, T. (2011). Signal transduction by reactive oxygen species. The Journal of cell biology *194*, 7-15.
Fung, S., Nishimura, T., Sasarman, F., and Shoubridge, E.A. (2013). The conserved interaction of C7orf30 with MRPL14 promotes biogenesis of the mitochondrial large ribosomal subunit and mitochondrial translation. Molecular biology of the cell *24*, 184-193.
Gagliardi, D., Stepien, P.P., Temperley, R.J., Lightowlers, R.N., and Chrzanowska-Lightowlers, Z.M. (2004). Messenger RNA stability in mitochondria: different means to an end. Trends in genetics : TIG *20*, 260-267.

Gaj, T., Gersbach, C.A., and Barbas, C.F., 3rd (2013). ZFN, TALEN, and CRISPR/Cas-based methods for genome engineering. Trends in biotechnology *31*, 397-405.
Galmiche, L., Serre, V., Beinat, M., Assouline, Z., Lebre, A.S., Chretien, D., Nietschke, P., Benes, V., Boddaert, N., Sidi, D., *et al.* (2011). Exome sequencing identifies MRPL3 mutation in mitochondrial cardiomyopathy. Human mutation *32*, 1225-1231.
Gardner, J.L., Craven, L., Turnbull, D.M., and Taylor, R.W. (2007). Experimental strategies towards treating mitochondrial DNA disorders. Bioscience reports *27*, 139-150.
Garrido, N., Griparic, L., Jokitalo, E., Wartiovaara, J., van der Bliek, A.M., and Spelbrink, J.N. (2003). Composition and dynamics of human mitochondrial nucleoids. Molecular biology of the cell *14*, 1583-1596.
Gelfand, R., and Attardi, G. (1981). Synthesis and turnover of mitochondrial ribonucleic acid in HeLa cells: the mature ribosomal and messenger ribonucleic acid species are metabolically unstable. Molecular and cellular biology *1*, 497-511.
Gilkerson, R.W., Schon, E.A., Hernandez, E., and Davidson, M.M. (2008). Mitochondrial nucleoids maintain genetic autonomy but allow for functional complementation. The Journal of cell biology *181*, 1117-1128.
Goldschmidt-Reisin, S., Kitakawa, M., Herfurth, E., Wittmann-Liebold, B., Grohmann, L., and Graack, H.R. (1998). Mammalian mitochondrial ribosomal proteins. N-terminal amino acid sequencing, characterization, and identification of corresponding gene sequences. The Journal of biological chemistry *273*, 34828-34836.
Goto, S., Muto, A., and Himeno, H. (2013). GTPases involved in bacterial ribosome maturation. Journal of biochemistry *153*, 403-414.
Graack, H.R., Bryant, M.L., and O'Brien, T.W. (1999). Identification of mammalian mitochondrial ribosomal proteins (MRPs) by N-terminal sequencing of purified bovine MRPs and comparison to data bank sequences: the large subribosomal particle. Biochemistry *38*, 16569-16577.
Gray, M.W., Burger, G., and Lang, B.F. (1999). Mitochondrial evolution. Science *283*, 1476-1481.
Greber, B.J., Boehringer, D., Leitner, A., Bieri, P., Voigts-Hoffmann, F., Erzberger, J.P., Leibundgut, M., Aebersold, R., and Ban, N. (2014). Architecture of the large subunit of the mammalian mitochondrial ribosome. Nature *505*, 515-519.
Green, R., Samaha, R.R., and Noller, H.F. (1997). Mutations at nucleotides G2251 and U2585 of 23 S rRNA perturb the peptidyl transferase center of the ribosome. Journal of molecular biology *266*, 40-50.
Guerrier-Takada, C., Gardiner, K., Marsh, T., Pace, N., and Altman, S. (1983). The RNA moiety of ribonuclease P is the catalytic subunit of the enzyme. Cell *35*, 849-857.
Guja, K.E., and Garcia-Diaz, M. (2012). Hitting the brakes: termination of mitochondrial transcription. Biochimica et biophysica acta *1819*, 939-947.
Haack, T.B., Kopajtich, R., Freisinger, P., Wieland, T., Rorbach, J., Nicholls, T.J., Baruffini, E., Walther, A., Danhauser, K., Zimmermann, F.A., *et al.* (2013). ELAC2 mutations cause a mitochondrial RNA processing defect associated with hypertrophic cardiomyopathy. American journal of human genetics *93*, 211-223.
Hager, J., Staker, B.L., Bugl, H., and Jakob, U. (2002). Active site in RrmJ, a heat shock-induced methyltransferase. The Journal of biological chemistry *277*, 41978-41986.
Hager, J., Staker, B.L., and Jakob, U. (2004). Substrate binding analysis of the 23S rRNA methyltransferase RrmJ. Journal of bacteriology *186*, 6634-6642.

Haque, M.E., Elmore, K.B., Tripathy, A., Koc, H., Koc, E.C., and Spremulli, L.L. (2010a). Properties of the C-terminal tail of human mitochondrial inner membrane protein Oxa1L and its interactions with mammalian mitochondrial ribosomes. The Journal of biological chemistry *285*, 28353-28362.
Haque, M.E., Grasso, D., Miller, C., Spremulli, L.L., and Saada, A. (2008). The effect of mutated mitochondrial ribosomal proteins S16 and S22 on the assembly of the small and large ribosomal subunits in human mitochondria. Mitochondrion *8*, 254-261.
Haque, M.E., Spremulli, L.L., and Fecko, C.J. (2010b). Identification of protein-protein and protein-ribosome interacting regions of the C-terminal tail of human mitochondrial inner membrane protein Oxa1L. The Journal of biological chemistry *285*, 34991-34998.
He, J., Cooper, H.M., Reyes, A., Di Re, M., Kazak, L., Wood, S.R., Mao, C.C., Fearnley, I.M., Walker, J.E., and Holt, I.J. (2012a). Human C4orf14 interacts with the mitochondrial nucleoid and is involved in the biogenesis of the small mitochondrial ribosomal subunit. Nucleic acids research *40*, 6097-6108.
He, J., Cooper, H.M., Reyes, A., Di Re, M., Sembongi, H., Litwin, T.R., Gao, J., Neuman, K.C., Fearnley, I.M., Spinazzola, A., *et al.* (2012b). Mitochondrial nucleoid interacting proteins support mitochondrial protein synthesis. Nucleic acids research *40*, 6109-6121.
Hensen, F., Cansiz, S., Gerhold, J.M., and Spelbrink, J.N. (2014). To be or not to be a nucleoid protein: a comparison of mass-spectrometry based approaches in the identification of potential mtDNA-nucleoid associated proteins. Biochimie *100*, 219-226.
Hodgkinson, A., Idaghdour, Y., Gbeha, E., Grenier, J.C., Hip-Ki, E., Bruat, V., Goulet, J.P., de Malliard, T., and Awadalla, P. (2014). High-resolution genomic analysis of human mitochondrial RNA sequence variation. Science *344*, 413-415.
Holt, I.J., Harding, A.E., and Morgan-Hughes, J.A. (1988). Deletions of muscle mitochondrial DNA in patients with mitochondrial myopathies. Nature *331*, 717-719.
Holt, I.J., and Reyes, A. (2012). Human mitochondrial DNA replication. Cold Spring Harbor perspectives in biology *4*.
Holzmann, J., Frank, P., Loffler, E., Bennett, K.L., Gerner, C., and Rossmanith, W. (2008). RNase P without RNA: identification and functional reconstitution of the human mitochondrial tRNA processing enzyme. Cell *135*, 462-474.
Iborra, F.J., Kimura, H., and Cook, P.R. (2004). The functional organization of mitochondrial genomes in human cells. BMC biology *2*, 9.
Jacobs, H.T., Lehtinen, S.K., and Spelbrink, J.N. (2000). No sex please, we're mitochondria: a hypothesis on the somatic unit of inheritance of mammalian mtDNA. BioEssays : news and reviews in molecular, cellular and developmental biology *22*, 564-572.
Jarrous, N. (2002). Human ribonuclease P: subunits, function, and intranuclear localization. RNA *8*, 1-7.
Jourdain, A.A., Koppen, M., Wydro, M., Rodley, C.D., Lightowlers, R.N., Chrzanowska-Lightowlers, Z.M., and Martinou, J.C. (2013). GRSF1 regulates RNA processing in mitochondrial RNA granules. Cell metabolism *17*, 399-410.
Kane, L.A., Lazarou, M., Fogel, A.I., Li, Y., Yamano, K., Sarraf, S.A., Banerjee, S., and Youle, R.J. (2014). PINK1 phosphorylates ubiquitin to activate Parkin E3 ubiquitin ligase activity. The Journal of cell biology *205*, 143-153.
Kash, J.C., Cunningham, D.M., Smit, M.W., Park, Y., Fritz, D., Wilusz, J., and Katze, M.G. (2002). Selective translation of eukaryotic mRNAs: functional molecular analysis of GRSF-1, a positive regulator of influenza virus protein synthesis. Journal of virology *76*, 10417-10426.

Kaufman, B.A., Newman, S.M., Hallberg, R.L., Slaughter, C.A., Perlman, P.S., and Butow, R.A. (2000). In organello formaldehyde crosslinking of proteins to mtDNA: identification of bifunctional proteins. Proceedings of the National Academy of Sciences of the United States of America *97*, 7772-7777.
Kaushal, P.S., Sharma, M.R., Booth, T.M., Haque, E.M., Tung, C.S., Sanbonmatsu, K.Y., Spremulli, L.L., and Agrawal, R.K. (2014). Cryo-EM structure of the small subunit of the mammalian mitochondrial ribosome. Proceedings of the National Academy of Sciences of the United States of America.
Kazak, L., Reyes, A., and Holt, I.J. (2012). Minimizing the damage: repair pathways keep mitochondrial DNA intact. Nature reviews Molecular cell biology *13*, 659-671.
Kim, S.J., Kwon, M.C., Ryu, M.J., Chung, H.K., Tadi, S., Kim, Y.K., Kim, J.M., Lee, S.H., Park, J.H., Kweon, G.R., *et al.* (2012). CRIF1 is essential for the synthesis and insertion of oxidative phosphorylation polypeptides in the mammalian mitochondrial membrane. Cell metabolism *16*, 274-283.
King, M.P., and Attardi, G. (1989). Human cells lacking mtDNA: repopulation with exogenous mitochondria by complementation. Science *246*, 500-503.
King, M.P., and Attardi, G. (1993). Post-transcriptional regulation of the steady-state levels of mitochondrial tRNAs in HeLa cells. The Journal of biological chemistry *268*, 10228-10237.
Kissil, J.L., Cohen, O., Raveh, T., and Kimchi, A. (1999). Structure-function analysis of an evolutionary conserved protein, DAP3, which mediates TNF-alpha- and Fas-induced cell death. The EMBO journal *18*, 353-362.
Koc, E.C., Burkhart, W., Blackburn, K., Koc, H., Moseley, A., and Spremulli, L.L. (2001a). Identification of four proteins from the small subunit of the mammalian mitochondrial ribosome using a proteomics approach. Protein science : a publication of the Protein Society *10*, 471-481.
Koc, E.C., Burkhart, W., Blackburn, K., Moyer, M.B., Schlatzer, D.M., Moseley, A., and Spremulli, L.L. (2001b). The large subunit of the mammalian mitochondrial ribosome. Analysis of the complement of ribosomal proteins present. The Journal of biological chemistry *276*, 43958-43969.
Koc, E.C., Cimen, H., Kumcuoglu, B., Abu, N., Akpinar, G., Haque, M.E., Spremulli, L.L., and Koc, H. (2013). Identification and characterization of CHCHD1, AURKAIP1, and CRIF1 as new members of the mammalian mitochondrial ribosome. Frontiers in physiology *4*, 183.
Koc, E.C., Haque, M.E., and Spremulli, L.L. (2010). Current Views of the Structure of the Mammalian Mitochondrial Ribosome. Isr J Chem *50*, 45-59.
Koc, E.C., Ranasinghe, A., Burkhart, W., Blackburn, K., Koc, H., Moseley, A., and Spremulli, L.L. (2001c). A new face on apoptosis: death-associated protein 3 and PDCD9 are mitochondrial ribosomal proteins. FEBS letters *492*, 166-170.
Koene, S., and Smeitink, J. (2009). Mitochondrial medicine: entering the era of treatment. Journal of internal medicine *265*, 193-209.
Kolanczyk, M., Pech, M., Zemojtel, T., Yamamoto, H., Mikula, I., Calvaruso, M.A., van den Brand, M., Richter, R., Fischer, B., Ritz, A., *et al.* (2011). NOA1 is an essential GTPase required for mitochondrial protein synthesis. Molecular biology of the cell *22*, 1-11.
Kopek, B.G., Shtengel, G., Xu, C.S., Clayton, D.A., and Hess, H.F. (2012). Correlative 3D superresolution fluorescence and electron microscopy reveal the relationship of mitochondrial nucleoids to membranes. Proceedings of the National Academy of Sciences of the United States of America *109*, 6136-6141.

Kotani, T., Akabane, S., Takeyasu, K., Ueda, T., and Takeuchi, N. (2013). Human G-proteins, ObgH1 and Mtg1, associate with the large mitochondrial ribosome subunit and are involved in translation and assembly of respiratory complexes. Nucleic acids research *41*, 3713-3722.
Krzyzosiak, W., Denman, R., Nurse, K., Hellmann, W., Boublik, M., Gehrke, C.W., Agris, P.F., and Ofengand, J. (1987). In vitro synthesis of 16S ribosomal RNA containing single base changes and assembly into a functional 30S ribosome. Biochemistry *26*, 2353-2364.
Kucej, M., and Butow, R.A. (2007). Evolutionary tinkering with mitochondrial nucleoids. Trends in cell biology *17*, 586-592.
Kujoth, G.C., Hiona, A., Pugh, T.D., Someya, S., Panzer, K., Wohlgemuth, S.E., Hofer, T., Seo, A.Y., Sullivan, R., Jobling, W.A., *et al.* (2005). Mitochondrial DNA mutations, oxidative stress, and apoptosis in mammalian aging. Science *309*, 481-484.
Kuzmenko, A., Atkinson, G.C., Levitskii, S., Zenkin, N., Tenson, T., Hauryliuk, V., and Kamenski, P. (2014). Mitochondrial translation initiation machinery: conservation and diversification. Biochimie *100*, 132-140.
Lafontaine, D.L., Preiss, T., and Tollervey, D. (1998). Yeast 18S rRNA dimethylase Dim1p: a quality control mechanism in ribosome synthesis? Molecular and cellular biology *18*, 2360-2370.
Lane, N., and Martin, W. (2010). The energetics of genome complexity. Nature *467*, 929-934.
Lee, K.W., and Bogenhagen, D.F. (2014). Assignment of 2'-O-methyltransferases to Modification Sites on the Mammalian Mitochondrial Large Subunit 16S rRNA. The Journal of biological chemistry.
Lee, K.W., Okot-Kotber, C., LaComb, J.F., and Bogenhagen, D.F. (2013). Mitochondrial ribosomal RNA (rRNA) methyltransferase family members are positioned to modify nascent rRNA in foci near the mitochondrial DNA nucleoid. The Journal of biological chemistry *288*, 31386-31399.
Legros, F., Malka, F., Frachon, P., Lombes, A., and Rojo, M. (2004). Organization and dynamics of human mitochondrial DNA. Journal of cell science *117*, 2653-2662.
Levinger, L., Morl, M., and Florentz, C. (2004a). Mitochondrial tRNA 3' end metabolism and human disease. Nucleic acids research *32*, 5430-5441.
Levinger, L., Oestreich, I., Florentz, C., and Morl, M. (2004b). A pathogenesis-associated mutation in human mitochondrial tRNALeu(UUR) leads to reduced 3'-end processing and CCA addition. Journal of molecular biology *337*, 535-544.
Levinger, L., and Serjanov, D. (2012). Pathogenesis-related mutations in the T-loops of human mitochondrial tRNAs affect 3' end processing and tRNA structure. RNA biology *9*, 283-291.
Lightowlers, R.N., and Chrzanowska-Lightowlers, Z.M. (2008). PPR (pentatricopeptide repeat) proteins in mammals: important aids to mitochondrial gene expression. The Biochemical journal *416*, e5-6.
Lightowlers, R.N., and Chrzanowska-Lightowlers, Z.M. (2010). Terminating human mitochondrial protein synthesis: a shift in our thinking. RNA biology *7*, 282-286.
Lightowlers, R.N., and Chrzanowska-Lightowlers, Z.M. (2013). Human pentatricopeptide proteins: only a few and what do they do? RNA biology *10*, 1433-1438.
Lightowlers, R.N., Rozanska, A., and Chrzanowska-Lightowlers, Z.M. (2014). Mitochondrial protein synthesis: Figuring the fundamentals, complexities and complications, of mammalian mitochondrial translation. FEBS letters.
Liu, M., and Spremulli, L. (2000). Interaction of mammalian mitochondrial ribosomes with the inner membrane. The Journal of biological chemistry *275*, 29400-29406.

Liu, P., Qian, L., Sung, J.S., de Souza-Pinto, N.C., Zheng, L., Bogenhagen, D.F., Bohr, V.A., Wilson, D.M., 3rd, Shen, B., and Demple, B. (2008). Removal of oxidative DNA damage via FEN1-dependent long-patch base excision repair in human cell mitochondria. Molecular and cellular biology *28*, 4975-4987.
Lovgren, J.M., and Wikstrom, P.M. (2001). The rlmB gene is essential for formation of Gm2251 in 23S rRNA but not for ribosome maturation in Escherichia coli. Journal of bacteriology *183*, 6957-6960.
Maden, B.E. (2001). Mapping 2'-O-methyl groups in ribosomal RNA. Methods *25*, 374-382.
Maden, B.E., and Hughes, J.M. (1997). Eukaryotic ribosomal RNA: the recent excitement in the nucleotide modification problem. Chromosoma *105*, 391-400.
Manam, S., and Van Tuyle, G.C. (1987). Separation and characterization of 5'- and 3'-tRNA processing nucleases from rat liver mitochondria. The Journal of biological chemistry *262*, 10272-10279.
Martin, R., Straub, A.U., Doebele, C., and Bohnsack, M.T. (2013). DExD/H-box RNA helicases in ribosome biogenesis. RNA biology *10*, 4-18.
Mason, P.A., and Lightowlers, R.N. (2003). Why do mammalian mitochondria possess a mismatch repair activity? FEBS letters *554*, 6-9.
Mason, P.A., Matheson, E.C., Hall, A.G., and Lightowlers, R.N. (2003). Mismatch repair activity in mammalian mitochondria. Nucleic acids research *31*, 1052-1058.
McLean, J.R., Cohn, G.L., Brandt, I.K., and Simpson, M.V. (1958). Incorporation of labeled amino acids into the protein of muscle and liver mitochondria. The Journal of biological chemistry *233*, 657-663.
Mears, J.A., Sharma, M.R., Gutell, R.R., McCook, A.S., Richardson, P.E., Caulfield, T.R., Agrawal, R.K., and Harvey, S.C. (2006). A structural model for the large subunit of the mammalian mitochondrial ribosome. Journal of molecular biology *358*, 193-212.
Mercer, T.R., Neph, S., Dinger, M.E., Crawford, J., Smith, M.A., Shearwood, A.M., Haugen, E., Bracken, C.P., Rackham, O., Stamatoyannopoulos, J.A., *et al.* (2011). The human mitochondrial transcriptome. Cell *146*, 645-658.
Metodiev, M.D., Lesko, N., Park, C.B., Camara, Y., Shi, Y., Wibom, R., Hultenby, K., Gustafsson, C.M., and Larsson, N.G. (2009). Methylation of 12S rRNA is necessary for in vivo stability of the small subunit of the mammalian mitochondrial ribosome. Cell metabolism *9*, 386-397.
Metodiev, M.D., Spahr, H., Loguercio Polosa, P., Meharg, C., Becker, C., Altmueller, J., Habermann, B., Larsson, N.G., and Ruzzenente, B. (2014). NSUN4 Is a Dual Function Mitochondrial Protein Required for Both Methylation of 12S rRNA and Coordination of Mitoribosomal Assembly. PLoS genetics *10*, e1004110.
Mick, D.U., Dennerlein, S., Wiese, H., Reinhold, R., Pacheu-Grau, D., Lorenzi, I., Sasarman, F., Weraarpachai, W., Shoubridge, E.A., Warscheid, B., *et al.* (2012). MITRAC links mitochondrial protein translocation to respiratory-chain assembly and translational regulation. Cell *151*, 1528-1541.
Miller, C., Saada, A., Shaul, N., Shabtai, N., Ben-Shalom, E., Shaag, A., Hershkovitz, E., and Elpeleg, O. (2004). Defective mitochondrial translation caused by a ribosomal protein (MRPS16) mutation. Annals of neurology *56*, 734-738.
Miller, W.L. (2013). Steroid hormone synthesis in mitochondria. Molecular and cellular endocrinology *379*, 62-73.

Minczuk, M., Kolasinska-Zwierz, P., Murphy, M.P., and Papworth, M.A. (2010). Construction and testing of engineered zinc-finger proteins for sequence-specific modification of mtDNA. Nature protocols *5*, 342-356.
Miyazaki, T., Shen, M., Fujikura, D., Tosa, N., Kim, H.R., Kon, S., Uede, T., and Reed, J.C. (2004). Functional role of death-associated protein 3 (DAP3) in anoikis. The Journal of biological chemistry *279*, 44667-44672.
Montoya, J., Ojala, D., and Attardi, G. (1981). Distinctive features of the 5'-terminal sequences of the human mitochondrial mRNAs. Nature *290*, 465-470.
Mootha, V.K., Lepage, P., Miller, K., Bunkenborg, J., Reich, M., Hjerrild, M., Delmonte, T., Villeneuve, A., Sladek, R., Xu, F., *et al.* (2003). Identification of a gene causing human cytochrome c oxidase deficiency by integrative genomics. Proceedings of the National Academy of Sciences of the United States of America *100*, 605-610.
Motorin, Y., and Helm, M. (2011). RNA nucleotide methylation. Wiley interdisciplinary reviews RNA *2*, 611-631.
Nagaike, T., Suzuki, T., Tomari, Y., Takemoto-Hori, C., Negayama, F., Watanabe, K., and Ueda, T. (2001). Identification and characterization of mammalian mitochondrial tRNA nucleotidyltransferases. The Journal of biological chemistry *276*, 40041-40049.
Nagao, A., Hino-Shigi, N., and Suzuki, T. (2008). Measuring mRNA decay in human mitochondria. Methods in enzymology *447*, 489-499.
Nicholls, T.J., and Minczuk, M. (2014). In D-loop: 40years of mitochondrial 7S DNA. Experimental gerontology *56*, 175-181.
Nolden, M., Ehses, S., Koppen, M., Bernacchia, A., Rugarli, E.I., and Langer, T. (2005). The m-AAA protease defective in hereditary spastic paraplegia controls ribosome assembly in mitochondria. Cell *123*, 277-289.
Noller, H.F. (1991). Ribosomal RNA and translation. Annual review of biochemistry *60*, 191-227.
Nomura, M. (1973). Assembly of bacterial ribosomes. Science *179*, 864-873.
Nomura, M., and Erdmann, V.A. (1970). Reconstitution of 50S ribosomal subunits from dissociated molecular components. Nature *228*, 744-748.
O'Brien, T.W. (1971). The general occurrence of 55 S ribosomes in mammalian liver mitochondria. The Journal of biological chemistry *246*, 3409-3417.
O'Brien, T.W. (2002). Evolution of a protein-rich mitochondrial ribosome: implications for human genetic disease. Gene *286*, 73-79.
O'Brien, T.W., Fiesler, S.E., Denslow, N.D., Thiede, B., Wittmann-Liebold, B., Mougey, E.B., Sylvester, J.E., and Graack, H.R. (1999). Mammalian mitochondrial ribosomal proteins (2). Amino acid sequencing, characterization, and identification of corresponding gene sequences. The Journal of biological chemistry *274*, 36043-36051.
O'Brien, T.W., and Kalf, G.F. (1967a). Ribosomes from rat liver mitochondira. II. Partial characterization. The Journal of biological chemistry *242*, 2180-2185.
O'Brien, T.W., and Kalf, G.F. (1967b). Ribosomes from rat liver mitochondria. I. Isolation procedure and contamination studies. The Journal of biological chemistry *242*, 2172-2179.
O'Brien, T.W., Liu, J., Sylvester, J.E., Mougey, E.B., Fischel-Ghodsian, N., Thiede, B., Wittmann-Liebold, B., and Graack, H.R. (2000). Mammalian mitochondrial ribosomal proteins (4). Amino acid sequencing, characterization, and identification of corresponding gene sequences. The Journal of biological chemistry *275*, 18153-18159.

O'Brien, T.W., O'Brien, B.J., and Norman, R.A. (2005). Nuclear MRP genes and mitochondrial disease. Gene *354*, 147-151.
Ofengand, J., and Bakin, A. (1997). Mapping to nucleotide resolution of pseudouridine residues in large subunit ribosomal RNAs from representative eukaryotes, prokaryotes, archaebacteria, mitochondria and chloroplasts. Journal of molecular biology *266*, 246-268.
Ojala, D., Merkel, C., Gelfand, R., and Attardi, G. (1980). The tRNA genes punctuate the reading of genetic information in human mitochondrial DNA. Cell *22*, 393-403.
Ojala, D., Montoya, J., and Attardi, G. (1981). tRNA punctuation model of RNA processing in human mitochondria. Nature *290*, 470-474.
Pagliarini, D.J., Calvo, S.E., Chang, B., Sheth, S.A., Vafai, S.B., Ong, S.E., Walford, G.A., Sugiana, C., Boneh, A., Chen, W.K., *et al.* (2008). A mitochondrial protein compendium elucidates complex I disease biology. Cell *134*, 112-123.
Papapetropoulos, S., Ffrench-Mullen, J., McCorquodale, D., Qin, Y., Pablo, J., and Mash, D.C. (2006). Multiregional gene expression profiling identifies MRPS6 as a possible candidate gene for Parkinson's disease. Gene expression *13*, 205-215.
Park, C.B., Asin-Cayuela, J., Camara, Y., Shi, Y., Pellegrini, M., Gaspari, M., Wibom, R., Hultenby, K., Erdjument-Bromage, H., Tempst, P., *et al.* (2007). MTERF3 is a negative regulator of mammalian mtDNA transcription. Cell *130*, 273-285.
Paul, M.F., Alushin, G.M., Barros, M.H., Rak, M., and Tzagoloff, A. (2012). The putative GTPase encoded by MTG3 functions in a novel pathway for regulating assembly of the small subunit of yeast mitochondrial ribosomes. The Journal of biological chemistry *287*, 24346-24355.
Peil, L., Virumae, K., and Remme, J. (2008). Ribosome assembly in Escherichia coli strains lacking the RNA helicase DeaD/CsdA or DbpA. The FEBS journal *275*, 3772-3782.
Petrossian, T.C., and Clarke, S.G. (2011). Uncovering the human methyltransferasome. Molecular & cellular proteomics : MCP *10*, M110 000976.
Pham, X.H., Farge, G., Shi, Y., Gaspari, M., Gustafsson, C.M., and Falkenberg, M. (2006). Conserved sequence box II directs transcription termination and primer formation in mitochondria. The Journal of biological chemistry *281*, 24647-24652.
Pintard, L., Bujnicki, J.M., Lapeyre, B., and Bonnerot, C. (2002). MRM2 encodes a novel yeast mitochondrial 21S rRNA methyltransferase. The EMBO journal *21*, 1139-1147.
Pinz, K.G., and Bogenhagen, D.F. (1998). Efficient repair of abasic sites in DNA by mitochondrial enzymes. Molecular and cellular biology *18*, 1257-1265.
Portnoy, V., Palnizky, G., Yehudai-Resheff, S., Glaser, F., and Schuster, G. (2008). Analysis of the human polynucleotide phosphorylase (PNPase) reveals differences in RNA binding and response to phosphate compared to its bacterial and chloroplast counterparts. RNA *14*, 297-309.
Purta, E., O'Connor, M., Bujnicki, J.M., and Douthwaite, S. (2009). YgdE is the 2'-O-ribose methyltransferase RlmM specific for nucleotide C2498 in bacterial 23S rRNA. Molecular microbiology *72*, 1147-1158.
Rackham, O., Davies, S.M., Shearwood, A.M., Hamilton, K.L., Whelan, J., and Filipovska, A. (2009). Pentatricopeptide repeat domain protein 1 lowers the levels of mitochondrial leucine tRNAs in cells. Nucleic acids research *37*, 5859-5867.
Rackham, O., and Filipovska, A. (2014). Supernumerary proteins of mitochondrial ribosomes. Biochimica et biophysica acta *1840*, 1227-1232.

Rackham, O., Mercer, T.R., and Filipovska, A. (2012). The human mitochondrial transcriptome and the RNA-binding proteins that regulate its expression. Wiley interdisciplinary reviews RNA *3*, 675-695.
Rackham, O., Shearwood, A.M., Mercer, T.R., Davies, S.M., Mattick, J.S., and Filipovska, A. (2011). Long noncoding RNAs are generated from the mitochondrial genome and regulated by nuclear-encoded proteins. RNA *17*, 2085-2093.
Raimundo, N., Song, L., Shutt, T.E., McKay, S.E., Cotney, J., Guan, M.X., Gilliland, T.C., Hohuan, D., Santos-Sacchi, J., and Shadel, G.S. (2012). Mitochondrial stress engages E2F1 apoptotic signaling to cause deafness. Cell *148*, 716-726.
Richter, R., Pajak, A., Dennerlein, S., Rozanska, A., Lightowlers, R.N., and Chrzanowska-Lightowlers, Z.M. (2010a). Translation termination in human mitochondrial ribosomes. Biochemical Society transactions *38*, 1523-1526.
Richter, R., Rorbach, J., Pajak, A., Smith, P.M., Wessels, H.J., Huynen, M.A., Smeitink, J.A., Lightowlers, R.N., and Chrzanowska-Lightowlers, Z.M. (2010b). A functional peptidyl-tRNA hydrolase, ICT1, has been recruited into the human mitochondrial ribosome. The EMBO journal *29*, 1116-1125.
Richter, U., Lahtinen, T., Marttinen, P., Myohanen, M., Greco, D., Cannino, G., Jacobs, H.T., Lietzen, N., Nyman, T.A., and Battersby, B.J. (2013). A mitochondrial ribosomal and RNA decay pathway blocks cell proliferation. Current biology : CB *23*, 535-541.
Ringel, R., Sologub, M., Morozov, Y.I., Litonin, D., Cramer, P., and Temiakov, D. (2011). Structure of human mitochondrial RNA polymerase. Nature *478*, 269-273.
Robberson, D.L., Kasamatsu, H., and Vinograd, J. (1972). Replication of mitochondrial DNA. Circular replicative intermediates in mouse L cells. Proceedings of the National Academy of Sciences of the United States of America *69*, 737-741.
Rorbach, J., Boesch, P., Gammage, P.A., Nicholls, T.J., Pearce, S.F., Patel, D., Hauser, A., Perocchi, F., and Minczuk, M. (2014). MRM2 and MRM3 are involved in biogenesis of the large subunit of the mitochondrial ribosome. Molecular biology of the cell.
Rorbach, J., Gammage, P.A., and Minczuk, M. (2012). C7orf30 is necessary for biogenesis of the large subunit of the mitochondrial ribosome. Nucleic acids research *40*, 4097-4109.
Rorbach, J., and Minczuk, M. (2012). The post-transcriptional life of mammalian mitochondrial RNA. The Biochemical journal *444*, 357-373.
Rorbach, J., Nicholls, T.J., and Minczuk, M. (2011). PDE12 removes mitochondrial RNA poly(A) tails and controls translation in human mitochondria. Nucleic acids research *39*, 7750-7763.
Rosa, I.D., Durigon, R., Pearce, S.F., Rorbach, J., Hirst, E.M., Vidoni, S., Reyes, A., Brea-Calvo, G., Minczuk, M., Woellhaf, M.W., *et al.* (2014). MPV17L2 is required for ribosome assembly in mitochondria. Nucleic acids research.
Rossmanith, W., Tullo, A., Potuschak, T., Karwan, R., and Sbisa, E. (1995). Human mitochondrial tRNA processing. The Journal of biological chemistry *270*, 12885-12891.
Ruzzenente, B., Metodiev, M.D., Wredenberg, A., Bratic, A., Park, C.B., Camara, Y., Milenkovic, D., Zickermann, V., Wibom, R., Hultenby, K., *et al.* (2012). LRPPRC is necessary for polyadenylation and coordination of translation of mitochondrial mRNAs. The EMBO journal *31*, 443-456.
Saada, A., Shaag, A., Arnon, S., Dolfin, T., Miller, C., Fuchs-Telem, D., Lombes, A., and Elpeleg, O. (2007). Antenatal mitochondrial disease caused by mitochondrial ribosomal protein (MRPS22) mutation. Journal of medical genetics *44*, 784-786.

Saikia, M., Dai, Q., Decatur, W.A., Fournier, M.J., Piccirilli, J.A., and Pan, T. (2006). A systematic, ligation-based approach to study RNA modifications. RNA *12*, 2025-2033.
Sanchez, M.I., Mercer, T.R., Davies, S.M., Shearwood, A.M., Nygard, K.K., Richman, T.R., Mattick, J.S., Rackham, O., and Filipovska, A. (2011). RNA processing in human mitochondria. Cell Cycle *10*, 2904-2916.
Sasarman, F., Brunel-Guitton, C., Antonicka, H., Wai, T., and Shoubridge, E.A. (2010). LRPPRC and SLIRP interact in a ribonucleoprotein complex that regulates posttranscriptional gene expression in mitochondria. Molecular biology of the cell *21*, 1315-1323.
Schatz, G. (1997). The hunt for mitochondrially synthesized proteins. Protein science : a publication of the Protein Society *6*, 728-734.
Schaub, M.C., Lopez, S.R., and Caputi, M. (2007). Members of the heterogeneous nuclear ribonucleoprotein H family activate splicing of an HIV-1 splicing substrate by promoting formation of ATP-dependent spliceosomal complexes. The Journal of biological chemistry *282*, 13617-13626.
Scheper, G.C., van der Knaap, M.S., and Proud, C.G. (2007). Translation matters: protein synthesis defects in inherited disease. Nature reviews Genetics *8*, 711-723.
Schmidt, O., Pfanner, N., and Meisinger, C. (2010). Mitochondrial protein import: from proteomics to functional mechanisms. Nature reviews Molecular cell biology *11*, 655-667.
Schwartz, M., and Vissing, J. (2002). Paternal inheritance of mitochondrial DNA. The New England journal of medicine *347*, 576-580.
Seidel-Rogol, B.L., McCulloch, V., and Shadel, G.S. (2003). Human mitochondrial transcription factor B1 methylates ribosomal RNA at a conserved stem-loop. Nature genetics *33*, 23-24.
Shajani, Z., Sykes, M.T., and Williamson, J.R. (2011). Assembly of bacterial ribosomes. Annual review of biochemistry *80*, 501-526.
Sharma, M.R., Koc, E.C., Datta, P.P., Booth, T.M., Spremulli, L.L., and Agrawal, R.K. (2003). Structure of the mammalian mitochondrial ribosome reveals an expanded functional role for its component proteins. Cell *115*, 97-108.
Shutt, T.E., and Gray, M.W. (2006). Bacteriophage origins of mitochondrial replication and transcription proteins. Trends in genetics : TIG *22*, 90-95.
Sirum-Connolly, K., Peltier, J.M., Crain, P.F., McCloskey, J.A., and Mason, T.L. (1995). Implications of a functional large ribosomal RNA with only three modified nucleotides. Biochimie *77*, 30-39.
Slomovic, S., Laufer, D., Geiger, D., and Schuster, G. (2005). Polyadenylation and degradation of human mitochondrial RNA: the prokaryotic past leaves its mark. Molecular and cellular biology *25*, 6427-6435.
Smeitink, J.A., Zeviani, M., Turnbull, D.M., and Jacobs, H.T. (2006). Mitochondrial medicine: a metabolic perspective on the pathology of oxidative phosphorylation disorders. Cell metabolism *3*, 9-13.
Smith, A.C., Blackshaw, J.A., and Robinson, A.J. (2012). MitoMiner: a data warehouse for mitochondrial proteomics data. Nucleic acids research *40*, D1160-1167.
Smith, A.C., and Robinson, A.J. (2009). MitoMiner, an integrated database for the storage and analysis of mitochondrial proteomics data. Molecular & cellular proteomics : MCP *8*, 1324-1337.
Smits, P., Smeitink, J., and van den Heuvel, L. (2010). Mitochondrial translation and beyond: processes implicated in combined oxidative phosphorylation deficiencies. Journal of biomedicine & biotechnology *2010*, 737385.

Sobek, S., and Boege, F. (2014). DNA topoisomerases in mtDNA maintenance and ageing. Experimental gerontology *56*, 135-141.
Spahr, H., Habermann, B., Gustafsson, C.M., Larsson, N.G., and Hallberg, B.M. (2012). Structure of the human MTERF4-NSUN4 protein complex that regulates mitochondrial ribosome biogenesis. Proceedings of the National Academy of Sciences of the United States of America *109*, 15253-15258.
Spelbrink, J.N. (2010). Functional organization of mammalian mitochondrial DNA in nucleoids: history, recent developments, and future challenges. IUBMB life *62*, 19-32.
Springer, M.S., and Douzery, E. (1996). Secondary structure and patterns of evolution among mammalian mitochondrial 12S rRNA molecules. Journal of molecular evolution *43*, 357-373.
Srivastava, S., and Moraes, C.T. (2001). Manipulating mitochondrial DNA heteroplasmy by a mitochondrially targeted restriction endonuclease. Human molecular genetics *10*, 3093-3099.
Steitz, T.A., and Moore, P.B. (2003). RNA, the first macromolecular catalyst: the ribosome is a ribozyme. Trends in biochemical sciences *28*, 411-418.
Stumpf, J.D., and Copeland, W.C. (2011). Mitochondrial DNA replication and disease: insights from DNA polymerase gamma mutations. Cellular and molecular life sciences : CMLS *68*, 219-233.
Sugiana, C., Pagliarini, D.J., McKenzie, M., Kirby, D.M., Salemi, R., Abu-Amero, K.K., Dahl, H.H., Hutchison, W.M., Vascotto, K.A., Smith, S.M., *et al.* (2008). Mutation of C20orf7 disrupts complex I assembly and causes lethal neonatal mitochondrial disease. American journal of human genetics *83*, 468-478.
Sun, L., Liu, Y., Fremont, M., Schwarz, S., Siegmann, M., Matthies, R., and Jost, J.P. (1998). A novel 52 kDa protein induces apoptosis and concurrently activates c-Jun N-terminal kinase 1 (JNK1) in mouse C3H10T1/2 fibroblasts. Gene *208*, 157-166.
Surovtseva, Y.V., and Shadel, G.S. (2013). Transcription-independent role for human mitochondrial RNA polymerase in mitochondrial ribosome biogenesis. Nucleic acids research *41*, 2479-2488.
Suzuki, T. (2014). A complete landscape of post-transcriptional modifications in mammalian mitochondrial tRNAs. Nucleic acids research *42*, 7346-7357.
Suzuki, T., and Nagao, A. (2011a). Human mitochondrial diseases caused by lack of taurine modification in mitochondrial tRNAs. Wiley interdisciplinary reviews RNA *2*, 376-386.
Suzuki, T., and Nagao, A. (2011b). Human mitochondrial tRNAs: biogenesis, function, structural aspects, and diseases. Annual review of genetics *45*, 299-329.
Suzuki, T., Terasaki, M., Takemoto-Hori, C., Hanada, T., Ueda, T., Wada, A., and Watanabe, K. (2001a). Proteomic analysis of the mammalian mitochondrial ribosome. Identification of protein components in the 28 S small subunit. The Journal of biological chemistry *276*, 33181-33195.
Suzuki, T., Terasaki, M., Takemoto-Hori, C., Hanada, T., Ueda, T., Wada, A., and Watanabe, K. (2001b). Structural compensation for the deficit of rRNA with proteins in the mammalian mitochondrial ribosome. Systematic analysis of protein components of the large ribosomal subunit from mammalian mitochondria. The Journal of biological chemistry *276*, 21724-21736.
Szklarczyk, R., Wanschers, B.F., Nijtmans, L.G., Rodenburg, R.J., Zschocke, J., Dikow, N., van den Brand, M.A., Hendriks-Franssen, M.G., Gilissen, C., Veltman, J.A., *et al.* (2013). A mutation in the FAM36A gene, the human ortholog of COX20, impairs cytochrome c oxidase assembly and is associated with ataxia and muscle hypotonia. Human molecular genetics *22*, 656-667.

Tachibana, M., Amato, P., Sparman, M., Gutierrez, N.M., Tippner-Hedges, R., Ma, H., Kang, E., Fulati, A., Lee, H.S., Sritanaudomchai, H., *et al.* (2013a). Human embryonic stem cells derived by somatic cell nuclear transfer. Cell *153*, 1228-1238.
Tachibana, M., Amato, P., Sparman, M., Woodward, J., Sanchis, D.M., Ma, H., Gutierrez, N.M., Tippner-Hedges, R., Kang, E., Lee, H.S., *et al.* (2013b). Towards germline gene therapy of inherited mitochondrial diseases. Nature *493*, 627-631.
Tachibana, M., Sparman, M., Sritanaudomchai, H., Ma, H., Clepper, L., Woodward, J., Li, Y., Ramsey, C., Kolotushkina, O., and Mitalipov, S. (2009). Mitochondrial gene replacement in primate offspring and embryonic stem cells. Nature *461*, 367-372.
Tang, T., Zheng, B., Chen, S.H., Murphy, A.N., Kudlicka, K., Zhou, H., and Farquhar, M.G. (2009). hNOA1 interacts with complex I and DAP3 and regulates mitochondrial respiration and apoptosis. The Journal of biological chemistry *284*, 5414-5424.
Taylor, R.W., and Turnbull, D.M. (2005). Mitochondrial DNA mutations in human disease. Nature reviews Genetics *6*, 389-402.
Temperley, R., Richter, R., Dennerlein, S., Lightowlers, R.N., and Chrzanowska-Lightowlers, Z.M. (2010a). Hungry codons promote frameshifting in human mitochondrial ribosomes. Science *327*, 301.
Temperley, R.J., Seneca, S.H., Tonska, K., Bartnik, E., Bindoff, L.A., Lightowlers, R.N., and Chrzanowska-Lightowlers, Z.M. (2003). Investigation of a pathogenic mtDNA microdeletion reveals a translation-dependent deadenylation decay pathway in human mitochondria. Human molecular genetics *12*, 2341-2348.
Temperley, R.J., Wydro, M., Lightowlers, R.N., and Chrzanowska-Lightowlers, Z.M. (2010b). Human mitochondrial mRNAs--like members of all families, similar but different. Biochimica et biophysica acta *1797*, 1081-1085.
Terzioglu, M., Ruzzenente, B., Harmel, J., Mourier, A., Jemt, E., Lopez, M.D., Kukat, C., Stewart, J.B., Wibom, R., Meharg, C., *et al.* (2013). MTERF1 binds mtDNA to prevent transcriptional interference at the light-strand promoter but is dispensable for rRNA gene transcription regulation. Cell metabolism *17*, 618-626.
Tkaczuk, K.L., Dunin-Horkawicz, S., Purta, E., and Bujnicki, J.M. (2007). Structural and evolutionary bioinformatics of the SPOUT superfamily of methyltransferases. BMC bioinformatics *8*, 73.
Trifunovic, A., Wredenberg, A., Falkenberg, M., Spelbrink, J.N., Rovio, A.T., Bruder, C.E., Bohlooly, Y.M., Gidlof, S., Oldfors, A., Wibom, R., *et al.* (2004). Premature ageing in mice expressing defective mitochondrial DNA polymerase. Nature *429*, 417-423.
Tucker, E.J., Hershman, S.G., Kohrer, C., Belcher-Timme, C.A., Patel, J., Goldberger, O.A., Christodoulou, J., Silberstein, J.M., McKenzie, M., Ryan, M.T., *et al.* (2011). Mutations in MTFMT underlie a human disorder of formylation causing impaired mitochondrial translation. Cell metabolism *14*, 428-434.
Uchiumi, T., Ohgaki, K., Yagi, M., Aoki, Y., Sakai, A., Matsumoto, S., and Kang, D. (2010). ERAL1 is associated with mitochondrial ribosome and elimination of ERAL1 leads to mitochondrial dysfunction and growth retardation. Nucleic acids research *38*, 5554-5568.
Ufer, C., Wang, C.C., Fahling, M., Schiebel, H., Thiele, B.J., Billett, E.E., Kuhn, H., and Borchert, A. (2008). Translational regulation of glutathione peroxidase 4 expression through guanine-rich sequence-binding factor 1 is essential for embryonic brain development. Genes & development *22*, 1838-1850.

Vafai, S.B., and Mootha, V.K. (2012). Mitochondrial disorders as windows into an ancient organelle. Nature *491*, 374-383.
Vilardo, E., Nachbagauer, C., Buzet, A., Taschner, A., Holzmann, J., and Rossmanith, W. (2012). A subcomplex of human mitochondrial RNase P is a bifunctional methyltransferase--extensive moonlighting in mitochondrial tRNA biogenesis. Nucleic acids research *40*, 11583-11593.
Vilardo, E., and Rossmanith, W. (2013). The amyloid-beta-SDR5C1(ABAD) interaction does not mediate a specific inhibition of mitochondrial RNase P. PloS one *8*, e65609.
Vogel, G. (2014). Assisted reproduction. FDA considers trials of 'three-parent embryos'. Science *343*, 827-828.
Wallace, D.C. (1999). Mitochondrial diseases in man and mouse. Science *283*, 1482-1488.
Wallace, D.C. (2007). Why do we still have a maternally inherited mitochondrial DNA? Insights from evolutionary medicine. Annual review of biochemistry *76*, 781-821.
Wallace, D.C. (2012). Mitochondria and cancer. Nature reviews Cancer *12*, 685-698.
Wallace, D.C., and Fan, W. (2009). The pathophysiology of mitochondrial disease as modeled in the mouse. Genes & development *23*, 1714-1736.
Wallace, D.C., Singh, G., Lott, M.T., Hodge, J.A., Schurr, T.G., Lezza, A.M., Elsas, L.J., 2nd, and Nikoskelainen, E.K. (1988). Mitochondrial DNA mutation associated with Leber's hereditary optic neuropathy. Science *242*, 1427-1430.
Wang, D.D., Guo, X.E., Modrek, A.S., Chen, C.F., Chen, P.L., and Lee, W.H. (2014a). Helicase SUV3, Polynucleotide Phosphorylase, and Mitochondrial Polyadenylation Polymerase Form a Transient Complex to Modulate Mitochondrial mRNA Polyadenylated Tail Lengths in Response to Energetic Changes. The Journal of biological chemistry *289*, 16727-16735.
Wang, D.D., Shu, Z., Lieser, S.A., Chen, P.L., and Lee, W.H. (2009). Human mitochondrial SUV3 and polynucleotide phosphorylase form a 330-kDa heteropentamer to cooperatively degrade double-stranded RNA with a 3'-to-5' directionality. The Journal of biological chemistry *284*, 20812-20821.
Wang, G., Chen, H.W., Oktay, Y., Zhang, J., Allen, E.L., Smith, G.M., Fan, K.C., Hong, J.S., French, S.W., McCaffery, J.M., *et al.* (2010). PNPASE regulates RNA import into mitochondria. Cell *142*, 456-467.
Wang, G., Shimada, E., Koehler, C.M., and Teitell, M.A. (2012). PNPASE and RNA trafficking into mitochondria. Biochimica et biophysica acta *1819*, 998-1007.
Wang, T., Sha, H., Ji, D., Zhang, H.L., Chen, D., Cao, Y., and Zhu, J. (2014b). Polar body genome transfer for preventing the transmission of inherited mitochondrial diseases. Cell *157*, 1591-1604.
Wang, Y., and Bogenhagen, D.F. (2006). Human mitochondrial DNA nucleoids are linked to protein folding machinery and metabolic enzymes at the mitochondrial inner membrane. The Journal of biological chemistry *281*, 25791-25802.
Wanschers, B.F., Szklarczyk, R., Pajak, A., van den Brand, M.A., Gloerich, J., Rodenburg, R.J., Lightowlers, R.N., Nijtmans, L.G., and Huynen, M.A. (2012). C7orf30 specifically associates with the large subunit of the mitochondrial ribosome and is involved in translation. Nucleic acids research *40*, 4040-4051.
Watanabe, K. (2010). Unique features of animal mitochondrial translation systems. The non-universal genetic code, unusual features of the translational apparatus and their relevance to human mitochondrial diseases. Proceedings of the Japan Academy Series B, Physical and biological sciences *86*, 11-39.

Weraarpachai, W., Antonicka, H., Sasarman, F., Seeger, J., Schrank, B., Kolesar, J.E., Lochmuller, H., Chevrette, M., Kaufman, B.A., Horvath, R., *et al.* (2009). Mutation in TACO1, encoding a translational activator of COX I, results in cytochrome c oxidase deficiency and late-onset Leigh syndrome. Nature genetics *41*, 833-837.
Weraarpachai, W., Sasarman, F., Nishimura, T., Antonicka, H., Aure, K., Rotig, A., Lombes, A., and Shoubridge, E.A. (2012). Mutations in C12orf62, a factor that couples COX I synthesis with cytochrome c oxidase assembly, cause fatal neonatal lactic acidosis. American journal of human genetics *90*, 142-151.
Wolf, A.R., and Mootha, V.K. (2014). Functional genomic analysis of human mitochondrial RNA processing. Cell reports *7*, 918-931.
Woodson, S.A. (2008). RNA folding and ribosome assembly. Current opinion in chemical biology *12*, 667-673.
Woodson, S.A. (2011). RNA folding pathways and the self-assembly of ribosomes. Accounts of chemical research *44*, 1312-1319.
Wredenberg, A., Lagouge, M., Bratic, A., Metodiev, M.D., Spahr, H., Mourier, A., Freyer, C., Ruzzenente, B., Tain, L., Gronke, S., *et al.* (2013). MTERF3 regulates mitochondrial ribosome biogenesis in invertebrates and mammals. PLoS genetics *9*, e1003178.
Xu, F., Ackerley, C., Maj, M.C., Addis, J.B., Levandovskiy, V., Lee, J., Mackay, N., Cameron, J.M., and Robinson, B.H. (2008). Disruption of a mitochondrial RNA-binding protein gene results in decreased cytochrome b expression and a marked reduction in ubiquinol-cytochrome c reductase activity in mouse heart mitochondria. The Biochemical journal *416*, 15-26.
Xu, F., Morin, C., Mitchell, G., Ackerley, C., and Robinson, B.H. (2004). The role of the LRPPRC (leucine-rich pentatricopeptide repeat cassette) gene in cytochrome oxidase assembly: mutation causes lowered levels of COX (cytochrome c oxidase) I and COX III mRNA. The Biochemical journal *382*, 331-336.
Yagi, M., Uchiumi, T., Takazaki, S., Okuno, B., Nomura, M., Yoshida, S., Kanki, T., and Kang, D. (2012). p32/gC1qR is indispensable for fetal development and mitochondrial translation: importance of its RNA-binding ability. Nucleic acids research *40*, 9717-9737.
Yakubovskaya, E., Guja, K.E., Eng, E.T., Choi, W.S., Mejia, E., Beglov, D., Lukin, M., Kozakov, D., and Garcia-Diaz, M. (2014). Organization of the human mitochondrial transcription initiation complex. Nucleic acids research *42*, 4100-4112.
Yakubovskaya, E., Guja, K.E., Mejia, E., Castano, S., Hambardjieva, E., Choi, W.S., and Garcia-Diaz, M. (2012). Structure of the essential MTERF4:NSUN4 protein complex reveals how an MTERF protein collaborates to facilitate rRNA modification. Structure *20*, 1940-1947.
Yan, H., Zareen, N., and Levinger, L. (2006). Naturally occurring mutations in human mitochondrial pre-tRNASer(UCN) can affect the transfer ribonuclease Z cleavage site, processing kinetics, and substrate secondary structure. The Journal of biological chemistry *281*, 3926-3935.
Yu, Y.T., Shu, M.D., and Steitz, J.A. (1997). A new method for detecting sites of 2'-O-methylation in RNA molecules. RNA *3*, 324-331.
Zhu, Z., Yao, J., Johns, T., Fu, K., De Bie, I., Macmillan, C., Cuthbert, A.P., Newbold, R.F., Wang, J., Chevrette, M., *et al.* (1998). SURF1, encoding a factor involved in the biogenesis of cytochrome c oxidase, is mutated in Leigh syndrome. Nature genetics *20*, 337-343.